

DELFT UNIVERSITY OF TECHNOLOGY

DEPARTMENT OF AEROSPACE ENGINEERING

Report LR - 248

**THE GENERATION OF MOTION CUES ON A
SIX-DEGREES-OF-FREEDOM MOTION SYSTEM**

by

M. Baarspul

DELFT - THE NETHERLANDS

June 1977



DELFT UNIVERSITY OF TECHNOLOGY

DEPARTMENT OF AEROSPACE ENGINEERING

Report LR - 248

**THE GENERATION OF MOTION CUES ON A
SIX-DEGREES-OF-FREEDOM MOTION SYSTEM**

by

M. Baarspul

DELFT - THE NETHERLANDS

June 1977

"Experiencing the motions of a six-degrees-of-freedom motion system is like listening to an orchestra. If you concentrate on one degree of freedom, you only hear the clarinet."

Jaap Veldhuijzen van Zanten

Foreword

The motion simulation described in this report has been performed at the Flight Crew Training Center of KLM, Royal Dutch Airlines at Schiphol Airport in 1975.

The author wishes to express his thanks to Capt. J. de Haas, Mr. M.G. van Staveren, Mr. J.A. Giel of KLM and Ir. J.A. van Ghesel Grothe of Delft University of Technology for their support and co-operation in organizing this project.

Summary

The mathematical formulation of motion cue generation on a six-degree-of-freedom motion base is described. From the mathematical model of the simulated aircraft, the specific forces and rotational accelerations at the aircraft c.g. are determined as primary control inputs to the motion drive laws. Because the specific forces are acting on the pilot inside the simulator cockpit, they should be transformed to the centroid location of the motion system.

As the motion possibilities of the moving platform are constrained, filtering of the specific forces and rotational accelerations is necessary. As far as possible, tilt angles are used to reproduce sustained specific forces, providing the motion system with "co-ordinated washout".

The scaled equations as programmed in the digital computer, including values for the time constants and damping ratio of the motion filters as applied to the KSS B-747 flight simulator, are represented in Appendix A. The listing of the main motion program for the SDS Sigma 2 computer of this flight simulator is represented in Appendix B.

Table of Contents

	<u>Page</u>
Summary	i
Symbols	iii
Systems of axes	vii
1. Introduction	1
2. General survey of the motion simulation concept	2
3. Flightpath to body-axes transformation of the total forces F_{x_w} , F_{y_w} and F_{z_w} .	4
4. Calculation of the body-axes specific forces A_{x_b} , A_{y_b} and A_{z_b} .	4
5. Centroid transformation of A_{x_b} , A_{y_b} and A_{z_b} .	5
6. Motion filters for the translational degrees of freedom	7
6.1. Longitudinal motion	7
6.2. Lateral motion	8
6.3. Heave motion	9
7. Body to inertial transformation of the motion platform translational accelerations	10
8. Translational washout	11
9. Motion filters for the rotational degrees of freedom	11
9.1. Pitch motion	11
9.2. Roll motion	14
9.3. Yaw motion	16
10. Body to inertial transformation of the motion platform rotational rates	17
11. Rotational washout	17
12. Lead compensation for dynamic lag in the motion system's translational and rotational degrees of freedom	17
13. Summary of the equations as applied in the motion simulation	18
14. Concluding remarks	21
15. References	23
16. Acknowledgements	23

Appendix A: Scaled equations as used in the KSS B-747 Main Motion
Simulation Program

(24 pages)

Appendix B: Listing of the "KSS B-747 Main Motion Simulation". Program

(48 pages).

4 Tables

4 Figures.

Symbols

A_{x_b}	body-axes longitudinal specific force at aircraft c.g.
$A_{x_b,c}$	body-axes longitudinal specific force at centroid location.
A_{y_b}	body-axes lateral specific force at aircraft c.g.
$A_{y_b,c}$	body-axes lateral specific force at centroid location.
A_{z_b}	body-axes vertical specific force at aircraft c.g.
$A_{z_b,c}$	body-axes vertical specific force at centroid location.
c.g.	center of gravity
F_x	total force along the X-axis, the subscript indicates the axes-system concerned.
F_y	total force along the Y-axis, the subscript indicates the axes-system concerned.
F_z	total force along the Z-axis, the subscript indicates the axes-system concerned.
g	acceleration due to gravity, m/sec^2 .
$H(P)$	transfer function.
m	aircraft mass.
p_b	roll-rate in body axes, rad/sec .
$p_{b,1_p}$	simulator roll-rate in body-axes to simulate lateral specific force, rad/sec .
p_{b,h_p}	simulator roll-rate in body-axes to simulate roll acceleration, rad/sec .
p_s	$= p_{b,1_p} + p_{b,h_p}$
P	Laplace operator.
q_b	pitch-rate in body-axes, rad/sec .
q_{b,h_p}	simulator pitch-rate in body-axes to simulate pitch acceleration, rad/sec .
$q_{b,1_p}$	simulator pitch-rate in body-axes to simulate longitudinal specific force, rad/sec .
q_s	$= q_{b,1_p} + q_{b,h_p}$

Symbols: cont'd

r_b	yaw-rate in body-axes, rad/sec.
r_{b,h_p}	simulator yaw-rate in body axes to simulate yaw acceleration, rad/sec.
R_x	$= x_p - x_{p,c}$
R_y	$= y_p - y_{p,c}$
R_z	$= z_p - z_{p,c}$
S	scale factor, the index indicates the variable concerned.
u_b	body-axis longitudinal velocity component, m/sec.
v_b	body-axis lateral velocity component, m/sec.
w_b	body-axis vertical velocity component, m/sec.
W	aircraft weight, kgf.
W_{x_b}	component of the aircraft weight along the X_b -axis.
W_{y_b}	component of the aircraft weight along the Y_b -axis.
W_{z_b}	component of the aircraft weight along the Z_b -axis.
$x_{b,1}$	longitudinal motion base position to simulate longitudinal specific force.
$x_{b,2}$	longitudinal motion base position to compensate for longitudinal specific force error.
x_c	lead compensated longitudinal position command input to the motion system.
x_m	inertial longitudinal position command input to the motion system.
x_p	x co-ordinate of pilot's station relative to the aircraft c.g. in body-axes.
$x_{p,c}$	x co-ordinate of centroid location relative to the pilot's station in body axes.
x_s	$= x_{b,1} + x_{b,2}$
$y_{b,1}$	lateral motion base position to simulate lateral specific force.
$y_{b,2}$	lateral motion base position to compensate for lateral specific force error.

Symbols cont'd

y_c	lead compensated lateral position command input to the motion system.
y_m	inertial lateral position command input to the motion system.
y_p	y co-ordinate of pilot's station relative to the aircraft c.g. in body-axes.
$y_{p,c}$	y co-ordinate of centroid location relative to the pilot's station in body-axes.
y_s	$= y_{b,1} + y_{b,2}$.
z_b	body-axes vertical motion base position.
z_c	lead compensated vertical position command input to the motion system.
z_m	inertial vertical position command input to the motion system.
z_p	z co-ordinate of pilot's station relative to the aircraft c.g. in body-axes.
$z_{p,c}$	z co-ordinate of centroid location relative to the pilot's station in body-axes.
α_b	aircraft body angle of attack, rad.
β	angle of sideslip, rad.
θ	aircraft body pitch attitude, rad.
θ_c	lead compensated pitch-input to the motion system, rad.
θ_{h_p}	body-axes simulator pitch angle, as a consequence of the simulation of pitch acceleration, rad.
θ_{l_p}	body-axes simulator pitch angle to simulate longitudinal specific force, rad.
θ_m	inertial pitch-input to the motion system, rad.
τ	time constant, the index indicating the variable concerned.
ϕ	roll angle, rad.
ϕ_c	lead compensated roll-input to the motion system, rad.
ϕ_{h_p}	body-axes simulator roll angle, as a consequence of the simulation of roll acceleration, rad.
ϕ_{l_p}	body-axes simulator roll angle to simulate lateral specific force.
ϕ_m	inertial roll-input to the motion system, rad.

Symbols cont'd

- Ψ yaw angle, rad.
- ψ_h _p body-axes simulator yaw angle, as a consequence of the simulation of yaw acceleration, rad.
- ψ_c lead compensated yaw-input to the motion system, rad.
- ψ_m inertial yaw-input to the motion system, rad.
- ζ damping ratio, the index indicating the variable concerned.

Subscripts

- b body-axes
- c centroid location
- h_p high-pass filtered
- i inertial axes
- l_p low-pass filtered
- w flightpath - (wind) axes
- x along x-axis
- y along y-axis
- z along z-axis.

A dot over a variable indicates the time derivative of that variable.

Systems of axes

In this report three systems of axes are used:

1. The aircraft "body-axes": an aircraft-fixed right-handed reference-frame $O_b X_b Y_b Z_b$. The origin O_b lies in the aircraft's center of gravity, the positive X_b -axis lies in the plane of symmetry $O_b X_b Z_b$ and points forward along the fuselage reference-line. The positive Y_b -axis is perpendicular to the $O_b X_b Z_b$ -plane and points to starboard. The positive Z_b -axis is perpendicular to the $O_b X_b Y_b$ -plane and points downward.
2. The flightpath-(wind) axes: a right-handed reference-frame $O_w X_w Y_w Z_w$. The origin O_w coincides with the aircraft c.g. the positive X_w -axis lies along the velocity-vector of the aircraft c.g. The positive Y_w -axis is perpendicular to the $O_w X_w Z_w$ -plane and points in the direction of the positive lateral force. The positive Z_w -axis is perpendicular to the velocity-vector, opposite to the direction of the lift and lies in the aircraft plane of symmetry, see Fig. 3.
3. An earth-fixed reference-frame $O_e X_e Y_e Z_e$. This reference-frame is identical to the $O_b X_b Y_b Z_b$ reference-frame with the exception of the orientation of the origin O_e and the direction of the X_e -axis. The origin O_e coincides with the centroid location of the motion system, see Fig. 4.
The X_e -axis lies in the plane of symmetry $O_e X_e Z_e$ of the flight simulator and in the horizontal plane.

1. Introduction

The addition of six-degree-of-freedom motion to a flight simulator cockpit provides realism and gives a greater consistency of training results between simulator- and flight training. Ideally, the simulator cockpit would be commanded to move about in accordance with the states that the real aircraft would possess. Generally, it is impossible to do this since the cockpit is mounted in a mechanical structure with limited possibilities of movement. In each degree of freedom the motion system cannot exceed physical limits on position, velocity and/or acceleration. These limits are given in Table 1 for motion in single degree of freedom operation, of the KLM 747 motion base.

Now the following dilemma arises. The pilot manipulates the controls of the simulator. The computer determines the resultant motion of the aircraft being simulated and sets the flight instruments and visual display to show this motion.

The computer also commands the simulator cockpit to move, preferably just as the aircraft would. However, since only limited motion of the cockpit is possible, some modifications of the computed motion is necessary before it can be used to command cockpit motion. Otherwise, the motion system might be driven into its structural limits and hence give totally erroneous motion impressions to the pilot.

The way in which the motion variables of the aircraft must be modified is closely related to the properties of the human vestibular system. The exact quantities "sensed" by a pilot's motion perceptive organisms are not yet completely understood. However, empirical knowledge combined with theoretical and practical considerations leads to the assumption that a pilot can "sense" the same quantities as can be measured by three linear- and three rotational accelerometers mounted along three perpendicular axes, see Refs. 1, 2 and 3.

A linear accelerometer does not measure acceleration but rather the difference between acceleration and gravitation. This difference is called specific force, e.g. in inertial navigation literature, see Ref. 4.

Three linear accelerometers are assumed to be appropriately mounted to measure the specific forces, denoted as A_{x_b} , A_{y_b} and A_{z_b} along the aircraft's X_b , Y_b and Z_b -axis respectively. The sum of these specific forces is the specific force vector, which is defined here as the positive sum of all non-gravitational forces per unit mass. According to the foregoing a pilot's motion perceptive organisms sense the specific force vector.

Three rotational accelerometers are assumed to be mounted along the aircraft's X_b , Y_b and Z_b -axis respectively, to measure the rotational accelerations along these axes. For sufficiently small rotations the rotational accelerations can be approximated by ψ , θ and ϕ respectively. During the simulation of aircraft motion the three components of specific force A_{x_b} , A_{y_b} and A_{z_b} and the rotational accelerations ψ , θ and ϕ acting on the pilot in the simulator cockpit should as much as possible agree with the magnitudes of the same variables in the aircraft cockpit during flight. As an example, the rolling response of an aircraft and the simulator are compared in a somewhat simplified form in Fig. 1. In the case considered here Fig. 1a shows that the bank angle ϕ of the real aircraft increases continuously. In about 1 sec. the aircraft roll rate $\dot{\phi}$ becomes constant, see Fig. 1b. The flight simulator cockpit however can only follow this motion partially, see Fig. 1a and has to return asymptotically to its neutral position, avoiding the generation of a false specific force, see section 9.2.

In spite of the great differences of the bank angle ϕ and the roll rate $\dot{\phi}$ between the aircraft and the simulator, Fig. 1c shows that the rotational accelerations agree very well.

The block diagram of Fig. 2 shows in great detail the modification of the specific forces and rotational accelerations of the simulated aircraft necessary to drive the motion system of the flight simulator.

In the subsequent Sections the motion drive signals for each degree of freedom of the motion system will be described. The motion limitations and restrictions mentioned in Table 1 are a major factor in the task suitability of the particular motion base as well as in the selection of the parameters in the motion simulation program, as further described in Appendix A.

The majority of the report is devoted to the mathematical formulation of motion generation, which aside from the physical characteristics of the hardware, see Ref. 5, is the major factor affecting the quality of a motion simulation.

2. General survey of the motion simulation concept

The emphasized parts of the motion simulation are illustrated in detailed form in Fig. 2. Frequent reference to Fig. 2 will be necessary in as much as the description of the motion cue generation consists of a block-by-block discussion.

From the equations of motion, describing the aircraft dynamics in flight and on the ground, the three total forces F_x , F_y and F_z and the three rotational accelerations \dot{r}_b , \dot{q}_b and \dot{p}_b are determined as primary control inputs of the motion drive laws. For the calculation of the body-axes specific forces, the total forces are required in body-axes. In the off-ground condition however, the total forces in the KSS B-747 flight simulation program are computed in flightpath- (wind) axes. They are transformed to body-axes before being used to compute the body-axes specific forces at the c.g. of the simulated aircraft, see Fig. 2, block 3. The centroid transformation converts the specific forces at the aircraft c.g. into specific forces, which, when applied at the centroid of the motion system, see Fig. 4, would produce the actual specific forces at the pilot's seat of the aircraft on the pilot inside the simulator cockpit. As the motion possibilities of the base are constrained, filtering of the specific forces at centroid location and the rotational accelerations is necessary. Sustained longitudinal and lateral specific forces can only be represented on a motion simulator by tilting the cockpit and utilizing the gravity-vector to generate the cue. However, the tilt angle must be obtained without pilot knowledge. Therefore the rotational acceleration of the cab, necessary to obtain the tilt angle should be below the threshold level of the pilot's perception. The initial part of the specific force, the onset, can only be generated by translational motion until the tilt angle is obtained. In this way translational and rotational motion of the flight simulator cockpit are co-ordinated to generate longitudinal and lateral specific forces.

In the case of the simulation of a rotational acceleration about the longitudinal or lateral axis by means of rotation alone, a false specific force may be obtained because of temporary misalignment of the gravity-vector relative to the simulator cockpit. Translational motion of the base is required to compensate for this specific force error.

This has been indicated in Fig. 2, see the boxes labeled "specific force error". The motion system operates in an earth-fixed, or inertial reference frame, so the filtered specific forces and rotational rates are transformed to inertial axes whereafter a second attenuation is applied.

Lead compensation of the six position and attitude command signals to the motion system is required to compensate for motion system lag. The actuator extension transformation routine transforms the six compensated position commands into the length of the servo-actuators of the motion system, see Fig. 2, block 13.

3. Flightpath to body-axes transformation of the total forces F_{x_w} , F_{y_w} and F_{z_w} .

For the calculation of the body-axes specific forces from the total forces F_x , F_y and F_z , see Fig. 2, the total forces are required in body-axes. However, in the off-ground condition, the total forces are computed in flightpath- (wind) axes. Therefore in the off-ground condition, the total forces F_{x_w} , F_{y_w} and F_{z_w} have to be transformed to body-axes, see Fig. 3.

The transformation equations read:

$$F_{x_b} = + \cos \alpha_b \cdot \cos \beta \cdot F_{x_w} - \cos \alpha_b \cdot \sin \beta \cdot F_{y_w} - \sin \alpha_b \cdot F_{z_w} \quad (3.1.)$$

$$F_{y_b} = + \sin \beta \cdot F_{x_w} + \cos \beta \cdot F_{y_w}$$

$$F_{z_b} = + \sin \alpha_b \cdot \cos \beta \cdot F_{x_w} - \sin \alpha_b \cdot \sin \beta \cdot F_{y_w} + \cos \alpha_b \cdot F_{z_w}$$

where: α_b is the aircraft body angle of attack and β is the side-slip angle.

When the aircraft is on the ground, the total forces F_x , F_y and F_z are computed in body-axes. As a consequence in the on-ground condition, transformation (3.1.) is not required, see Fig. 2, blocks 1, 2 and 3.

4. Calculation of the body-axes specific forces A_{x_b} , A_{y_b} and A_{z_b} .

For the total forces F_{x_b} , F_{y_b} and F_{z_b} in body-axes can be written, see Ref. 6:

$$F_{x_b} = m (\ddot{u}_b - r_b \cdot v_b) \quad *)$$

$$F_{y_b} = m (\dot{v}_b + r_b \cdot u_b - p_b \cdot w_b) \quad (4.1.)$$

$$F_{z_b} = m (\dot{w}_b - q_b \cdot u_b + p_b \cdot v_b)$$

where: $m = \frac{W}{g}$ is the aircraft mass.

\ddot{u}_b is the aircraft body-axes longitudinal acceleration, denoted as V'_{x_b} in Ref. 6.

u_b is the body-axes longitudinal velocity component, denoted as V'_{x_b} in Ref. 6.

\dot{v}_b is the aircraft body-axes lateral acceleration, denoted as V'_{y_b} in Ref. 6.

v_b is the body-axes lateral velocity component, denoted as V'_{y_b} in Ref. 6.

\dot{w}_b is the aircraft body-axes vertical acceleration, denoted as V'_{z_b} in Ref. 6.

w_b is the body-axes vertical velocity component, denoted as V'_{z_b} in Ref. 6.

*) In Ref. 6 the term $q_b w_b$ in the equation for F_{x_b} is neglected, because its magnitude is small.

From the total forces, the specific forces in body-axes can be easily derived by subtraction of the component of the aircraft weight and deviding the result by the aircraft mass, see Fig. 2, block 4:

$$A_{x_b} = (F_{x_b} - W_{x_b}) \cdot g/W$$

where: $W_{x_b} \cdot g/W = -g \cdot \sin \theta$

$$A_{y_b} = (F_{y_b} - W_{y_b}) \cdot g/W$$

where: $W_{y_b} \cdot g/W = +g \cdot \cos \theta \cdot \sin \phi \quad (4.2.)$

$$A_{z_b} = (F_{z_b} - W_{z_b}) \cdot g/W$$

where: $W_{z_b} \cdot g/W = +g \cdot \cos \theta \cdot \cos \phi$

According to (4.1.):

$$F_{x_b} \cdot g/W = a_b - r_b \cdot v_b$$

$$F_{y_b} \cdot g/W = \dot{v}_b + r_b \cdot u_b - p_b \cdot w_b$$

$$F_{z_b} \cdot g/W = \dot{w}_b - q_b \cdot u_b + p_b \cdot v_b \quad (4.3.)$$

Combination of (4.2.) and (4.3.) results in the specific forces in body-axes at the c.g. of the simulated aircraft:

$$A_{x_b} = \dot{u}_b - r_b \cdot v_b + g \cdot \sin \theta$$

$$A_{y_b} = \dot{v}_b + r_b \cdot u_b - p_b \cdot w_b - g \cdot \cos \theta \cdot \sin \phi \quad (4.4.)$$

$$A_{z_b} = \dot{w}_b - q_b \cdot u_b + p_b \cdot v_b - g \cdot \cos \theta \cdot \cos \phi$$

5. Centroid transformation of A_{x_b} , A_{y_b} and A_{z_b} .

The purpose of the centroid transformation is to provide the motion filters with the unconstrained motions of the base that would be necessary to produce all the cues to which a pilot would be subjected at the pilot's station, see Fig. 2 block 5. Thus it is necessary to locate hypothetically the centroid of the motion base, see Fig. 4, in the simulated aircraft with respect to the pilot's station, and then transform the motion, derived for the center of gravity of the simulated aircraft, to this hypothetical location. This location with respect to the aircraft c.g. is defined as:

$$R_x = x_p - x_{p,c}$$

$$R_y = y_p - y_{p,c}$$

$$R_z = z_p - z_{p,c}$$

where x_p , y_p and z_p locate the pilot's station with respect to the aircraft c.g. and $x_{p,c}$, $y_{p,c}$ and $z_{p,c}$ locate the centroid with respect to the pilot's station.

Now the specific forces A_{x_b} , A_{y_b} and A_{z_b} (4.4.) can be computed at centroid location:

$$A_{x_b,c} = A_{x_b} - (q_b^2 + r_b^2) \cdot R_x + (q_b \cdot p_b - t_b) \cdot R_y + (r_b \cdot p_b + \dot{q}_b) \cdot R_z$$
$$A_{y_b,c} = A_{y_b} + (p_b \cdot q_b + t_b) \cdot R_x - (p_b^2 + r_b^2) \cdot R_y + (r_b \cdot q_b - \dot{p}_b) \cdot R_z$$
$$A_{z_b,c} = A_{z_b} + (p_b \cdot r_b - \dot{q}_b) \cdot R_x + (q_b \cdot r_b + \dot{p}_b) \cdot R_y - (p_b^2 + q_b^2) \cdot R_z$$

For the KSS B-747 flight simulator:

$$y_p = y_{p,c}, \text{ therefore: } R_y = 0$$
$$z_p = z_{p,c}, \text{ therefore: } R_z = 0$$

Introducing these simplifications and substitution of (4.4.) for A_{x_b} , A_{y_b} and A_{z_b} results in:

$$A_{x_b,c} = \dot{u}_b - r_b \cdot v_b + g \cdot \sin \theta - (q_b^2 + r_b^2) \cdot R_x$$
$$A_{y_b,c} = \dot{v}_b + r_b \cdot u_b - p_b \cdot w_b - g \cdot \cos \theta \cdot \sin \phi + (p_b \cdot q_b + t_b) \cdot R_x \quad (5.1)$$
$$A_{z_b,c} = \dot{w}_b - q_b \cdot u_b + p_b \cdot v_b - g \cdot \cos \theta \cdot \cos \phi + (p_b \cdot r_b - \dot{q}_b) \cdot R_x$$

Now the following notations are introduced:

$$\dot{u}_{b,c} = \dot{u}_b - r_b \cdot v_b - (q_b^2 + r_b^2) \cdot R_x$$

$$\dot{v}_{b,c} = \dot{v}_b + r_b \cdot u_b - p_b \cdot w_b + (p_b \cdot q_b + t_b) \cdot R_x$$

$$\dot{w}_{b,c} = \dot{w}_b - q_b \cdot u_b + p_b \cdot v_b + (p_b \cdot r_b - \dot{q}_b) \cdot R_x$$

Substituting $\dot{u}_{b,c}$, $\dot{v}_{b,c}$ and $\dot{w}_{b,c}$ in the expressions (5.1.) results in the specific forces at the centroid location in the simulated aircraft:

$$A_{x_b,c} = \dot{u}_{b,c} + g \cdot \sin \theta \quad (5.2.)$$

$$A_{y_b,c} = \dot{v}_{b,c} - g \cdot \cos \theta \cdot \sin \phi \quad (5.3.)$$

$$A_{z_b,c} = \dot{w}_{b,c} - g \cdot \cos \theta \cdot \cos \phi \quad (5.4.)$$

6. Motion filters for the translational degrees of freedom

6.1. Longitudinal motion

The simulation of longitudinal specific forces is performed by means of the co-ordinated longitudinal and pitch motion of the simulator cockpit. The longitudinal motion is used to reproduce the high-frequency onset cue of the longitudinal specific force until the pitch motion has had time to align the simulator cockpit relative to the gravity vector to present the sustained, or low frequency portion of the longitudinal specific force.

High-pass filtering of $A_{x_b,c}$ removes the low-frequency portion of the longitudinal specific force, likely to exceed the motion platform position limits in X-direction, see Fig. 2, block 6.1.

The longitudinal specific force at the centroid position inside the simulator cockpit can be written as:

$$(A_{x_b,c})_{\text{sim}} = A_{x_b,1,c} + g \cdot \theta_{1p} \quad (6.1.)$$

where $A_{x_b,1,c}$ is the high-frequency portion of the longitudinal specific force, reproduced by means of the simulator longitudinal translational motion and θ_{1p} is the simulator pitch angle needed to reproduce sustained longitudinal specific force, see Section 9.1.

Combining the two expressions for the longitudinal specific force at the centroid location, (5.2.) and (6.1.), gives:

$$A_{x_b,1,c} = \dot{u}_{b,c} + g \cdot \sin \theta - g \cdot \theta_{1p}$$

The low frequency gravity component $g \cdot \sin \theta$ of $A_{x_b,c}$ will be simulated separately by means of θ_{1p} , as discussed in section 9.1.

So, for the simulator, the high-frequency longitudinal specific force becomes:

$$A_{x_b,1,c} = \dot{u}_{b,c} - g \cdot \theta_{1p} \quad (6.2.)$$

The transfer function of the applied high-pass second order filter reads:

$$\frac{\ddot{x}_{b,1}(P)}{(\dot{u}_{b,c} - g \cdot \theta_{1p})(P)} = H(P) = \frac{\tau_x^2 \cdot P^2}{1 + 2 \cdot \tau_x \cdot \zeta_x \cdot P + \tau_x^2 \cdot P^2}$$

Substituting (6.2.) and applying the inverse Laplace transform results in:

$$x_{b,1} + 2 \cdot \tau_x \cdot \zeta_x \cdot \dot{x}_{b,1} + \tau_x^2 \cdot \ddot{x}_{b,1} - \tau_x^2 \cdot (\dot{u}_{b,c} - g \cdot \theta_{1p}) = 0$$

* Note: In order to stay with the existing notation of the KSS B-747 motion simulation program, time constants τ (sec) have been used, rather than the more usual natural frequencies ω_0 (sec^{-1}), where $\tau = \frac{1}{\omega_0}$.

The resulting longitudinal acceleration of the motion base now can be written as:

$$\ddot{x}_{b,1} = \dot{v}_{b,c} - g \cdot \theta_{1_p} - \frac{2\zeta_x}{\tau_x} \cdot \dot{x}_{b,1} - \frac{1}{\tau_x^2} \cdot x_{b,1} \quad (6.3.)$$

If the computer sample time for the sequential calculations is 50 msec (20 times/sec) rectangular integration of $\dot{x}_{b,1}$ gives at time t_n :

$$\dot{x}_{b,1_n} = \dot{x}_{b,1_{n-1}} + 0,05 \cdot \ddot{x}_{b,1_{n-1}}$$

$$x_{b,1_n} = x_{b,1_{n-1}} + 0,05 \cdot \dot{x}_{b,1_n}$$

The correction for specific force error as a consequence of the simulation of aircraft pitch acceleration, see section 9.1., reads:

$$\dot{x}_{b,2} = -g \cdot \theta_{h_p}$$

where θ_{h_p} is the simulator pitch angle resulting as a consequence of the simulation of pitch acceleration, see Fig. 2, block 9.1.2.

The resulting body-axes longitudinal translational acceleration of the motion base now becomes:

$$\ddot{x}_s = \ddot{x}_{b,1} + \dot{x}_{b,2} \quad (6.4.)$$

6.2. Lateral motion

The simulation of lateral specific forces is performed in a way similar to the longitudinal case by means of the co-ordinated lateral and roll motions of the motion base, see Fig. 2, block 6.2.

The lateral specific force at the centroid location inside the simulator cockpit is:

$$(A_{y_b,c})_{sim} = A_{y_{b,1},c} - g \cdot \phi_{1_p} \quad (6.5.)$$

where $A_{y_{b,1},c}$ is the high-frequency part of the lateral specific force, reproduced by the simulator lateral translational motion and ϕ_{1_p} is the simulator roll angle needed to reproduce sustained lateral specific force, see section 9.2.

Equating the lateral specific force at centroid location (5.3.) and (6.5.) gives:

$$A_{y_{b,1},c} = \dot{v}_{b,c} - g \cdot \cos \theta \cdot \sin \phi + g \cdot \phi_{1_p} \quad (6.6.)$$

The transfer function of the applied high-pass second order filter reads:

$$\frac{\dot{y}_{b,1}(P)}{(\dot{v}_{b,c} - g \cdot \cos \theta \cdot \sin \phi + g \cdot \phi_{1_p})(P)} = H(P)^{*} = \frac{\tau_y^2 \cdot P^2}{1 + 2\tau_y \zeta_y \cdot P + \tau_y^2 \cdot P^2}$$

* See note on page 7.

Substituting (6.6.) and applying the inverse Laplace transform results in:

$$y_{b,1} + 2 \tau_y \zeta_y \cdot \ddot{y}_{b,1} + \tau_y^2 \cdot \ddot{y}_{b,1} - \tau_y^2 \cdot (v_{b,c} - g \cdot \cos \theta \cdot \sin \phi + g \cdot \phi_{1_p}) = 0$$

The resulting lateral acceleration of the motion base now can be written as:

$$\ddot{y}_{b,1} = v_{b,c} - g \cdot \cos \theta \cdot \sin \phi + g \cdot \phi_{1_p} - \frac{2\zeta_y}{\tau_y} \cdot \ddot{y}_{b,1} - \frac{1}{\tau_y^2} \cdot y_{b,1} \quad (6.7.)$$

Rectangular integration at a rate of 20 times/sec results at time t_n :

$$\dot{y}_{b,1_n} = \dot{y}_{b,1_{n-1}} + 0,05 \ddot{y}_{b,1_{n-1}}$$

$$y_{b,1_n} = y_{b,1_{n-1}} + 0,05 \dot{y}_{b,1_n}$$

The correction for specific force error as a consequence of the simulation of aircraft roll acceleration, see section 9.2., reads:

$$\dot{y}_{b,2} = +g \cdot \phi_{h_p}$$

where ϕ_{h_p} is the simulator roll angle resulting as a consequence of the simulation of roll acceleration, see Fig. 2, block 9.2.2.

The total body-axes lateral translational acceleration of the motion base now becomes:

$$y_s = y_{b,1} + y_{b,2} \quad (6.8.)$$

6.3. Heave motion

The simulation of vertical specific forces is, because of the restricted stroke of the servo-actuators, see Table 1, only possible in a very limited way. No tilt angle is available to reproduce the low-frequency part of the vertical specific force and thus the low-frequency part cannot be simulated. This results in the limitation of simulating only relatively small normal accelerations during a short time. Specific forces or normal accelerations as a result of atmospheric turbulence or touch down can therefore be simulated very well, but the longer lasting specific forces occurring in a steep turn or during a pull up from a dive can only be simulated approximately. That is why also in this degree of freedom a high-pass filter is applied, see Fig. 2, block 6.3., to suppress the low frequency changes of the vertical specific force.

The vertical specific force at the centroid location inside the simulator cockpit is:

$$(A_{z_b,c})_{sim} = z_b - g \quad (6.9.)$$

Combining the two expressions for the vertical specific force at the centroid location, (5.4.) and (6.9.), gives:

$$\hat{w}_{b,c} = g \cdot \cos \theta \cdot \cos \phi = z_b^* - g \quad (6.10.)$$

where \hat{z}_b^* is the not yet filtered vertical acceleration of the simulator cockpit in body-axes.

The transfer function of the applied high-pass filter reads:

$$H(P)^* = \frac{z_b(P)}{z_b^*(P)} = \frac{\tau_z^2 \cdot P^2}{1 + 2 \tau_z \zeta_z \cdot P + \tau_z^2 \cdot P^2}$$

Substituting (6.10.) for \hat{z}_b^* and applying the inverse Laplace transform results in:

$$z_b + 2 \tau_z \cdot \zeta_z \cdot \dot{z}_b + \tau_z^2 \cdot z_b - \tau_z^2 \cdot \hat{w}_{b,c} - \tau_z^2 \cdot g(1 - \cos \theta \cdot \cos \phi) = 0$$

The term $\tau_z^2 \cdot g(1 - \cos \theta \cdot \cos \phi)$ in this equation will be neglected, because of its low magnitude and its relatively low frequency.

The resulting vertical acceleration of the simulator cockpit can now be written as:

$$\ddot{z}_b = \hat{w}_{b,c} - \frac{2\zeta_z}{\tau_z} \cdot \dot{z}_b - \frac{1}{\tau_z^2} \cdot z_b \quad (6.11.)$$

Rectangular integration of \ddot{z}_b at a rate of 20 times/sec gives at time t_n :

$$\dot{z}_{b_n} = \dot{z}_{b_{n-1}} + 0,05 \ddot{z}_{b_{n-1}}$$

$$z_{b_n} = z_{b_{n-1}} + 0,05 \dot{z}_{b_n}$$

7. Body to inertial transformation of the motion platform translational accelerations.

The translational degrees of freedom of the motion base operate in an earth-fixed inertial reference frame. Therefore the body-axes translational accelerations \ddot{x}_s (6.4.), \ddot{y}_s (6.8.) and \ddot{z}_b (6.11.) are transformed to inertial co-ordinates.

According to Table 14 of Ref. 7, for the inertial translational accelerations can be written successively:

$$\begin{aligned} \ddot{x}_i &= \cos \theta_m \cdot \cos \psi_m \cdot \ddot{x}_s + (\sin \phi_m \cdot \sin \theta_m \cdot \cos \psi_m - \cos \phi_m \cdot \sin \psi_m) \cdot \ddot{y}_s \\ &\quad + (\cos \phi_m \cdot \sin \theta_m \cdot \cos \psi_m + \sin \phi_m \cdot \sin \psi_m) \cdot \ddot{z}_b \end{aligned} \quad (7.1.)$$

$$\begin{aligned} \ddot{y}_i &= \cos \theta_m \cdot \sin \psi_m \cdot \ddot{x}_s + (\sin \phi_m \cdot \sin \theta_m \cdot \sin \psi_m + \cos \phi_m \cdot \cos \psi_m) \cdot \ddot{y}_s \\ &\quad + (\cos \phi_m \cdot \sin \theta_m \cdot \sin \psi_m - \sin \phi_m \cdot \cos \psi_m) \cdot \ddot{z}_b \end{aligned} \quad (7.2.)$$

* See note on page 7.

$$\ddot{z}_i = -\sin \theta_m \cdot \dot{x}_s + \sin \phi_m \cdot \cos \theta_m \cdot \dot{y}_s + \cos \phi_m \cdot \cos \theta_m \cdot \dot{z}_b \quad (7.3.)$$

where ψ_m , θ_m and ϕ_m are the simulator yaw, pitch and roll angles respectively, see Section 11.

8. Translational wash-out.

To prevent the motion platform from running into its limits, translational wash-out is carried out on the inertial accelerations \ddot{x}_i , \ddot{y}_i and \ddot{z}_i by means of second-order high-pass filters of the form:

$$\begin{aligned}\ddot{x}_m &= \ddot{x}_i - \frac{2\zeta_{x_T}}{\tau_{x_T}^2} \cdot \dot{x}_m - \frac{1}{\tau_{x_T}^2} \cdot x_m \\ \ddot{y}_m &= \ddot{y}_i - \frac{2\zeta_{y_T}}{\tau_{y_T}^2} \cdot \dot{y}_m - \frac{1}{\tau_{y_T}^2} \cdot y_m \\ \ddot{z}_m &= \ddot{z}_i - \frac{2\zeta_{z_T}}{\tau_{z_T}^2} \cdot \dot{z}_m - \frac{1}{\tau_{z_T}^2} \cdot z_m\end{aligned}\quad (8.1.)$$

The inertial motion platform positions x_m , y_m and z_m , not yet compensated for the motion system's dynamic lag, see section 12, and velocities \dot{x}_m , \dot{y}_m and \dot{z}_m are obtained by rectangular integration of \ddot{x}_m , \ddot{y}_m and \ddot{z}_m respectively at a rate of 20 times/sec.

9. Motion filters for the rotational degrees of freedom.

9.1. Pitch motion

The pitch motion of the flight simulator is used for the simulation of the sustained portion of the longitudinal specific force, see Section 6.1., and for the simulation of aircraft pitch acceleration, see Fig. 2, blocks 9.1.1. and 9.1.2.

The sustained portion of the longitudinal specific force $A_{x_b,c}$ is created in the simulator by means of a component of gravity:

$$A_{x_b,c} = g \cdot \sin \theta_{1_p} \quad (9.1.)$$

The generation of the simulator pitch angle θ_{1_p} necessary for this purpose is inevitably associated with pitch acceleration. As the pilot should not notice this acceleration, it should be kept below the threshold level of the pilot's perception. That is why a low-pass filter is used in the computation of θ_{1_p} , see Fig. 2, block 9.1.1.

The computation of θ_{1_p} occurs in the following way.

Equating the longitudinal specific force at the centroid location (5.2.) and the longitudinal specific force at the centroid position inside the simulator cockpit (9.1.) gives:

$$\dot{u}_{b,c} + g \cdot \sin \theta = g \cdot \sin \theta_{1p}^*$$

where θ_{1p}^* is the not yet filtered pitch angle of the simulator cockpit to simulate the sustained portion of longitudinal specific forces.

As the longitudinal specific force acting inside a B-747 cockpit is normally less than 0,3g, resulting in $\theta_{1p}^* < 16^\circ$, $\sin \theta_{1p}^*$ is approximated by θ_{1p}^* :

$$\sin \theta_{1p}^* = \theta_{1p}^*$$

For θ_{1p}^* now can be written:

$$\theta_{1p}^* = \frac{\dot{u}_{b,c}}{g} + \sin \theta \quad (9.2.)$$

θ_{1p}^* is fed through a low-pass filter, see Fig. 2, block 9.1.1., the transfer function of which reads:

$$H(P) = \frac{\theta_{1p}^*(P)}{\theta_{1p}(P)} = \frac{1}{1 + 2 \cdot \tau_{\theta_{1p}} \cdot \zeta_{\theta_{1p}} \cdot P + \tau_{\theta_{1p}}^2 \cdot P^2}$$

Substituting (9.2.) for θ_{1p}^* and applying the inverse Laplace transform gives:

$$\theta_{1p} + 2\tau_{\theta_{1p}} \cdot \zeta_{\theta_{1p}} \cdot q_{b,1p} + \tau_{\theta_{1p}}^2 \cdot \dot{q}_{b,1p} - \frac{\dot{u}_{b,c}}{g} - \sin \theta = 0$$

The resulting pitch acceleration reads:

$$\dot{q}_{b,1p} = \frac{\dot{u}_{b,c}}{\tau_{\theta_{1p}}^2 \cdot g} + \frac{\sin \theta}{\tau_{\theta_{1p}}^2} - \frac{2\zeta_{\theta_{1p}}}{\tau_{\theta_{1p}}^2} \cdot q_{b,1p} - \frac{1}{\tau_{\theta_{1p}}^2} \cdot \theta_{1p} \quad (9.3.)$$

Rectangular integration at a rate of 20 times/sec gives at time t_n :

$$q_{b,1p_n} = q_{b,1p_{n-1}} + 0,05 \dot{q}_{b,1p} \quad (9.4.)$$

$$\theta_{1p_n} = \theta_{1p_{n-1}} + 0,05 q_{b,1p_n}$$

* See note on page 7.

The simulation of the aircraft pitch acceleration \dot{q}_b on the simulator gives also rise to a simulator pitch angle θ_{h_p} .

According to the foregoing θ_{h_p} , is sensed by the pilot as an erroneous specific force.

Therefore, the pitch angle θ_{h_p} of the simulator as a result of the simulation of the pitch acceleration \dot{q}_b should remain as small as possible. This can be achieved by applying a high-pass filter in the computation of the pitch acceleration \dot{q}_{b,h_p} of the simulator.

The computation of the simulator pitch angle θ_{h_p} for the simulation of pitch acceleration occurs in the following way. The transfer function of the applied high-pass second order filter reads:

$$\frac{\theta_{h_p}(P)^*)}{\theta(P)} = \frac{\tau_{\theta_{h_p}}^2 \cdot P^2}{1 + 2\tau_{\theta_{h_p}} \cdot \zeta_{\theta_{h_p}} \cdot P + \tau_{\theta_{h_p}}^2 \cdot P^2}$$

Applying the inverse Laplace transform results in:

$$\theta_{h_p} + 2\tau_{\theta_{h_p}} \cdot \zeta_{\theta_{h_p}} \cdot q_{b,h_p} + \tau_{\theta_{h_p}}^2 \cdot \dot{q}_{b,h_p} - \tau_{\theta_{h_p}}^2 \cdot \dot{q}_b = 0$$

The simulator pitch acceleration now can be written as:

$$q_{b,h_p} = \dot{q}_b - \frac{2\zeta_{\theta_{h_p}}}{\tau_{\theta_{h_p}}} \cdot q_{b,h_p} - \frac{1}{\tau_{\theta_{h_p}}^2} \cdot \theta_{h_p}$$

Rectangular integration at a rate of 20 times/sec gives at time t_n :

$$q_{b,h_p_n} = q_{b,h_p_{n-1}} + 0,05 \cdot q_{b,h_p_n}$$

$$\theta_{h_p_n} = \theta_{h_p_{n-1}} + 0,05 \cdot q_{b,h_p_n}$$

The flight simulator pitch angle θ_{h_p} as a consequence of the simulation of pitch acceleration \dot{q}_b results in a specific force error:

$$(A_{x_b,c})_{\text{error}} = -g \cdot \theta_{h_p}$$

This longitudinal specific force error can be compensated by means of the longitudinal translational motion of the base:

$$\ddot{x}_{b,2} = -g \cdot \theta_{h_p}, \text{ see Section 6.1.}$$

* See note on page 7.

The total body-axes pitch acceleration, used for lead-compensation of the motion system, see section 12, reads:

$$\dot{q}_s = \dot{q}_{b,l_p} + \dot{q}_{b,h_p} \quad (9.5.)$$

The total body-axes pitch rate, to be transformed into inertial axes, see section 10, reads:

$$q_s = q_{b,l_p} + q_{b,h_p} \quad (9.6.)$$

9.2. Roll motion

The roll motion of the flight simulator is used for the simulation of the sustained portion of the lateral specific force, see Section 6.2. and for the simulation of aircraft roll acceleration, see Fig. 2, blocks 9.2.1. and 9.2.2. respectively.

The simulation of the lateral specific force $A_{y_{b,c}}$ occurs in just the same manner as the simulation of the longitudinal specific force $A_{x_{b,c}}$, described in the previous section:

$$A_{y_{b,c}} = -g \cdot \sin \phi_{l_p} \quad (9.7.)$$

where $g \cdot \sin \phi_{l_p}$ is the lateral component of gravity inside the simulator cockpit. Note, that for the simulation of a positive lateral specific force ϕ_{l_p} is negative.

Equating the lateral specific force at the centroid location (5.3.) and the lateral specific force at the centroid position inside the simulator cockpit (9.7.) results in:

$$\dot{v}_{b,c} - g \cdot \cos \theta \cdot \sin \phi = -g \cdot \sin \phi_{l_p}^* \quad *$$

where $\phi_{l_p}^*$ is the not yet filtered roll angle of the simulator to generate lateral specific forces.

Also here the approximation is made:

$$\sin \phi_{l_p}^* \approx \phi_{l_p}^*$$

as $A_{y_{b,c}}$ normally $< 0,3g$.

For $\phi_{l_p}^*$ now can be written:

$$\phi_{l_p}^* = -\frac{\dot{v}_{b,c}}{g} + \cos \theta \cdot \sin \phi \quad (9.8.)$$

* See note on page 7.

$\dot{\phi}_{1p}^*$ is fed through a low-pass filter to keep the roll acceleration of the cab below the threshold level of the pilot's perception. The transfer function of this filter reads:

$$\frac{\phi_{1p}^*(P)}{\dot{\phi}_{1p}^*(P)} = \frac{1}{1 + 2\tau_{\phi_{1p}} \cdot \zeta_{\phi_{1p}} \cdot P + \tau_{\phi_{1p}}^2 \cdot P^2}$$

Substituting (9.8.) for $\dot{\phi}_{1p}^*$ and applying the inverse Laplace transform gives:

$$\dot{\phi}_{1p} + 2\tau_{\phi_{1p}} \cdot \zeta_{\phi_{1p}} \cdot p_{b,1p} + \tau_{\phi_{1p}}^2 \cdot \dot{p}_{b,1p} + \frac{\dot{v}_{b,c}}{g} - \cos \theta \cdot \sin \phi = 0$$

The resulting roll acceleration $\dot{p}_{b,1p}$ reads:

$$\dot{p}_{b,1p} = -\frac{\dot{v}_{b,c}}{\tau_{\phi_{1p}}^2 \cdot g} + \frac{\cos \theta \cdot \sin \phi}{\tau_{\phi_{1p}}^2} - \frac{2\zeta_{\phi_{1p}}}{\tau_{\phi_{1p}}^2} \cdot p_{b,1p} - \frac{1}{\tau_{\phi_{1p}}^2} \cdot \dot{\phi}_{1p} \quad (9.9.)$$

Rectangular integration at a rate of 20 times/sec gives at time t_n :

$$p_{b,1p_n} = p_{b,1p_{n-1}} + 0,05 \cdot \dot{p}_{b,1p_{n-1}}$$

$$\dot{\phi}_{1p_n} = \dot{\phi}_{1p_{n-1}} + 0,05 \cdot p_{b,1p_n}$$

The computation of the simulator roll angle ϕ_{hp} to simulate aircraft roll accelerations occurs in the same manner as the computation of θ_{hp} .

The transfer function of the applied high-pass second order filter reads:

$$\frac{\phi_{hp}(P)}{\phi(P)} = \frac{\tau_{\phi_{hp}}^2 \cdot P^2}{1 + 2\tau_{\phi_{hp}} \cdot \zeta_{\phi_{hp}} \cdot P + \tau_{\phi_{hp}}^2 \cdot P^2}$$

The resulting simulator roll acceleration $\dot{p}_{b,hp}$ can be written as:

$$\dot{p}_{b,hp} = \dot{p}_b - \frac{2\zeta_{\phi_{hp}}}{\tau_{\phi_{hp}}^2} \cdot p_{b,hp} - \frac{1}{\tau_{\phi_{hp}}^2} \cdot \dot{\phi}_{hp}$$

Rectangular integration of $\dot{p}_{b,hp}$ gives at time t_n :

$$p_{b,hp_n} = p_{b,hp_{n-1}} + 0,05 \cdot \dot{p}_{b,hp_{n-1}}$$

* See note on page 7.

$$\phi_{h_{p_n}} = \phi_{h_{p_{n-1}}} + 0,05 \cdot p_{b,h_{p_n}}$$

The specific force error as a result of ϕ_{h_p} reads:

$$(A_{y_{b,c}})_{\text{error}} = + g \cdot \phi_{h_p}$$

This lateral specific force error is compensated by means of the lateral translational motion of the base:

$$\dot{y}_{b,2} = + g \cdot \phi_{h_p}, \text{ see Section 6.2.}$$

The total body-axes roll acceleration, used for lead-compensation of the motion system, see Section 12, reads:

$$p_s = p_{b,l_p} + p_{b,h_p} \quad (9.10.)$$

The total body-axes roll rate, to be transformed into inertial axes, see Section 10, reads:

$$p_s = p_{b,l_p} + p_{b,h_p} \quad (9.11.)$$

9.3. Yaw motion

Because of the restricted freedom in yaw of the motion base, see Table 1, also here a high-pass filter is applied to suppress the low-frequency changes of aircraft yaw acceleration \dot{r}_b .

The transfer function of the applied high-pass second order filter reads:

$$\frac{\dot{r}_{b,h_p}}{\dot{r}_b} = H(P)^*) = \frac{\tau_\psi^2 \cdot P^2}{1 + 2\tau_\psi \cdot \zeta_\psi \cdot P + \tau_\psi^2 \cdot P^2}$$

The resulting body-axes yaw acceleration \dot{r}_{b,h_p} can be written as:

$$\dot{r}_{b,h_p} = \dot{r}_b - \frac{2\zeta_\psi}{\tau_\psi} \cdot r_{b,h_p} - \frac{1}{\tau_\psi^2} \cdot \psi_{h_p} \quad (9.12.)$$

Rectangular integration gives at time t_n :

$$r_{b,h_{p_n}} = r_{b,h_{p_{n-1}}} + 0,05 \cdot \dot{r}_{b,h_{p_{n-1}}} \quad (9.13.)$$

$$\psi_{h_{p_n}} = \psi_{h_{p_{n-1}}} + 0,05 \cdot r_{b,h_{p_n}} \quad (9.14.)$$

* See note on page 7.

10. Body to inertial transformation of the motion system rotational rates.

Just as the translational degrees of freedom, the rotational degrees of freedom of the motion base operate in an inertial axes system.

Therefore, the rotational rates (9.6.), (9.11.) and (9.13.) are transformed to Euler rates. According to Table 33 of Ref. 7, the Euler rates $\dot{\psi}_i$, $\dot{\theta}_i$ and $\dot{\phi}_i$ can be written as:

$$\dot{\psi}_i = \frac{\sin \phi_m}{\cos \theta_m} \cdot q_s + \frac{\cos \phi_m}{\cos \theta_m} \cdot r_{b,h_p}$$

$$\dot{\theta}_i = \cos \phi_m \cdot q_s - \sin \phi_m \cdot r_{b,h_p} \quad (10.1.)$$

$$\dot{\phi}_i = p_s + \sin \phi_m \cdot \tan \theta_m \cdot q_s + \cos \phi_m \cdot \tan \theta_m \cdot r_{b,h_p}$$

where θ_m and ϕ_m are the simulator pitch and roll angles respectively, see also section 11.

11. Rotational washout.

In accordance with section 8, an attenuation is applied also to the Euler rates $\dot{\psi}_i$, $\dot{\theta}_i$ and $\dot{\phi}_i$ of the motion platform, see Fig. 2, block 11, to prevent the platform from running into its limits.

Use is made here of first order high-pass washout filters.

$$\dot{\psi}_m = \dot{\psi}_i - \frac{1}{\tau_{\psi_R}} \cdot \psi_m$$

$$\dot{\theta}_m = \dot{\theta}_i - \frac{1}{\tau_{\theta_R}} \cdot \theta_m \quad (11.1.)$$

$$\dot{\phi}_m = \dot{\phi}_i - \frac{1}{\tau_{\phi_R}} \cdot \phi_m$$

The yaw angle ψ_m , pitch angle θ_m and roll angle ϕ_m of the motion platform, not yet compensated for the platform's dynamic lag, are obtained by rectangular integration of $\dot{\psi}_m$, $\dot{\theta}_m$ and $\dot{\phi}_m$ respectively at a rate of 20 times/sec.

12. Lead compensation for dynamic lag in the motion system's translational and rotational degrees of freedom.

An analysis of the motion system's response characteristics revealed that the hardware had dominant second-order phase lag characteristics, see Ref. 5.

Compensation for these lags could be achieved by introducing in the software program of the motion simulation appropriate second-order lead terms. Both the first and second derivatives are required of the signal to be compensated. For the translational degrees of freedom, both the transformed first and second derivatives \dot{x}_m , \ddot{x}_m , \dot{z}_m , \ddot{z}_m , \dot{y}_m , and \ddot{y}_m are available for this purpose, see section 8. For the rotational degrees of freedom, however, the second derivatives (9.5.), (9.10.) and (9.12.) are available only in body-axes and thus they will be used for the compensation. The six compensated position and attitude command signals, to be sent to the actuator extension transformation, see Fig. 2, block 13, read:

$$\begin{aligned}x_c &= x_m + B_1 \cdot \dot{x}_m + A_1 \cdot \ddot{x}_m \\y_c &= y_m + B_2 \cdot \dot{y}_m + A_2 \cdot \ddot{y}_m \\z_c &= z_m + B_3 \cdot \dot{z}_m + A_3 \cdot \ddot{z}_m \\\theta_c &= \theta_m + B_4 \cdot \dot{\theta}_m + A_4 \cdot \ddot{\theta}_m \\phi_c &= \phi_m + B_5 \cdot \dot{\phi}_m + A_5 \cdot \ddot{\phi}_m \\\psi_c &= \psi_m + B_6 \cdot \dot{\psi}_m + A_6 \cdot \ddot{\psi}_m\end{aligned}\quad (12.1.)$$

Numerical values for the "time-constants"^{x)}, damping ratio and other parameters as applied to the KSS B-747 motion simulation are presented in Appendices A and B.

13. Summary of the equations as applied in the motion simulation.

Flightpath to body-axes transformation of the total forces F_{x_w} , F_{y_w} and F_{z_w} in the off-ground condition:

$$\begin{aligned}F_{x_b} &= + \cos \alpha_b \cdot \cos \beta \cdot F_{x_w} - \cos \alpha_b \cdot \sin \beta \cdot F_{y_w} - \sin \alpha_b \cdot F_{z_w} \\F_{y_b} &= \quad \quad \quad + \sin \beta \cdot F_{x_w} \quad + \quad \quad \quad \cos \beta \cdot F_{y_w} \\F_{z_b} &= + \sin \alpha_b \cdot \cos \beta \cdot F_{x_w} - \sin \alpha_b \cdot \sin \beta \cdot F_{y_w} + \cos \alpha_b \cdot F_{z_w}\end{aligned}\quad (3.1.)$$

The body-axes specific forces:

$$\begin{aligned}A_{x_b} &= \dot{u}_b - r_b \cdot v_b + g \cdot \sin \theta \\A_{y_b} &= \dot{v}_b + r_b \cdot u_b - p_b \cdot w_b - g \cdot \cos \theta \cdot \sin \phi \\A_{z_b} &= \dot{w}_b - q_b \cdot u_b + p_b \cdot v_b - g \cdot \cos \theta \cdot \cos \phi\end{aligned}\quad (4.4.)$$

x) See note on page 7.

Centroid transformation:

$$A_{x_b,c} = \dot{u}_{b,c} + g \cdot \sin \theta \quad (5.2.)$$

where:

$$\dot{u}_{b,c} = \dot{u}_b - r_b \cdot v_b - (q_b^2 + r_b^2) \cdot R_x$$

$$A_{y_b,c} = \dot{v}_{b,c} - g \cdot \cos \theta \cdot \sin \phi \quad (5.3.)$$

where:

$$\dot{v}_{b,c} = \dot{v}_b + r_b \cdot u_b - p_b \cdot w_b + (p_b \cdot q_b + r_b) \cdot R_x$$

$$A_{z_b,c} = \dot{w}_{b,c} - g \cdot \cos \theta \cdot \cos \phi \quad (5.4.)$$

where:

$$\dot{w}_{b,c} = \dot{w}_b - q_b \cdot u_b + p_b \cdot v_b + (p_b \cdot r_b - q_b) \cdot R_x$$

Longitudinal motion:

$$\ddot{x}_{b,1} = \dot{u}_{b,c} - g \cdot \theta_{h_p} - \frac{2\zeta_x}{\tau_x} \cdot \dot{x}_{b,1} - \frac{1}{\tau_x^2} \cdot x_{b,1} \quad (6.3.)$$

$$\ddot{x}_{b,2} = -g \cdot \theta_{h_p} \quad (\text{specific force error})$$

$$\ddot{x}_s = \dot{x}_{b,1} + \ddot{x}_{b,2} \quad (6.4.)$$

Lateral motion:

$$\ddot{y}_{b,1} = \dot{v}_{b,c} - g \cdot \cos \theta \cdot \sin \phi + g \cdot \phi_{h_p} - \frac{2\zeta_y}{\tau_y} \cdot \dot{y}_{b,1} - \frac{1}{\tau_y^2} \cdot y_{b,1} \quad (6.7.)$$

$$\ddot{y}_{b,2} = +g \cdot \phi_{h_p} \quad (\text{specific force error})$$

$$\ddot{y}_s = \dot{y}_{b,1} + \ddot{y}_{b,2} \quad (6.8.)$$

Heave motion:

$$\ddot{z}_b = \dot{w}_{b,c} - \frac{2\zeta_z}{\tau_z} \cdot \dot{z}_b - \frac{1}{\tau_z^2} \cdot z_b \quad (6.11.)$$

Body to inertial transformation of the motion platform translational accelerations:

$$\begin{aligned} \ddot{x}_i &= \cos \theta_m \cdot \cos \psi_m \cdot \ddot{x}_s + (\sin \phi_m \cdot \sin \theta_m \cdot \cos \psi_m - \cos \phi_m \cdot \sin \psi_m) \cdot \ddot{y}_s \\ &\quad + (\cos \phi_m \cdot \sin \theta_m \cdot \cos \psi_m + \sin \phi_m \cdot \sin \psi_m) \cdot \ddot{z}_b \end{aligned} \quad (7.1.)$$

$$\begin{aligned} \ddot{y}_i &= \cos \theta_m \cdot \sin \psi_m \cdot \ddot{x}_s + (\sin \phi_m \cdot \sin \theta_m \cdot \sin \psi_m + \cos \phi_m \cdot \cos \psi_m) \cdot \ddot{y}_s \\ &\quad + (\cos \phi_m \cdot \sin \theta_m \cdot \sin \psi_m - \sin \phi_m \cdot \cos \psi_m) \cdot \ddot{z}_b \end{aligned} \quad (7.2.)$$

$$\ddot{z}_i = -\sin \theta_m \cdot \ddot{x}_s + \sin \phi_m \cdot \cos \theta_m \cdot \ddot{y}_s + \cos \phi_m \cdot \cos \theta_m \cdot \ddot{z}_b \quad (7.3.)$$

Translational washout:

$$\begin{aligned} \ddot{x}_m &= \ddot{x}_i - \frac{2\zeta_{x_T}}{\tau_{x_T}} \cdot \dot{x}_m - \frac{1}{\tau_{x_T}^2} \cdot x_m \\ \ddot{y}_m &= \ddot{y}_i - \frac{2\zeta_{y_T}}{\tau_{y_T}} \cdot \dot{y}_m - \frac{1}{\tau_{y_T}^2} \cdot y_m \\ \ddot{z}_m &= \ddot{z}_i - \frac{2\zeta_{z_T}}{\tau_{z_T}} \cdot \dot{z}_m - \frac{1}{\tau_{z_T}^2} \cdot z_m \end{aligned} \quad (8.1.)$$

Pitch motion:

$$\begin{aligned} \dot{q}_{b,1_p} &= \frac{\dot{u}_{b,c}}{\tau_{\theta_{1_p}}^2 \cdot g} + \frac{\sin \theta}{\tau_{\theta_{1_p}}^2} - \frac{2\zeta_{\theta_{1_p}}}{\tau_{\theta_{1_p}}} \cdot q_{b,1_p} - \frac{1}{\tau_{\theta_{1_p}}^2} \cdot \theta_{1_p} \\ \dot{q}_{b,h_p} &= \dot{q}_b - \frac{2\zeta_{\theta_{h_p}}}{\tau_{\theta_{h_p}}} \cdot q_{b,h_p} - \frac{1}{\tau_{\theta_{h_p}}^2} \cdot \theta_{h_p} \end{aligned} \quad (9.3.)$$

$$q_s = q_{b,1_p} + q_{b,h_p} \quad (9.5.)$$

$$q_s = q_{b,1_p} + q_{b,h_p} \quad (9.6.)$$

Roll motion:

$$\begin{aligned} \dot{p}_{b,1_p} &= -\frac{\dot{v}_{b,c}}{\tau_{\phi_{1_p}}^2 \cdot g} + \frac{\cos \theta \cdot \sin \phi}{\tau_{\phi_{1_p}}^2} - \frac{2\zeta_{\phi_{1_p}}}{\tau_{\phi_{1_p}}} \cdot p_{b,1_p} - \frac{1}{\tau_{\phi_{1_p}}^2} \cdot \phi_{1_p} \\ \dot{p}_{b,h_p} &= \dot{p}_b - \frac{2\zeta_{\phi_{h_p}}}{\tau_{\phi_{h_p}}} \cdot p_{b,h_p} - \frac{1}{\tau_{\phi_{h_p}}^2} \cdot \phi_{h_p} \end{aligned} \quad (9.9.)$$

$$p_s = p_{b,1_p} + p_{b,h_p} \quad (9.10.)$$

$$p_s = p_{b,1_p} + p_{b,h_p} \quad (9.11.)$$

Yaw motion:

$$\dot{r}_{b,h_p} = \dot{r}_b - \frac{2\zeta_\psi}{\tau_\psi} \cdot r_{b,h_p} - \frac{1}{\tau_\psi^2} \cdot \dot{\psi}_{h_p} \quad (9.12.)$$

Euler rates:

$$\dot{\psi}_i = \frac{\sin \phi_m}{\cos \theta_m} \cdot q_s + \frac{\cos \phi_m}{\cos \theta_m} \cdot r_{b,h_p}$$

$$\dot{\theta}_i = \cos \phi_m \cdot q_s - \sin \phi_m \cdot r_{b,h_p} \quad (10.1.)$$

$$\dot{\phi}_i = p_s + \sin \phi_m \cdot \tan \theta_m \cdot q_s + \cos \phi_m \cdot \tan \theta_m \cdot r_{b,h_p}$$

Rotational washout:

$$\dot{\psi}_m = \dot{\psi}_i - \frac{1}{\tau_{\psi_R}} \cdot \psi_m$$

$$\dot{\theta}_m = \dot{\theta}_i - \frac{1}{\tau_{\theta_R}} \cdot \theta_m \quad (11.1.)$$

$$\dot{\phi}_m = \dot{\phi}_i - \frac{1}{\tau_{\phi_R}} \cdot \phi_m$$

Motion system lead compensation:

$$x_c = x_m + B_1 \cdot \dot{x}_m + A_1 \cdot \ddot{x}_m$$

$$y_c = y_m + B_2 \cdot \dot{y}_m + A_2 \cdot \ddot{y}_m$$

$$z_c = z_m + B_3 \cdot \dot{z}_m + A_3 \cdot \ddot{z}_m$$

$$\theta_c = \theta_m + B_4 \cdot \dot{\theta}_m + A_4 \cdot \ddot{\theta}_m \quad (12.1.)$$

$$\phi_c = \phi_m + B_5 \cdot \dot{\phi}_m + A_5 \cdot \ddot{\phi}_m$$

$$\psi_c = \psi_m + B_6 \cdot \dot{\psi}_m + A_6 \cdot \ddot{\psi}_m + \dot{r}_{b,h_p}$$

14. Concluding remarks

In this report the mathematical formulation of the generation of motion cues is described. From the mathematical model of the simulated aircraft, the specific forces and rotational accelerations at the aircraft c.g. are determined as primary control inputs of the motion drive laws. Because the specific forces are acting on the pilot inside the simulator cockpit, they should be transformed to the so called centroid location of the motion system.

As the motion possibilities of the base are constrained, filtering of the specific forces and rotational accelerations is necessary and as far as possible, tilt angles are used to reproduce sustained specific forces, providing the motion system with so called "co-ordinated wash-out".

The dynamic characteristics of the motion system should be such, that for the reproduction of the high frequencies, the high frequency-response of the base is of sufficient quality. On the other hand the smoothness of the base is important to keep the low-frequency "wash-out" below the threshold level of the pilot's perception.

Experience obtained from the development of the motion simulation software, presented in Appendix B, has shown that realistic motion cues are obtained, especially in the approach, landing and take-off phases of flight. Among other difficulties, problems such as lateral pilot-induced-oscillations in the final part of the visual approach were solved.

15. References

1. S.F. Schmidt,
B. Conrad
"Motion Drive Signals For Piloted Flight
Simulators", Analytical Mechanics Associates,
Inc. Palo Alto, California, 1970.
2. R.L. Stapleford
R.A. Peters
F.K. Alex
"Experiments and a Model for Pilot Dynamics
with Visual on Motion Inputs", NASA CR 1325,
May 1969.
3. D.T. McRuer et al.
"New Approaches to Human Pilot/Vehicle Dynamic
Analysis", Systems Technology Inc., Techn.
Report AFDL-TR-76-150, 1968.
4. C. Broxmeyer
"Inertial Navigation Systems", Electronic
Services Series, McGraw-Hill, 1964.
5. M. Baarspul
"Hardware Modifications to improve the frequency
response and smoothness of a synergistic six-
degree-of-freedom motion system", (KLM report to
be published).
6. J. Schlien
CAE Program Specification Flight part 1 and 4,
CAE Electronics Ltd., Canada, November 1971.
7. W.G. Vermeulen
"Overzicht van in de vliegmechanica veel gebruikte
assenstelsels en de daarmee samenhangende trans-
formatie formules", Memo VH-69-035, National
Aerospace Laboratory NLR, The Netherlands.

16. Acknowledgements

The author wishes to acknowledge the efficient and cheerful co-operation with his team-members: Captain J.L. Veldhuyzen van Zanten, Chief-Instructor B-747 of KLM and Mr. B. Baarschers, Simulator Engineer at KLM, responsible for the hard- and software of the KSS B-747 flight simulator. Special thanks are due to Prof. Dr. Ir. O.H. Gerlach of Delft University of Technology for his support and valuable suggestions in the conducting of this project and for reading the concept of this report.

		Performance limits		
Degree of freedom	Position	Velocity	Acceleration	Rate of change accelerations
Horizontal x	forward 1,24 m	± 0,610 m/sec	± 0,5 g	± 30g/sec
	aft 1,24 m			
Lateral y	left 1,21 m	± 0,610 m/sec	± 0,5 g	± 30g/sec
	right 1,21 m			
Vertical z	up 0,85 m	± 0,91 m/sec	± 0,75 g	± 50g/sec
	down 0,85 m			
Yaw ψ	+ 36°	± 20°/sec	± 20°/sec ²	
Pitch θ	+ 34°	± 20°/sec	± 30°/sec ²	
	- 32°			
Roll ϕ	+ 28°	± 16°/sec	± 20°/sec ²	

Table 1: Performance limits for single degree of freedom operation.

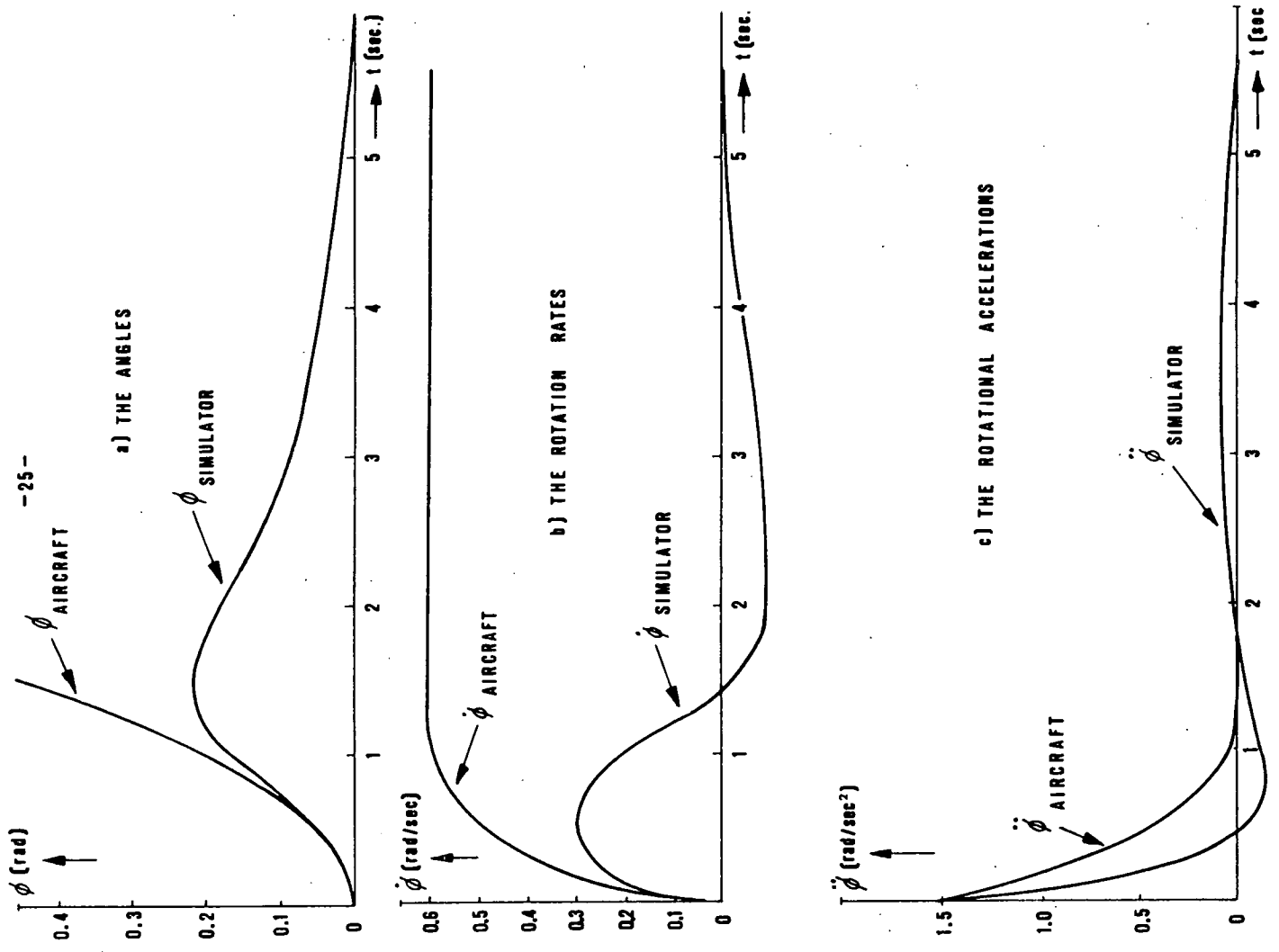
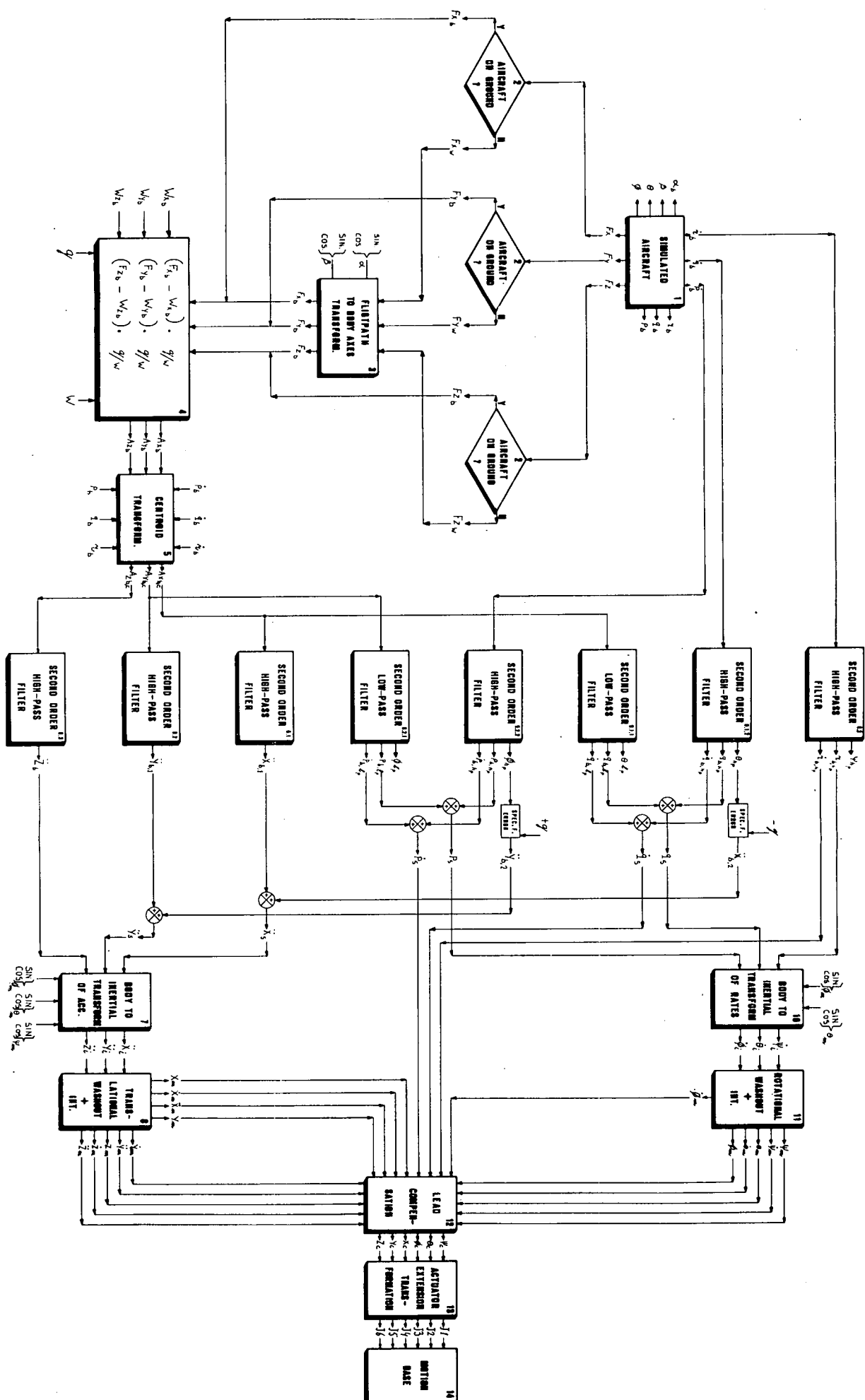


FIG. 1 THE RESPONSES OF THE BANK ANGLE (ϕ) AND THE ROLL RATE ($\dot{\phi}$) AND THE ROLL ACCELERATION ($\ddot{\phi}$) OF AN AIRCRAFT AND THE FLIGHT SIMULATOR TO AN AILERON STEP INPUT

FIG. 2: KSS BOEING 747 MOTION SIMULATION



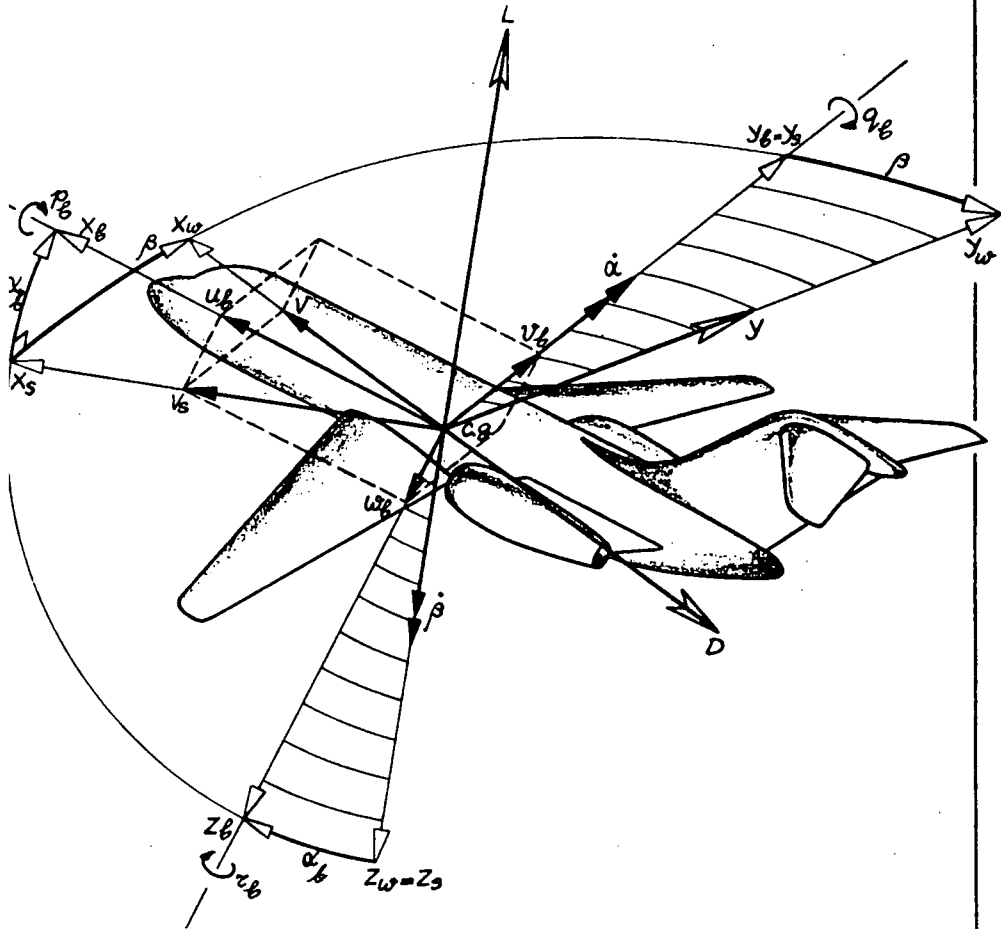


FIG 3 THE RELATION BETWEEN BODY AXES AND FLIGHTPATH- (WIND) AXES

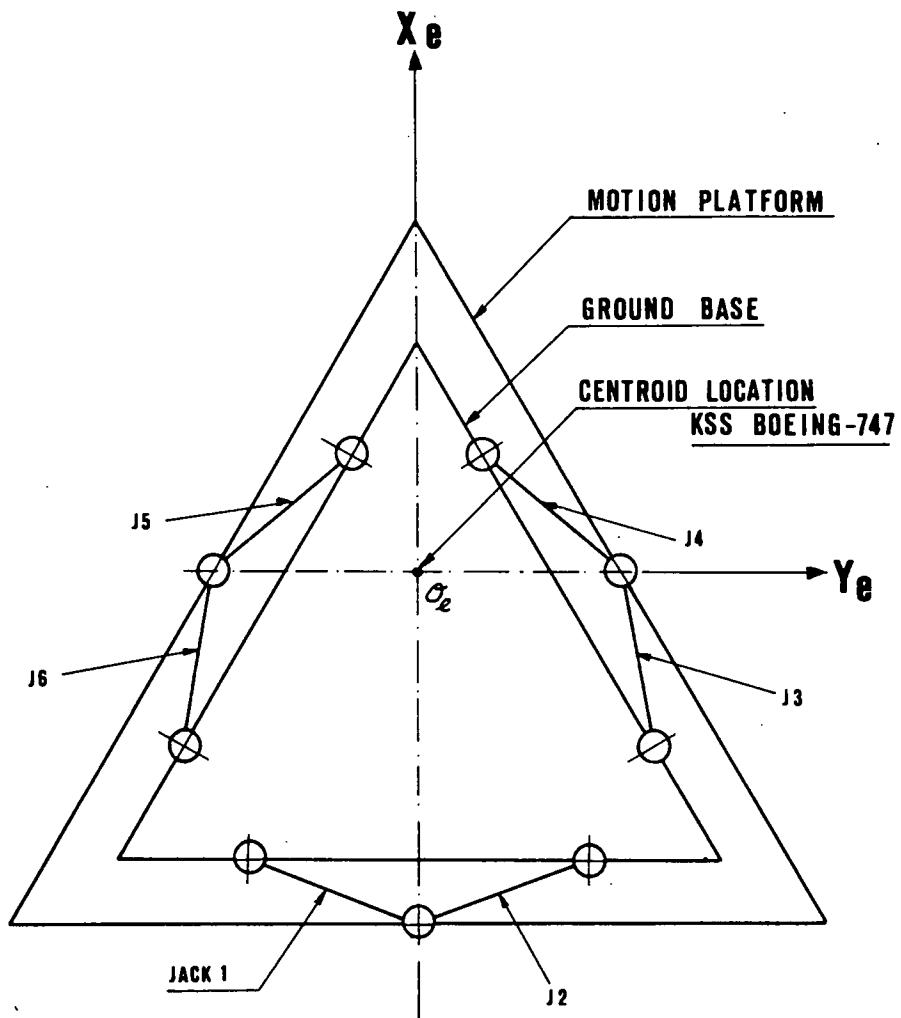


FIG. 4 ARRANGEMENT OF THE KSS BOEING-747 MOTION SYSTEM,
DEFINING THE $\sigma_e X_e Y_e Z_e$ - REFERENCE FRAME AND THE CENTROID LOCATION

Appendix A. Scaled equations as used in the KSS Boeing 747 Main Motion Simulation Program.

The scaled equations of the KSS Boeing 747 Main Motion Simulation Program in the sequence as followed by the digital computer are given below. The parameters used in the software are summarized in Table 2.

Computations in behalf of the specific forces, see section 4; on ground:

$$\dot{u}_b = r_b \cdot v_b = \frac{F_{x_b}}{W} \cdot g$$
$$\frac{\dot{u}_b - r_b \cdot v_b}{10} = (\frac{F_{x_b}}{W \cdot 1,748}) \cdot \frac{1,748}{10} \cdot 9,81$$

$$UBD = MFXWB \cdot KXU1$$

Off ground:

$$UWD = MFXWB \cdot KXU1$$

$$KXU1 = K SCALE = \frac{1,748}{10} \cdot 9,81 = 1,71479 = 0,428697 SALD 3. *$$

On ground:

$$\dot{v}_b + r_b \cdot u_b - p_b \cdot w_b = \frac{F_{y_b}}{W} \cdot g$$
$$\frac{\dot{v}_b + r_b \cdot u_b - p_b \cdot w_b}{8} = \frac{F_{y_b}}{W \cdot 2} \cdot \frac{2}{8} \cdot 9,81$$

$$VBDM = MFYWB \cdot KYV1$$

Off ground:

$$VWD = MFYWB \cdot KYV1$$

$$KYV1 = K SCALE = \frac{2}{8} \cdot 9,81 = 2,4525 = 0,613124 SALD 3.$$

On ground:

$$\dot{w}_b - q_b \cdot u_b + p_b \cdot v_b = \frac{F_{z_b}}{W} \cdot g$$
$$\frac{\dot{w}_b - q_b \cdot u_b + p_b \cdot v_b}{40} = (\frac{F_{z_b}}{W \cdot 6}) \cdot \frac{6}{40} \cdot 9,81$$

$$WBD = MFZWB \cdot KZW1$$

Off ground:

$$WWD = MFZWB \cdot KZW1$$

* Note: SALD 3 means arithm. left shift double (3 = z^2 effectively).

$$KZW1 = K \text{ SCALE} = \frac{6}{40} \cdot 9,81 = 1,4715 = 0,367875 \text{ SALD } 3.$$

The above computations are performed by means of LOOP 1 and 2 in part 1 of KSS Boeing 747 Main Motion Simulation, see line 41 of Appendix B, part 1.

Wind- to body-axes transformation of UWD, VWD and WWD, when the aircraft is off-ground, see section 3:

$$\begin{aligned} UBD &= UWD \cdot \cos \alpha_b \cdot \cos \beta - VWD \cdot \cos \alpha_b \cdot \sin \beta - WWD \cdot \sin \alpha_b \\ \frac{UBD}{10} &= \frac{UWD}{10} \cdot \frac{\cos \alpha_b}{1} \cdot \frac{\cos \beta}{1} - \frac{1}{10} \cdot \left(\frac{VWD}{8}\right) \cdot 8 \cdot \frac{\cos \alpha_b}{1} \cdot \frac{\sin \beta}{1} - \frac{1}{10} \cdot \left(\frac{WWD}{40}\right) \cdot \\ &\quad \cdot 40 \cdot \frac{\sin \alpha_b}{1} \end{aligned}$$

$$\overline{UBD} = \overline{UWD} \cdot VCSAB \cdot VCSB - \overline{VWD} \cdot VCSAB \cdot VSNB \cdot KUBBD - \overline{WWD} \cdot VSNAB \cdot 4$$

$$KUBBD = \frac{8}{10} = 0,8, \text{ see line 81 of Appendix B.}$$

$$VBDM = UWD \cdot \sin \beta + VWD \cdot \cos \beta$$

$$\frac{VBDM}{8} = \frac{1}{8} \cdot \left(\frac{UWD}{10}\right) \cdot 10 \cdot \frac{\sin \beta}{1} + \frac{VWD}{8} \cdot \frac{\cos \beta}{1}$$

$$\overline{VBDM} = \overline{UWD} \cdot VSNB \cdot KVBBB + \overline{VWD} \cdot VCSB$$

$$KVBBB = \frac{10}{8} = 1,25 = 0,625 \text{ SALD } 2, \text{ see line 98 and 99 of Appendix B, part 1}$$

$$WBD = UWD \cdot \sin \alpha_b \cdot \cos \beta - VWD \cdot \sin \alpha_b \cdot \sin \beta + WWD \cdot \cos \alpha_b$$

$$\begin{aligned} \frac{WBD}{40} &= \frac{1}{40} \cdot \left(\frac{UWD}{10}\right) \cdot 10 \cdot \frac{\sin \alpha_b}{1} \cdot \frac{\cos \beta}{1} - \frac{1}{40} \cdot \left(\frac{VWD}{8}\right) \cdot 8 \cdot \frac{\sin \alpha_b}{1} \cdot \frac{\sin \beta}{1} + \\ &\quad + \frac{WWD}{40} \cdot \frac{\cos \alpha_b}{1} \end{aligned}$$

$$\overline{WBD} = \overline{UWD} \cdot VSNAB \cdot VCSB \cdot KWBBB1 - \overline{VWD} \cdot VSNAB \cdot VSNB \cdot KWBBB2 + \overline{WWD} \cdot VS$$

$$KWBBB1 = \frac{10}{40} = 0,25, \text{ see line 120 of Appendix B, part 1.}$$

$$KWBBB2 = \frac{8}{40} = 0,2, \text{ see line 129 of Appendix B, part 1.}$$

To avoid discontinuity problems during the transition from on- to off-ground, the calculation is stopped for 1 sec in case of a condition change see line 141 of Appendix B, part 1.

Pitch acceleration, see section 9.1:

$$\zeta_{\theta_{hp}} = 0,7$$

$$\tau_{\theta_{hp}} = 6 \text{ sec.}$$

$$S_{\dot{q}_b, hp} = 2 \text{ rad/sec}^2$$

$$S_{q_b, hp} = 1 \text{ rad/sec}$$

$$S_{\theta_{hp}} = 1 \text{ rad}$$

$$S_{\dot{q}_b} = 2 \text{ rad/sec}^2$$

$$\dot{q}_{b,h_p} = \dot{q}_b - \frac{2\zeta_{\theta_{hp}}}{\tau_{\theta_{hp}}} \cdot q_{b,h_p} - \frac{1}{\tau_{\theta_{hp}}^2} \cdot \theta_{hp}$$

$$\frac{\dot{q}_{b,h_p}}{2} = \frac{\dot{q}_b}{2} - \frac{2\zeta_{\theta_{hp}}}{2\tau_{\theta_{hp}}} \cdot \frac{q_{b,h_p}}{1} - \frac{1}{2\tau_{\theta_{hp}}^2} \cdot \frac{\theta_{hp}}{1}$$

$$MPITCHDD = VPRD - (KP1 \cdot MPITCHDM + KP2 \cdot MPITCHM)$$

$$KP1 = \frac{2\zeta_{\theta_{hp}}}{2\tau_{\theta_{hp}}} = \frac{2 \cdot 0,7}{2 \cdot 6} = 0,11666 \text{ (line 359)}$$

$$KP2 = \frac{1}{2\tau_{\theta_{hp}}^2} = \frac{1}{2 \cdot 36} = 0,01388 \text{ (line 360)}$$

Rectangular integration:

$$q_{b,h_p} = q_{b,h_p} + 0,05 \cdot \dot{q}_{b,h_p}$$

$$\frac{q_{b,h_p}}{1} = \frac{q_{b,h_p}}{1} + \frac{0,05}{1} \cdot \left(\frac{\dot{q}_{b,h_p}}{2} \right) \cdot 2$$

$$MPITCHDM = MPITCHDM + KP3 \cdot MPITCHDD$$

$$KP3 = \frac{0,05}{1} \cdot 2 = 0,1$$

$$\theta_{h_p} = \theta_{h_p} + 0,05 \cdot a_{b,h_p}$$

$$\frac{\theta_{h_p}}{1} = \frac{\theta_{h_p}}{1} + \frac{0,05}{1} \cdot \frac{a_{b,h_p}}{1}$$

MPITCHM = MPITCHM + KP4 . MPITCHDM

$$KP4 = \frac{0,05}{1} = 0,05$$

Roll acceleration, see section 9.2:

$$\zeta_{\phi_{h_p}} = 0,7$$

$$\tau_{\phi_{h_p}} = 6 \text{ sec}$$

$$S_{p_b,h_p} = 4 \text{ rad/sec}^2$$

$$S_{p_b,h_p} = 2 \text{ rad/sec}$$

$$S_{\dot{\phi}_{h_p}} = 2 \text{ rad}$$

$$S_{\ddot{p}_b} = 4 \text{ rad/sec}^2$$

$$\dot{p}_{b,h_p} = \dot{p}_b - \frac{2\zeta_{\phi_{h_p}}}{\tau_{\phi_{h_p}}} \cdot p_{b,h_p} - \frac{1}{\tau_{\phi_{h_p}}^2} \cdot \dot{\phi}_{h_p}$$

$$\frac{\dot{p}_{b,h_p}}{4} = \frac{\dot{p}_b}{4} - \frac{2\zeta_{\phi_{h_p}}}{4\tau_{\phi_{h_p}}} \cdot \left(\frac{p_{b,h_p}}{2}\right) \cdot 2 - \frac{1}{4\tau_{\phi_{h_p}}^2} \cdot \left(\frac{\dot{\phi}_{h_p}}{2}\right) \cdot 2$$

MROLLDD = VRRD - (KR1 . MROLLDM + KR2 . MROLLM)

$$KR1 = \frac{2\zeta_{\phi_{h_p}}}{4\tau_{\phi_{h_p}}} \cdot 2 = \frac{2 \cdot 0,7 \cdot 2}{4 \cdot 6} = 0,11666$$

$$KR2 = \frac{1}{4\tau_{\phi_{h_p}}^2} \cdot 2 = \frac{2}{4 \cdot 36} = 0,01388$$

Rectangular integration:

$$p_{b,h_p} = p_{b,h_p} + 0,05 \dot{p}_{b,h_p}$$

$$\frac{p_{b,h_p}}{2} = \frac{p_{b,h_p}}{2} + \frac{0,05}{2} \cdot (\frac{\dot{p}_{b,h_p}}{4}) \cdot 4$$

$$MROLLDM = MROLLDM + KR3 \cdot MROLLDD$$

$$KR3 = \frac{0,05}{2} \cdot 4 = 0,1$$

$$\phi_{h_p} = \phi_{h_p} + 0,05 p_{b,h_p}$$

$$\frac{\phi_{h_p}}{2} = \frac{\phi_{h_p}}{2} + \frac{0,05}{2} \cdot (\frac{p_{b,h_p}}{2}) \cdot 2$$

$$MROLLM = MROLLM + KR4 \cdot MROLLDM$$

$$KR4 = \frac{0,05}{2} \cdot 2 = 0,05$$

Yaw acceleration, see section 9.3:

$$\zeta_\psi = 0,7$$

$$\tau_\psi = 1,5 \text{ sec}$$

$$S_{\dot{r}_{b,h_p}} = 2 \text{ rad/sec}^2$$

$$S_{r_{b,h_p}} = 1 \text{ rad/sec}$$

$$S_{\psi_{h_p}} = 1 \text{ rad}$$

$$S_{\dot{r}_b} = 2 \text{ rad/sec}^2$$

$$\dot{r}_{b,h_p} = \dot{r}_b - \frac{2\zeta_\psi}{\tau_\psi} \cdot r_{b,h_p} - \frac{1}{\tau_\psi^2} \cdot \psi_{h_p}$$

$$\frac{\dot{r}_{b,h_p}}{2} = \frac{\dot{r}_b}{2} - \frac{2\zeta_\psi}{2\tau_\psi} \cdot \frac{r_{b,h_p}}{1} - \frac{1}{2\tau_\psi^2} \cdot \frac{\psi_{h_p}}{1}$$

$$MYAWDD = VHRD - (KJ1 \cdot MYAWDM + KJ2 \cdot MYAWM)$$

$$KJ1 = \frac{2\zeta_\psi}{2\tau_\psi} = \frac{2 \cdot 0,7}{2 \cdot 1,5} = 0,233332 \cdot 2 \text{ (line 377)}$$

$$KJ2 = \frac{1}{2\tau_\psi^2} = \frac{1}{2 \cdot 2,25} = 0,05552 \cdot 4 \text{ (line 378)}$$

Rectangular integration:

$$r_{b,h_p} = r_{b,h_p} + 0,05 \dot{r}_{b,h_p}$$

$$\frac{r_{b,h_p}}{1} = \frac{r_{b,h_p}}{1} + \frac{0,05}{1} \cdot (\frac{\dot{r}_{b,h_p}}{2}) \cdot 2$$

$$MYAWDM = MYAWDM + KJ3 \cdot MYAWDD$$

$$KJ3 = \frac{0,05}{1} \cdot 2 = 0,1$$

$$\psi_{h_p} = \psi_{h_p} + 0,05 \cdot r_{b,h_p}$$

$$\frac{\psi_{h_p}}{1} = \frac{\psi_{h_p}}{1} + \frac{0,05}{1} \cdot \frac{r_{b,h_p}}{1}$$

$$MYAWM = MYAWM + KJ4 \cdot MYAWDM$$

$$KJ4 = \frac{0,05}{1} = 0,05$$

Specific force errors, see section 9.1. and 9.2.:

$$\dot{x}_{b,2} = -g \cdot \theta_{h_p}$$

$$\frac{\dot{x}_{b,2}}{10} = \frac{-g}{10} \cdot \frac{\theta_{h_p}}{1}$$

$$MXDD = KX1 \cdot MPITCHM$$

The program value of KX1 has been adjusted to:

$$KX1 = -0,12 \text{ (see line 380 of Appendix B, part 1)}$$

to prevent the motion platform from running into its longitudinal position limits.

$$\dot{y}_{b,2} = +g \cdot \phi_{h_p}$$

$$\frac{\dot{y}_{b,2}}{8} = \frac{+g}{8} \cdot (\frac{\phi_{h_p}}{2}) \cdot 2$$

$$MYDD = KY1 \cdot MROLLM$$

For the same reason, KY1 has been adjusted to:

$$KY1 = 0,3 \text{ (see line 381).}$$

Centroid transformation, see section 5:

$$\dot{u}_{b,c} = \dot{u}_b - r_b \cdot v_b - (q_b^2 + r_b^2) \cdot R_x$$

$$\frac{\dot{u}_{b,c}}{10} = \frac{\dot{u}_b - r_b \cdot v_b - (q_b^2 + r_b^2)}{10} \cdot \frac{R_x}{10}$$

$$UBCD = UBD - (VPR \cdot VPR + VHR \cdot VHR) \cdot KUBC$$

$$KUBC = \frac{25,9}{10} = 2,59 = 0,6475 \text{ SALD 3 (line 353)}$$

$$\dot{v}_{b,c} = \dot{v}_b + r_b \cdot u_b - p_b \cdot w_b + (p_b \cdot q_b + t_b) \cdot R_x$$

$$\frac{\dot{v}_{b,c}}{8} = \frac{\dot{v}_b + r_b \cdot u_b - p_b \cdot w_b}{8} + (\frac{p_b}{2} \cdot 2 \cdot \frac{q_b}{1} + \frac{t_b}{2} \cdot 2) \cdot \frac{R_x}{8}$$

$$VBCD = VBDM + (VRR \cdot VPR + VHRD) \cdot KVBC$$

$$KVBC = \frac{25,9 \cdot 2}{8} = 6,475 = 0,8094 \text{ SALD 4 (line 354)}$$

$$\dot{w}_{b,c} = \dot{w}_b - q_b \cdot u_b + p_b \cdot v_b + (p_b \cdot r_b - \dot{q}_b) \cdot R_x$$

$$\frac{\dot{w}_{b,c}}{40} = \frac{\dot{w}_b - q_b \cdot u_b + p_b \cdot v_b}{40} + (\frac{p_b}{2} \cdot 2 \cdot \frac{r_b}{1} - \frac{\dot{q}_b}{2} \cdot 2) \cdot \frac{R_x}{40}$$

$$WBCD = WBD + (VRR \cdot VHR - VPRD) \cdot KWBC$$

$$KWBC = \frac{2 \cdot 25,9}{40} = 1,295 = 0,6475 \text{ SALD 2 (line 355)}$$

LONGITUDINAL SPECIFIC FORCE.

Longitudinal highpass filter, see section 6.1.:

$$\zeta_x = 0,7$$

$$\tau_x = 0,7$$

$$S_{\ddot{x}} = 10 \text{ m/sec}^2$$

$$S_x = 10 \text{ m/sec}$$

$$S_{\dot{x}} = 11,3952 \text{ m}$$

$$S_{\ddot{u}_{b,c}} = 10 \text{ m/sec}^2$$

$$\ddot{x}_{b,1} = \dot{u}_{b,c} - g \cdot \theta_{1,p} - \frac{2\zeta_x}{\tau_x} \cdot \dot{x}_{b,1} - \frac{1}{\tau_x^2} \cdot x_{b,1} \quad (6.3.)$$

$$\frac{\ddot{x}_{b,1}}{10} = \frac{\dot{u}_{b,c}}{10} - \frac{g}{10} \cdot \frac{\theta_{1,p}}{1} - \frac{2}{10} \cdot \frac{\zeta_x}{\tau_x} \cdot (\frac{\dot{x}_{b,1}}{10}) \cdot 10 - \frac{1}{10\tau_x^2} \cdot (\frac{x_{b,1}}{11,3952}) \cdot 11,3952$$

$$BXDD = UBCD - BPITCHM - KX10 \cdot BXDM - KX11 \cdot BXM$$

$$KX10 = \frac{2}{10} \cdot \frac{0,7}{0,7} \cdot 10 = 2 = 0,9999 \text{ SALD 2 (line 482)}$$

$$KX11 = \frac{11,3952}{10 \cdot 0,49} = 2,3255 = 0,581377 \text{ SALD 3 (line 358)}$$

Rectangular integration:

$$\dot{x}_{b,1} = \dot{x}_{b,1} + 0,05 \dot{x}_{b,1}$$

$$\frac{\dot{x}_{b,1}}{10} = \frac{\dot{x}_{b,1}}{10} + \frac{0,05}{10} \cdot \left(\frac{\dot{x}_{b,1}}{10} \right) \cdot 10$$

$$BXDM = BXDM + KX12 \cdot BXDD$$

$$KX12 = \frac{0,05}{10} \cdot 10 = 0,05$$

$$x_{b,1} = x_{b,1} + 0,05 \dot{x}_{b,1}$$

$$\frac{x_{b,1}}{11,3952} = \frac{x_{b,1}}{11,3952} + \frac{0,05}{11,3952} \cdot \left(\frac{\dot{x}_{b,1}}{10} \right) \cdot 10$$

$$BXM = BXM + KX13 \cdot BXDM$$

$$KX13 = \frac{0,05 \cdot 10}{11,3952} = 0,043877$$

Longitudinal low-pass filter, see section 9.1.

$$\zeta_{\theta_1 p} = 0,7$$

$$\tau_{\theta_1 p} = 2 \text{ sec}$$

$$S_{q_{b,1p}} = 1 \text{ rad/sec}^2$$

$$S_{\dot{q}_{b,1p}} = 1 \text{ rad/sec}$$

$$S_{\theta_1 p} = 1 \text{ rad}$$

$$S_{\dot{u}_{b,c}} = 10 \text{ m/sec}^2$$

$$\ddot{q}_{b,1p} = \frac{\dot{q}_{b,c}}{\tau_{\theta_1 p}^2 \cdot g} + \frac{\sin \theta}{\tau_{\theta_1 p}^2} - \frac{2\zeta_{\theta_1 p}}{\tau_{\theta_1 p}^2} \cdot q_{b,1p} - \frac{1}{\tau_{\theta_1 p}^2} \cdot \theta_1 p \quad (9.3.)$$

$$\frac{\dot{q}_{b,1p}}{1} = \frac{1}{\tau_{\theta_1 p}^2 \cdot g} \cdot \left(\frac{\dot{u}_{b,c}}{10} \right) \cdot 10 + \frac{\sin \theta}{1 \cdot \tau_{\theta_1 p}^2} - \frac{2\zeta_{\theta_1 p}}{\tau_{\theta_1 p}^2} \cdot \frac{q_{b,1p}}{1} - \frac{1}{\tau_{\theta_1 p}^2} \cdot \frac{\theta_1 p}{1}$$

BPITCHDD = KP13 . UBCD + KP14 . VSNPB - KP15 . BPITCHDM - KP16 . BPITCHM

$$KP13 = \frac{10}{4 \cdot 10} = 0,25 \text{ (line 361)}$$

$$KP14 = \frac{1}{4} = 0,25 \text{ (line 362)}$$

$$KP15 = \frac{2 + 0,7}{2} = 0,7 \text{ (line 363)}$$

$$KP16 = \frac{1}{4} = 0,25 \text{ (line 364)}$$

Rectangular integration of $q_{b,1_p}$:

$$q_{b,1_p} = q_{b,1_p} + 0,05 q_{b,1_p}$$

$$\frac{q_{b,1_p}}{1} = \frac{q_{b,1_p}}{1} + \frac{0,05}{1} \cdot \frac{q_{b,1_p}}{1}$$

BPITCHDM = BPITCHDM + KP17 . BPITCHDD

$$KP17 = 0,05$$

$$\theta_{1_p} = \theta_{1_p} + 0,05 q_{b,1_p}$$

$$\frac{\theta_{1_p}}{1} = \frac{\theta_{1_p}}{1} + \frac{0,05}{1} \cdot \frac{q_{b,1_p}}{1}$$

BPITCHM = BPITCHM + KP18 . BPITCHDM

$$KP18 = 0,05$$

Remark: BXDD and BPITCHDD are forced to hold their momentary values for 1 sec, when the aircraft condition changes from on- to off ground and from off- to on ground, see page A-2.

LATERAL SPECIFIC FORCE

Lateral high-pass filter, see section 6.2.:

$$\zeta_y = 0,7$$

$$\tau_y = 1 \text{ sec}$$

$$S_{\dot{y}_{b,1}} = 8 \text{ m/sec}^2$$

$$S_{y_{b,1}} = 10 \text{ m/sec}$$

$$S_y = 11,3952 \text{ m}$$

$$S_{\dot{v}_{b,c}} = 8 \text{ m/sec}^2$$

$$\dot{y}_{b,1} = \dot{v}_{b,c} - g \cdot \cos \theta \cdot \sin \phi + g \cdot \phi_{1p} - \frac{2\zeta_y}{\tau_y} \cdot \dot{y}_{b,1} - \frac{1}{\tau_y^2} \cdot y_{b,1} \quad (6.7)$$

$$\frac{\dot{y}_{b,1}}{8} = \frac{\dot{v}_{b,c}}{8} - \frac{g}{8} \cdot \frac{\cos \theta}{1} \cdot \frac{\sin \phi}{1} + \frac{g}{8} \cdot \frac{\phi_{1p}}{1} - \frac{2}{8} \cdot \frac{\zeta_y}{\tau_y} \cdot \left(\frac{\dot{y}_{b,1}}{10}\right) \cdot 10 +$$

$$- \frac{1}{8\tau_y^2} \cdot \left(\frac{\dot{y}_{b,1}}{11,3952}\right) \cdot 11,3952$$

BYDD = VBCD - KR28 . VCSPB . VSNRB + KR12 . BROLLM - KY10 . BYDM +
- KY11 . BYM

$$KR28 = \frac{g}{8} \cdot \frac{1}{1} = 1,25 = 0,625 \text{ SALD 2 (line 371)}$$

KR12 = $\frac{g}{8} \cdot \frac{1}{1} = 1,25$. In Appendix B: KR12 has been experimentally reduced
to $\frac{1,25}{2} = 0,625$ (line 367)

$$KY10 = \frac{2}{8} \cdot \frac{07}{1} \cdot 10 = 1,750 = 0,875 \text{ SALD 2 (line 365)}$$

$$KY11 = \frac{1}{8} \cdot \frac{1}{1} \cdot 11,3952 = 1,4244 = 0,7122 \text{ SALD 2 (line 366)}$$

Rectangular integration:

$$\dot{y}_{b,1} = \dot{y}_{b,1} + 0,05 \dot{y}_{b,1}$$

$$\frac{\dot{y}_{b,1}}{10} = \frac{\dot{y}_{b,1}}{10} + \frac{0,05}{10} \cdot \left(\frac{\dot{y}_{b,1}}{8}\right) \cdot 8$$

$$BYDM = BYDM + KY12 \cdot BYDD$$

$$KY12 = \frac{0,05}{10} \cdot 8 = 0,04$$

$$y_{b,1} = y_{b,1} + 0,05 \dot{y}_{b,1}$$

$$\frac{y_{b,1}}{11,3952} = \frac{y_{b,1}}{11,3952} + \frac{0,05}{11,3952} \cdot \left(\frac{\dot{y}_{b,1}}{10}\right) \cdot 10$$

$$BYM = BYM + KY13 \cdot BYDM$$

$$KY13 = \frac{0,05 \cdot 10}{11,3952} = 0,043878$$

Lateral low-pass filter, see section 9.2.:

$$\zeta_{\phi_{1p}} = 0,7$$

$$\tau_{\phi_{1p}} = 2 \text{ sec}$$

$$S_{\phi_{1p}} = 2 \text{ rad/sec}^2$$

$$S_{p_b,1_p} = 1 \text{ rad/sec}$$

$$S_{\phi_1 p} = 1 \text{ rad}$$

$$S_{v_b,c} = 8 \text{ m/sec}^2$$

$$\dot{p}_{b,1_p} = -\frac{\dot{v}_{b,c}}{\tau_{\phi_1 p}^2 \cdot g} + \frac{\cos \theta \cdot \sin \phi}{\tau_{\phi_1 p}^2} - \frac{2\zeta_{\phi_1 p}}{\tau_{\phi_1 p}^2} \cdot p_{b,1_p} - \frac{1}{\tau_{\phi_1 p}^2} \cdot \phi_{1_p} \quad (9.9.)$$

$$\frac{\dot{p}_{b,1_p}}{2} = -\frac{1}{2\tau_{\phi_1 p}^2 \cdot g} \cdot (\frac{\dot{v}_{b,c}}{8})_8 + \frac{1}{2\tau_{\phi_1 p}^2} \cdot \frac{\cos \theta}{1} \cdot \frac{\sin \phi}{1} - \frac{2\zeta_{\phi_1 p}}{2\tau_{\phi_1 p}^2} \cdot$$

$$\cdot \frac{p_{b,1_p}}{1} - \frac{1}{2\tau_{\phi_1 p}^2} \cdot \frac{\phi_{1_p}}{1}$$

$$\text{BROLLDD} = -(\text{KR13} \cdot \text{VBCD} + \text{KR14} \cdot \text{VCSPB} \cdot \text{VSNRB} + \text{KR15} \cdot \text{BROLLIM} + \text{KR16} \cdot \text{BROLLM}).$$

$$\text{KR13} = \frac{1}{2.4.10} \cdot 8 = 0,1$$

$$\text{KR14} = -\frac{1}{2.4} = -0,125 \text{ (line 368)}$$

$$\text{KR15} = \frac{2 \cdot 0,7}{2.2} = 0,35 \text{ (line 369)}$$

$$\text{KR16} = \frac{1}{2.4} = 0,125 \text{ (line 370)}$$

Rectangular integration:

$$p_{b,1_p} = p_{b,1_p} + 0,05 \dot{p}_{b,1_p}$$

$$\frac{p_{b,1_p}}{1} = \frac{p_{b,1_p}}{1} + \frac{0,05}{1} \cdot (\frac{\dot{p}_{b,1_p}}{2}) \cdot 2$$

$$\text{BROLLIM} = \text{BROLLIM} + \text{KR17} \cdot \text{BROLLDD}.$$

$$\text{KR17} = \frac{0,05}{1} \cdot 2 = 0,1$$

$$\phi_{1_p} = \phi_{1_p} + 0,05 p_{b,1_p}$$

$$\frac{\phi_{1_p}}{1} = \frac{\phi_{1_p}}{1} + \frac{0,05}{1} \cdot \frac{p_{b,1_p}}{1}$$

$$\text{BROLLM} = \text{BROLLM} + \text{KR18} \cdot \text{BROLLIM}$$

KR18 = 0,05

Vertical high-pass filter, see section 6.3.:

$$\zeta_z = 0,7$$

$$\tau_z = 0,7$$

$$S_{\dot{z}_b} = 40 \text{ m/sec}^2$$

$$S_{\dot{z}_b} = 10 \text{ m/sec}$$

$$S_{z_b} = 49,854 \text{ m}$$

$$S_{\dot{w}_{b,c}} = 40 \text{ m/sec}^2$$

$$\ddot{z}_b = \dot{w}_{b,c} - \frac{2\zeta_z}{\tau_z} \cdot \dot{z}_b - \frac{1}{\tau_z^2} \cdot z_b \quad (6.11.)$$

$$\frac{\ddot{z}_b}{40} = \frac{\dot{w}_{b,c}}{40} - \frac{2}{40} \cdot \frac{\zeta_z}{\tau_z} \cdot \left(\frac{\dot{z}_b}{10}\right) \cdot 10 - \frac{1}{40\tau_z^2} \cdot \left(\frac{z_b}{49,854}\right) \cdot 49,854$$

$$BZDD = WBCD - KZ1 \cdot BZDM - KZ2 \cdot BZM$$

$$KZ1 = \frac{2}{40} \cdot \frac{0,7}{0,7} \cdot 10 = 0,5 \quad (\text{line 694})$$

$$KZ2 = \frac{49,854}{40 \cdot 0,7^2} = 2,54356 = 0,63589 \text{ SALD 3 (line 382)}$$

Rectangular integration:

$$\dot{z}_b = \dot{z}_b + 0,05 \cdot \ddot{z}_b$$

$$\frac{\dot{z}_b}{10} = \frac{\dot{z}_b}{10} + \frac{0,05}{10} \cdot \left(\frac{\dot{z}_b}{40}\right) \cdot 40$$

$$BZDM = BZDM + KZ3 \cdot BZDD$$

$$KZ3 = \frac{0,05}{10} \cdot 40 = 0,2$$

$$z_b = z_b + 0,05 \cdot \dot{z}_b$$

$$\frac{z_b}{49,854} = \frac{z_b}{49,854} + \frac{0,05}{49,854} \cdot \left(\frac{\dot{z}_b}{10}\right) \cdot 10$$

$$BZM = BZM + KZ4 \cdot BZDM$$

$$KZ4 = \frac{0,05 \cdot 10}{49,854} = 0,0100294$$

KSS Boeing 747 Main motion simulation, part 2:

Sum of body-axes rotational accelerations, see sections 9.1., 9.2. and 12.

$$\dot{q}_s = \dot{q}_{b,1_p} + \dot{q}_{b,h_p} \quad (9.5.)$$

$$\frac{\dot{q}_s}{2} = \frac{\dot{q}_{b,1_p}}{2} + \left(\frac{\dot{q}_{b,h_p}}{2} \right) \cdot 2$$

SPITCHDD = BPITCHDD + KP26 . MPITCHDD

KP26 = 2 (see line 41 of Appendix B, part 2)

$$\dot{p}_s = \dot{p}_{b,1_p} + \dot{p}_{b,h_p} \quad (9.10.)$$

$$\frac{\dot{p}_s}{2} = \frac{\dot{p}_{b,1_p}}{2} + \frac{\dot{p}_{b,h_p}}{2}$$

SROLLDD = BROLLDD + MROLLDD

Sum of body-axes rotational rates, see sections 9.1., 9.2. and 10.

$$q_s = q_{b,1_p} + q_{b,h_p} \quad (9.6.)$$

$$\frac{q_s}{1} = \frac{q_{b,1_p}}{1} + \frac{q_{b,h_p}}{1}$$

SPITCHDM = BPITCHDM + MPITCHDM

$$p_s = p_{b,1_p} + p_{b,h_p} \quad (9.11.)$$

$$\frac{p_s}{1} = \frac{p_{b,1_p}}{1} + \frac{p_{b,h_p}}{1}$$

SROLLDM = BROLLDM + MROLLDM

Euler rates, see section 10:

$$\dot{\theta}_i = q_s \cdot \cos \phi_m - r_{b,h_p} \cdot \sin \phi_m$$

$$\frac{\dot{\theta}_i}{1} = \frac{q_s}{1} \cdot \frac{\cos \phi_m}{1} - \frac{r_{b,h_p}}{1} \cdot \frac{\sin \phi_m}{1}$$

MPITCHSD = SPITCHDM . cos(MROLLSM) - MYAWDM . sin(MROLLSM)

$$\dot{\phi}_i = p_s + q_s \cdot \sin \phi_m \cdot \frac{\sin \theta_m}{\cos \theta_m} + r_{b,h_p} \cdot \cos \phi_m \cdot \frac{\sin \theta_m}{\cos \theta_m}$$

$$\frac{\dot{\phi}_i}{1} = \frac{p_s}{1} + \frac{q_s}{1} \cdot \frac{\sin \phi_m}{1} \cdot \frac{\sin \theta_m}{\cos \theta_m} + \frac{r_{b,h_p}}{1} \cdot \frac{\cos \phi_m}{1} \cdot \frac{\sin \theta_m}{\cos \theta_m}$$

$$MROLLSD = SROLLDM + SPITCHDM \cdot \sin(MROLLSM) \cdot \sin(MPITCHSM)$$

$$/\cos(MPITCHSM) + MYAWDM \cdot \cos(MROLLSM) \cdot \sin(MPITCHSM)$$

$$/\cos(MPITCHSM).$$

$$\dot{\psi}_i = q_s \cdot \frac{\sin \phi_m}{\cos \theta_m} + r_b, h_p \cdot \frac{\cos \phi_m}{\cos \theta_m}$$

$$\frac{\dot{\psi}_i}{T} = \frac{q_s}{T} \cdot \frac{\sin \phi_m}{\cos \theta_m} + \frac{r_b, h_p}{T} \cdot \frac{\cos \phi_m}{\cos \theta_m}$$

$$MYAWSD = SPITCHDM \cdot \sin(MROLLSM)/\cos MPITCHSM + MYAWDM \cdot \cos(MROLLSM)$$

$$/\cos MPITCHSM.$$

Return to ground check: When the simulated aircraft is returned to ground by means of the "return to ground button" on the instructor's console, the following variables in the motion program are set to zero:

$$\dot{\theta}_i, \dot{\theta}_m \text{ and } \theta_m$$

$$\dot{\phi}_i, \dot{\phi}_m \text{ and } \phi_m$$

$$\dot{\psi}_i, \dot{\psi}_m \text{ and } \psi_m,$$

see Appendix B, part 2, line 142 - 157.

Rotational washout, see section 11:

$$\text{Pitch: } \tau_{\theta_R} = 200 \text{ sec}$$

$$S_{\theta_m} = 1 \text{ rad.}$$

$$\dot{\theta}_m = \dot{\theta}_i - \frac{1}{\tau_{\theta_R}} \cdot \theta_m$$

$$\frac{\dot{\theta}_m}{T} = \frac{\dot{\theta}_i}{T} - \frac{1}{\tau_{\theta_R}} \cdot \frac{\theta_m}{T}$$

$$MPITCHMD = MPITCHSD - KP24 \cdot MPITCHSM$$

$$KP24 = \frac{1}{200} = 0,005$$

Rectangular integration:

$$\theta_m = \theta_m + 0,05 \dot{\theta}_m$$

$$\frac{\theta_m}{T} = \frac{\theta_m}{T} + \frac{0,05}{T} \cdot \frac{\dot{\theta}_m}{T}$$

$$MPITCHSM = MPITCHSM + KP18 \cdot MPITCHMD$$

$$KP18 = 0,05$$

Motion system lead compensation, see section 12:

$$\theta_c = \theta_m + B_4 \cdot \dot{\theta}_m + A_4 \cdot \ddot{\theta}_s$$

$$\frac{\theta_c}{T} = \frac{\theta_m}{T} + B_4 \cdot \frac{\dot{\theta}_m}{T} + A_4 \cdot \frac{\ddot{\theta}_s}{T}$$

$$MPITCHC = MPITCHSM + KP19 \cdot MPITCHMD + KP20 \cdot SPITCHDD$$

$$KP19 = 0,28$$

$$KP20 = 0,044$$

Roll:

$$\tau_{\phi_R} = 200 \text{ sec}$$

$$S_{\phi_m} = 1 \text{ rad.}$$

$$\dot{\phi}_m = \dot{\phi}_i - \frac{1}{\tau_{\phi_R}} \cdot \phi_m$$

$$\frac{\dot{\phi}_m}{T} = \frac{\dot{\phi}_i}{T} - \frac{1}{\tau_{\phi_R}} \cdot \frac{\phi_m}{T}$$

$$MROLLMD = MROLLSD - KR23 \cdot MROLLSM$$

$$KR23 = \frac{1}{200} = 0,005$$

Rectangular integration:

$$\phi_m = \phi_m + 0,05 \cdot \dot{\phi}_m$$

$$\frac{\phi_m}{T} = \frac{\phi_m}{T} + \frac{0,05}{1} \cdot \frac{\dot{\phi}_m}{T}$$

$$MROLLSM = MROLLSM + KR18 \cdot MROLLMD$$

$$KR18 = 0,05$$

Motion system lead compensation:

$$\phi_c = \phi_m + B_5 \cdot \dot{\phi}_m + A_5 \cdot \ddot{\phi}_s$$

$$\frac{\phi_c}{T} = \frac{\phi_m}{T} + B_5 \cdot \frac{\dot{\phi}_m}{T} + A_5 \cdot \left(\frac{\ddot{\phi}_s}{2}\right) \cdot 2$$

$$MROLLC = MROLLSM + KR19 \cdot MROLLMD + KR20 \cdot SROLLDD$$

$$KR19 = 0,28$$

$$KR20 = 0,044 \cdot 2 = 0,088$$

Yaw:

$$\tau_{\psi_R} = 20 \text{ sec}$$

$$S_{\psi_m} = 1 \text{ rad}$$

$$\dot{\psi}_m = \dot{\psi}_i - \frac{1}{\tau_{\psi_R}} \cdot \psi_m$$

$$\frac{\dot{\psi}_m}{T} = \frac{\dot{\psi}_i}{T} - \frac{1}{\tau_{\psi_R}} \cdot \frac{\psi_m}{T}$$

$$MYAWMD = MYAWSI - KJ11 \cdot MYAWSM$$

$$KJ11 = \frac{1}{20} = 0,05$$

Rectangular integration:

$$\psi_m = \psi_m + 0,05 \dot{\psi}_m$$

$$\frac{\psi_m}{T} = \frac{\psi_m}{T} + 0,05 \cdot \frac{\dot{\psi}_m}{T}$$

$$MYAWSM = MYAWSM + KJ4 \cdot MYAWMD$$

$$KJ4 = 0,05$$

Motion system lead compensation:

$$\psi_c = \psi_m + B_6 \cdot \dot{\psi}_m + A_6 \cdot \dot{r}_{b,h_p}$$

$$\frac{\psi_c}{T} = \frac{\psi_m}{T} + B_6 \cdot \frac{\dot{\psi}_m}{T} + A_6 \cdot (\frac{\dot{r}_{b,h_p}}{2}) \cdot 2$$

$$MYAWC = MYAWSM + KJ5 \cdot MYAWMD + KJ6 \cdot MYAWDD$$

$$KJ5 = 0,28$$

$$KJ6 = 0,044 \cdot 2 = 0,088.$$

Sum of body-axes translational accelerations, see section 6:

$$\ddot{x}_s = \ddot{x}_{b,1} + \ddot{x}_{b,2} \quad (6.4.)$$

$$\frac{\ddot{x}_s}{10} = \frac{\ddot{x}_{b,1}}{10} + \frac{\ddot{x}_{b,2}}{10}$$

$$SXDD = BXDD + MXDD$$

$$\ddot{y}_s = \ddot{y}_{b,1} + \ddot{y}_{b,2}$$

$$\frac{\ddot{y}_s}{8} = \frac{\ddot{y}_{b,1}}{8} + \frac{\ddot{y}_{b,2}}{8}$$

SYDD = BYDD + MYDD (see line 351 - 357 of Appendix B, part 2)

Body to inertial transformation of the motion platform translational accelerations, see section 7:

$$\begin{aligned} \ddot{x}_i &= \ddot{x}_s \cdot \cos \theta_m \cdot \cos \psi_m + \ddot{y}_s (\sin \phi_m \cdot \sin \theta_m \cdot \cos \psi_m + \\ &\quad + \cos \phi_m \cdot \sin \psi_m) \end{aligned} \quad (*) \quad (7.1.)$$

$$\begin{aligned} \frac{\ddot{x}_i}{10} &= \frac{\ddot{x}_s}{10} \cdot \frac{\cos \theta_m}{1} \cdot \frac{\cos \psi_m}{1} + \frac{1}{10} \cdot \left(\frac{\ddot{y}_s}{8}\right) \cdot 8 \cdot \left(\frac{\sin \phi_m}{1} \cdot \frac{\sin \theta_m}{1} \cdot \frac{\cos \psi_m}{1} + \right. \\ &\quad \left. - \frac{\cos \phi_m}{1} \cdot \frac{\sin \psi_m}{1}\right) \end{aligned}$$

$$MXSDD = SXDD \cdot \cos(MPITCHSM) \cdot \cos(MYAWSM) + KY16 \cdot SYDD .$$

$$\begin{aligned} &\{ \sin(MROLLSM) \cdot \sin(MPITCHSM) \cdot \cos(MYAWSM) - \cos(MROLLSM) \cdot \\ &\quad \cdot \sin(MYAWSM) \} \end{aligned}$$

$$KY16 = \frac{8}{10} = 0,8$$

$$\begin{aligned} \ddot{y}_i &= \ddot{x}_s \cdot \cos \theta_m \cdot \sin \psi_m + \ddot{y}_s \cdot (\sin \phi_m \cdot \sin \theta_m \cdot \sin \psi_m + \\ &\quad + \cos \phi_m \cdot \cos \psi_m) \end{aligned} \quad (*) \quad (7.2.)$$

$$\begin{aligned} \frac{\ddot{y}_i}{8} &= \frac{1}{8} \cdot \left(\frac{\ddot{x}_s}{10}\right) \cdot 10 \cdot \frac{\cos \theta_m}{1} \cdot \frac{\sin \psi_m}{1} + \frac{\ddot{y}_s}{8} \cdot \left(\frac{\sin \phi_m}{1} \cdot \frac{\sin \theta_m}{1} \cdot \frac{\sin \psi_m}{1} + \right. \\ &\quad \left. + \left(\frac{\cos \phi_m}{1} \cdot \frac{\cos \psi_m}{1}\right)\right) \end{aligned}$$

$$MYSDD = KX16 \cdot SXDD \cdot \cos(MPITCHSM) \cdot \sin(MYAWSM) + SYDD .$$

$$\begin{aligned} &\{ \sin(MROLLSM) \cdot \sin(MPITCHSM) \cdot \sin(MYAWSM) + \cos(MROLLSM) \cdot \\ &\quad \cdot \cos(MYAWSM) \} \end{aligned}$$

$$KX16 = \frac{10}{8} = 1,25 = 0,625 \text{ SALD 2}$$

*) Note: The contribution of \ddot{z}_b to \ddot{x}_i and \ddot{y}_i is neglected in the KSS Boeing 747 Motion Simulation Program, because this contribution is small and the computation-time required for the transformation is less.

$$\ddot{z}_i = -\ddot{x}_s \cdot \sin \theta_m + \ddot{y}_s \cdot \sin \phi_m \cdot \cos \theta_m + \ddot{z}_b \cdot \cos \phi_m \cdot \cos \theta_m$$

$$\frac{\ddot{z}_i}{40} = -\frac{1}{40} \cdot \left(\frac{\ddot{x}_s}{10}\right) \cdot 10 \cdot \frac{\sin \theta_m}{1} + \frac{1}{40} \cdot \left(\frac{\ddot{y}_s}{8}\right) \cdot 8 \cdot \frac{\sin \phi_m}{1} \cdot \frac{\cos \theta_m}{1} + \frac{\ddot{z}_b}{40} \cdot$$

$$\cdot \frac{\cos \phi_m}{1} \cdot \frac{\cos \theta_m}{1}$$

$$Mzsdd = Kx17 \cdot SXDD \cdot \sin(MPITCHSM) + KY17 \cdot SYDD \cdot \sin(MROLLSM) \cdot$$

$$\cdot \cos(MPITCHSM) + BZDD \cdot \cos(MROLLSM) \cdot \cos(MPITCHSM).$$

$$Kx17 = -\frac{10}{40} = -0,25$$

$$KY17 = \frac{8}{40} = 0,2$$

Translational washout, see section 8:

$$\zeta_{x_T} = 0,7$$

$$\tau_{x_T} = 2 \text{ sec}$$

$$\dot{x}_m = \dot{x}_i - \frac{2\zeta_{x_T}}{\tau_{x_T}} \cdot \dot{x}_m - \frac{1}{\tau_{x_T}^2} \cdot x_m$$

$$\frac{\dot{x}_m}{10} = \frac{\dot{x}_i}{10} - \frac{2\zeta_{x_T}}{10\tau_{x_T}} \cdot \left(\frac{\dot{x}_m}{10}\right) \cdot 10 - \frac{1}{10\tau_{x_T}^2} \cdot \left(\frac{x_m}{11,3952}\right) \cdot 11,3952$$

$$MXMDD = MXSDD - KX18 \cdot MXDM - KX19 \cdot MXM$$

$$KX18 = \frac{2}{10} \cdot \frac{0,7}{2} \cdot 10 = 0,7$$

$$KX19 = \frac{11,3952}{10} \cdot \frac{0,7}{4} = 0,28488$$

Rectangular integration:

$$\dot{x}_m = \dot{x}_m + 0,05 \dot{x}_m$$

$$\frac{\dot{x}_m}{10} = \frac{\dot{x}_m}{10} + \frac{0,05}{10} \cdot \left(\frac{\dot{x}_m}{10}\right) \cdot 10$$

$$MXDM = MXDM + KX12 \cdot MXMDD$$

$$KX12 = \frac{0,05}{10} \cdot 10 = 0,05$$

$$x_m = x_m + 0,05 \dot{x}_m$$

$$\frac{x_m}{11,3952} = \frac{x_m}{11,3952} + \frac{0,05}{11,3952} \cdot \left(\frac{\dot{x}_m}{10}\right) \cdot 10$$

$$MXM = MXM + KX13 \cdot MXDM$$

$$KX13 = \frac{0,05}{11,3952} \cdot \frac{10}{10} = 0,043878$$

Motion system lead compensation, see section 12:

$$x_c = x_m + B_1 \cdot \dot{x}_m + A_1 \cdot \ddot{x}_m$$

$$\frac{x_c}{11,3952} = \frac{x_m}{11,3952} + \frac{B_1}{11,3952} \cdot \left(\frac{\dot{x}_m}{10}\right) \cdot 10 + \frac{A_1}{11,3952} \cdot \left(\frac{\ddot{x}_m}{10}\right) \cdot 10$$

$$MXC = MXM + KX14 \cdot MXDM + KX15 \cdot MXMDD$$

$$KX14 = \frac{0,28}{11,3952} \cdot \frac{10}{10} = 0,24572$$

$$KX15 = \frac{0,044}{11,3952} \cdot \frac{10}{10} = 0,038613$$

$$\zeta_{y_T} = 0,7$$

$$\tau_{y_T} = 2 \text{ sec}$$

$$\ddot{y}_m = \ddot{y}_i - \frac{2\zeta_{y_T}}{\tau_{y_T}} \cdot \dot{y}_m - \frac{1}{\tau_{y_T}^2} \cdot y_m$$

$$\frac{\ddot{y}_m}{8} = \frac{\ddot{y}_i}{8} - \frac{2\zeta_{y_T}}{\tau_{y_T} \cdot 8} \cdot \left(\frac{\dot{y}_m}{10}\right) \cdot 10 - \frac{1}{8\tau_{y_T}^2} \cdot \left(\frac{y_m}{11,3952}\right) \cdot 11,3952$$

$$MYMDD = MYSDD - (KY18 \cdot MYDM) - (KY19 \cdot MYM)$$

$$KY18 = \frac{2}{8} \cdot \frac{0,7}{2} \cdot 10 = 0,875$$

$$KY19 = \frac{11,3952}{8} \cdot \frac{4}{4} = 0,3561$$

Rectangular integration:

$$\dot{y}_m = \dot{y}_m + 0,05 \dot{y}_m$$

$$\frac{\dot{y}_m}{10} = \frac{\dot{y}_m}{10} + \frac{0,05}{10} \cdot \left(\frac{\dot{y}_m}{8}\right) \cdot 8$$

$$MYDM = MYDM + KY12 \cdot MYMDD$$

$$KY12 = \frac{0,05}{10} \cdot 8 = 0,04$$

$$y_m = y_m + 0,05 \dot{y}_m$$

$$\frac{y_m}{11,3952} = \frac{y_m}{11,3952} + \frac{0,05}{11,3952} \cdot \left(\frac{\dot{y}_m}{10}\right) \cdot 10$$

$$MYM = MYM + KY13 \cdot MYDM$$

$$KY13 = \frac{0,05}{11,3952} \cdot 10 = 0,043878$$

Motion system lead compensation:

$$y_C = y_m + B_2 \cdot \dot{y}_m + A_2 \cdot \ddot{y}_m$$

$$\frac{y_C}{11,3952} = \frac{y_m}{11,3952} + \frac{B_2}{11,3952} \cdot \left(\frac{\dot{y}_m}{10}\right) \cdot 10 + \frac{A_2}{11,3952} \cdot \left(\frac{\ddot{y}_m}{8}\right) \cdot 8$$

$$MYC = MYM + KY14 \cdot MYDM + KY15 \cdot MYMDD$$

$$KY14 = \frac{0,28 \cdot 10}{11,3952} = 0,245718$$

$$KY15 = \frac{0,044 \cdot 8}{11,3952} = 0,03089$$

$$\zeta_{z_T} = 0,7$$

$$\tau_{z_T} = 2 \text{ sec.}$$

$$\ddot{z}_m = \ddot{z}_i - \frac{2\zeta_{z_T}}{\tau_{z_T}} \cdot \dot{z}_m - \frac{1}{\tau_{z_T}^2} \cdot z_m$$

$$\frac{\ddot{z}_m}{40} = \frac{\ddot{z}_i}{40} - \frac{2\zeta_{z_T}}{40\tau_{z_T}} \cdot \left(\frac{\dot{z}_m}{10}\right) \cdot 10 - \frac{1}{40\tau_{z_T}^2} \cdot \left(\frac{z_m}{49,854}\right) \cdot 49,854$$

$$MZMDD = MZSDD - (KZ8 \cdot MZDM) - (KZ9 \cdot MZM)$$

$$KZ8 = \frac{2 \cdot 0,7}{40 \cdot 2} \cdot 10 = 0,175$$

$$KZ9 = \frac{49,854}{40 \cdot 4} = 0,311587$$

Rectangular integration:

$$z_m = z_m + 0,05 \cdot \ddot{z}_m$$

$$\frac{\dot{z}_m}{10} = \frac{\dot{z}_m}{10} + \frac{0,05}{10} \cdot \left(\frac{\ddot{z}_m}{40}\right) \cdot 40$$

$$MZDM = MZDM + KZ3 \cdot MZMDD$$

$$KZ3 = \frac{0,05 + 40}{10} = 0,2$$

$$z_m = z_m + 0,05 \cdot \dot{z}_m$$

$$\frac{z_m}{49,854} = \frac{z_m}{49,854} + \frac{0,05}{49,854} \cdot \left(\frac{\dot{z}_m}{10} \right) \cdot 10$$

$$MZM = MZM + KZ4 \cdot MZDM$$

$$KZ4 = \frac{0,05}{49,854} \cdot 10 = 0,0100294$$

Motion system lead compensation:

$$z_c = z_m + B_3 \cdot \dot{z}_m + A_3 \cdot \ddot{z}_m$$

$$\frac{z_c}{49,854} = \frac{z_m}{49,854} + \frac{B_3}{49,854} \cdot \left(\frac{\dot{z}_m}{10} \right) 10 + \frac{A_3}{49,854} \cdot \left(\frac{\ddot{z}_m}{40} \right) \cdot 40$$

$$MZC = MZM + KZ5 \cdot MZDM + KZ6 \cdot MZMDD$$

$$KZ5 = \frac{0,28}{49,854} \cdot 10 = 0,056164$$

$$KZ6 = \frac{0,044 \cdot 40}{49,854} = 0,035302$$

The KSS Boeing 747 main motion simulation program, represented in Appendix B, is executed each 50 msec on a SDS Sigma 2 computer.

Timing runs of this program show, that the average computation time required for execution amounts to 7 msec, see Table 3.

Table 4 shows a timing-run of the complete KSS Boeing 747 flight simulation program, including motion simulation, with the aircraft in the on-ground condition. The average time required for the computation remains within 50 msec.

Parameter	Value in SI units	Program value	Parameter	Value in SI units	Program value
KXU1	1,71479	0,428697	KJ3	0,1	0,1
KYV1	2,4525	0,613125	KJ4	0,05	0,05
KZW1	1,4715	0,367875	KX1	-0,12	-0,12
KUBBD	0,8	0,8	KY1	0,3	0,3
KVBBB	1,25	0,625	KUBC	2,59	0,6475
KWBBB1	0,25	0,25	KVBC	6,475	0,8094
KWBBB2	0,2	0,2	KWBC	1,295	0,6475
$\zeta_{\theta_{hp}}$	0,7	0,7	KX10	2,0	0,9999
$\tau_{\theta_{hp}}$, sec	6	6	KX11	2,3255	0,581377
KP1	0,11666	0,11666	ζ_x	0,7	0,7
KP2	0,01388	0,01388	τ_x	0,7	0,7
KP3	0,1	0,1	$\zeta_{\theta_{1p}}$	0,7	0,7
KP4	0,05	0,05	$\tau_{\theta_{1p}}$, sec	2	2
$\zeta_{\phi_{hp}}$	0,7	0,7	KP13	0,25	0,25
$\tau_{\phi_{hp}}$, sec	6	6	KP14	0,25	0,25
KR1	0,11666	0,11666	KP15	0,7	0,7
KR2	0,01388	0,01388	KP16	0,25	0,25
KR3	0,1	0,1	KX12	0,05	0,05
KR4	0,05	0,05	KX13	0,043878	0,043878
ζ_ψ	0,7	0,7	KP17	0,05	0,05
τ_ψ , sec	1,5	1,5	KP18	0,05	0,05
KJ1	0,466664	0,233332	ζ_y	0,7	0,7
KJ2	0,22228	0,055552	τ_y , sec	1	1

Table 2: Parameter values as used in the KSS B-747 Motion simulation.

Parameter	Value in SI units	Program value	Parameter	Value in SI units	Program value
KR28	1,25	0,625	KP20	0,044	0,044
KR12	0,625	0,625	KR23	0,005	0,005
KY10	1,750	0,875	KR19	0,28	0,28
KY11	1,4244	0,7122	KR20	0,088	0,088
KY12	0,04	0,04	KJ11	0,05	0,05
KY13	0,043878	0,043878	KJ5	0,28	0,28
ζ_{ϕ_1} _p	0,7	0,7	KJ6	0,088	0,088
τ_{ϕ_1} , sec	2	2	KJ9	0,31831	0,31831
KR13	0,1	0,1	KY16	0,8	0,8
KR14	-0,125	-0,125	KP25	0,31831	0,31831
KR15	0,35	0,35	KR24	0,31831	0,31831
KR16	0,125	0,125	KX16	1,25	0,625
KR17	0,1	0,1	KX17	-0,25	-0,25
KR18	0,05	0,05	KY17	0,2	0,2
ζ_z	0,7	0,7	KX18	0,7	0,7
τ_z , sec	0,7	0,7	KX19	0,28488	0,28488
KZ1	0,5	0,5 (shift)	KX14	0,24572	0,24572
KZ2	2,543572	0,635893	KX15	0,038613	0,038613
KZ3	0,2	0,2	KY18	0,875	0,875
KZ4	0,010029	0,010029	KY19	0,3561	0,3561
KP26	2,0	2,0 (shift)	KY14	0,24572	0,24572
KP24	0,005	0,005	KY15	0,03089	0,03089
KP19	0,28	0,28	KZ8	0,175	0,175
			KZ9	0,311587	0,311587
			KZ5	0,056164	0,056164
			KZ6	0,035302	0,035302

Table 2: Parameter values as used in the KSS B-747 Motion simulation.
(cont'd)

!SL
!XE
TIMING FOR SYSTEM '4089'
-AVERAGE AFTER 01 MINUTES 26 SECONDS-
BAND MAX MIN AVG (IN MS ECS)
#00 09.0 06.0 07.0
#01 06.5 06.0 06.0
#02 06.5 06.0 06.0
#03 08.5 06.0 06.0
#04 09.0 06.0 06.5
#05 08.5 06.0 07.0
#06 06.5 06.0 06.0
#07 06.5 06.0 06.0
#08 08.5 06.0 07.0
#09 08.5 06.0 06.5
#10 09.0 06.0 07.0
#11 08.0 06.0 06.0
#12 08.5 06.0 06.5
#13 08.5 06.0 07.0
#14 06.5 06.0 06.0
#15 06.5 06.0 06.0

Table 3: Timing-run of KSS Boeing 747 main motion simulation program.

TIMING FOR SYSTEM '408F'
-AVERAGE AFTER 00 MINUTES 42 SECONDS-
BAND MAX MIN AVG (IN MS ECS)
#00 50.0 45.5 47.5
#01 50.5 43.5 46.5
#02 52.0 45.0 47.5
#03 50.5 42.5 46.0
#04 49.5 44.0 46.5
#05 47.0 40.5 43.5
#06 55.0 46.5 49.5
#07 50.0 45.0 47.0
#08 49.5 45.0 46.5
#09 48.5 41.0 44.0
#10 48.5 42.5 44.5
#11 50.0 42.0 46.0
#12 48.5 42.0 45.5
#13 47.0 40.5 43.5
#14 52.5 46.5 49.5
#15 52.5 47.5 49.5

Table 4: Timing-run of total system; aircraft on ground.

APPENDIX B, PART 1

1 * KSS B-747 MAIN MOTION SIMULATION. PART 1
2 *
3 * MAINMN1 FILE NO : K-817-1
4 * MAINMN2 FILE NO : K-817-2
5 *
6 *
7 * TEST PILOT : CAPTAIN J.L. VELDHUYZEN VAN ZANTEN
8 *
9 * DESIGN : IR. M.BAARSPUL
10 *
11 * SOFTWARE : B.BAARSCHERS
12 *
13 * ASSEMBLE THIS PROGRAM WITH :
14 * EXT. X-REF
15 * SLV SP
16 * MOTION X-REF
17 * FLIGHT INT. X-REF.
18 *
19 * ISSUE 3
20 * AUG. 1975
21 *
22 * DEF MAINMN1
23 *
24 * CSECT
25 * ORG X'0000'
26 *
27 0000 8CC9 A MAINMN1 LDA ACTFL GO4 FLIGHT OR TOTAL FREEZE ?
28 0001 98C9 A AND BIT4&8
29 0002 6402 A BAZ NOFRZE NO
30 0003 44FD A B *PROGRETN YES
31 *
32 * BASE X'1000'
33 *
34 0004 80BD A NOFRZE LDA BASE10
35 0005 74D7 A RCPY A,B
36 *

37	PAGE	
38	*	
39	*	RESCALING FOR TRANSFORMATION FROM WIND TO BODY
40	*	
41	0006 C0D8 A	LDX M3
42	0007 83AB A LOOP1	LDA MFZWB+1,1
43	0008 3AAE A	MUL KSCALE,1
44	0009 20A3 A	SALD 3
45	000A 74F6 A	RCPY E,A
46	000B E3AE A	STA WWD+1,1
47	000C 67FB A	BIX LOOP1
48	*	
49	*	DECIDE FOR ON OR OFF GROUND.
50	*	
51	000D 8CBB A	LDA VBOG
52	000E 6E02 A	BAN ONGROUND
53	000F 4808 A	B TRANSFORM
54	0010 C0D8 A ONGROUND	LDX M3
55	0011 8C80 A LOOP2	LDA VVXBP
56	0012 6402 A	BAZ ZERO
57	0013 83AE A	LDA WWD+1,1
58	0014 E3B1 A ZERO	STA WBD+1,1
59	0015 67FC A	BIX LOOP2
60	0016 483D A	B TIMEX

61 PAGE
62 *
63 * TRANSFORMATION OF X WIND TO BODY-AXIS ACCEL'S.
64 * UBD = (UWD*VCSAB*VCSB)-(VWD*VCSAB*VSNB*KUBBD)
65 * -(VWD*VSNB*4) (=SALD 3)
66 *

67 0017 81AB A TRANSFOR LDA UWD W-AXIS X ACCEL.
68 0018 3CA2 A MUL VCSAB COS.ALPHA BODY
69 0019 20A1 A SALD 1
70 001A 74F6 A RCPY E,A
71 001B 3CA0 A MUL VCSB COS.BETA
72 001C 20A1 A SALD 1
73 001D 74F6 A RCPY E,T SAVE IT
74 001E 81AC A LDA VWD W-AXIS Y ACCEL.
75 001F 3C98 A MUL VCSAB COS.ALPHA BODY
76 0020 20A1 A SALD 1
77 0021 74F6 A RCPY E,A
78 0022 3C9A A MUL VSNB SINE BETA
79 0023 20A1 A SALD 1
80 0024 74F6 A RCPY E,A
81 0025 3891 A MUL KUBBD .8
82 0026 20A1 A SALD 1
83 0027 703E A RADDI *E,T SUBTRACT IN T REG.
84 0028 81AD A LDA VWD W-AXIS Z ACCEL.
85 0029 3C94 A MUL VSNB SINE ALPHA BODY
86 002A 20A3 A SALD 3 *4
87 002B 703E A RADDI *E,T SUBTRACT IN T REG.
88 002C 74F3 A RCPY T,A
89 002D E1AE A STA UBD
90 *
91 * TRANSFORMATION OF Y WIND TO BODY-AXIS ACCEL.
92 * VBDM = (UWD*VSNB) * KVBBDD + (VWD*VCSB)
93 *
94 002E 81AB A LDA UWD W-AXIS LONGITUDINAL ACCEL.
95 002F 3C8D A MUL VSNB SINE BETA
96 0030 20A1 A SALD 1
97 0031 74F6 A RCPY E,A
98 0032 3885 A MUL KVBBDD .625
99 0033 20A2 A SALD 2 *2 = 1.25
100 0034 74F6 A RCPY E,T SAVE IT
101 0035 81AC A LDA VWD W-AXIS LATERAL ACCEL.
102 0036 3C85 A MUL VCSB COS.BETA
103 0037 20A1 A SALD 1
104 0038 7C36 A RADD E,T SUM IT
105 0039 74F3 A RCPY T,A
106 003A E1AF A STA VBDM

107	PAGE	
108	*	
109	*	
110	*	
111	*	
112	*	
113 003B 81AB A	LDA UWD	W-AXIS X ACCEL.
114 003C 3C81 A	MUL VSNA8	SINE ALPHA BODY
115 003D 20A1 A	SALD 1	
116 003E 74F6 A	RCPY E,A	
117 003F 3C7C A	MUL VCSB	COS.BETA
118 0040 20A1 A	SALD 1	
119 0041 74F6 A	RCPY E,A	
120 0042 3876 A	MUL KWBD1	.25
121 0043 74B6 A	RCPY E,T	SAVE IT
122 0044 81AC A	LDA WWD	W-AXIS Y ACCEL.
123 0045 3C78 A	MUL VSNA8	SINE ALPHA BODY
124 0046 20A1 A	SALD 1	
125 0047 74F6 A	RCPY E,A	
126 0048 3C74 A	MUL VSNB	SINE BETA
127 0049 20A1 A	SALD 1	
128 004A 74F6 A	RCPY E,A	
129 004B 386E A	MUL KWBD2	.2
130 004C 7D3E A	RADDI *E,T	SUBTRACT IN T REG.
131 004D 81AD A	LDA WWD	W-AXIS Z ACCEL.
132 004E 3C6C A	MUL VCSAB	COS.ALPHA BODY
133 004F 20A1 A	SALD 1	
134 0050 7C36 A	RADD E,T	SUM IT
135 0051 74F3 A	RCPY T,A	
136 0052 E1B0 A	STA WBD	Z-BODY AXIS ACCEL.

PAGE		
137	*	
138	*	
139	*	TIMER TO STOP THE CALCULATIONS DURING ON/OFF GRD TRANSITION
140	*	
141 0053 888A A	TIMEX	LDA TIMER
142 0054 6403 A		BAZ TIMEUP
143 0055 F888 A		IM TIMER
144 0056 480C A		B GO1
145 0057 8C71 A	TIMEUP	LDA VBOG
146 0058 D886 A		CP LTCONDIT
147 0059 6203 A		BNC \$+3
148 005A 74F0 A		RCPY Z,A
149 005B 4804 A		B \$+4
150 005C 8883 A		LDA 20ITERS
151 005D E880 A		STA TIMER
152 005E 74F8 A		RCPY *Z,A
153 005F E881 A		STA STOPFLAG
154 0060 8C68 A		LDA VBOG
155 0061 E870 A		STA LTCONDIT
		TIME WAS NOT YET UP
		CONDITION CHANGED ?
		YES
		NO
		RESET STOPFLAG
		1 SECOND
		SET STOPFLAG
		STORE PRESENT CONDITION
		IN LAST TIME CONDITION

156	PAGE
157	*
158	*
159	*
160	*
161	*
162	*
163	*
164	*
165	*
166	*
167	*
168	*
169	*
170 0062 81B7 A G01	LDA MPITCHDM
171 0063 386F A	MUL KP1
172 0064 74B6 A	RCPY E,T
173 0065 81BA A	LDA MPITCHM
174 0066 386D A	MUL KP2
175 0067 7C36 A	RADD E,T
176 0068 10C0 A	RD X'CO'
177 0069 8C5D A	LDA VPRD
178 006A 7D7B A	RADDI *T,A
179 006B E1B4 A	STA MPITCHDD
180	*
181	*
182	*
183	*
184	*
185 006C 31CE A	MUL KP3
186 006D A879 A	ADD MPITCHDL
187 006E E878 A	STA MPITCHDL
188 006F 10C0 A	RD X'CO'
189 0070 81B7 A	LDA MPITCHDM
190 0071 7E76 A	RADD C E,A
191 0072 E1B7 A	STA MPITCHDM
192	*
193	*
194	*
195 0073 31CF A	MUL KP4
196 0074 A875 A	ADD MPITCHL
197 0075 E874 A	STA MPITCHL
198 0076 10C0 A	RD X'CO'
199 0077 81BA A	LDA MPITCHM
200 0078 7E76 A	RADD C E,A
201 0079 E1BA A	STA MPITCHM

PITCH BODY ACCELERATIONS

MPITCHDD = VPRD - ((KP1*MPITCHDM) + (KP2*MPITCHM))

PITCH RATE

MPITCHDM = MPITCHDM + (KP3*MPITCHDD)

MPITCHM = MPITCHM + (KP4*MPITCHDM)

L/S PART
NEW L/S PART
RESET COF
M/S PART
L/S PART
NEW L/S PART
RESET COF
M/S PART

202 PAGE
203
204 ROLL BODY ACCELERATIONS
205
206 TAU PHI HI-PASS = 6 SEC
207 ZETA PHI HI-PASS = .7
208 S PHI HP DD = 4 RAD/SEC 2
209 S PHI HP D = 2 RAD/SEC
210 S PHI HP = 2 RAD
211
212 VRD = 4 RAD/SEC 2
213
214 MROLLDD = VRD - ((KR1*MROLLDM) + (KR2*MROLLM))
215
216 007A 81BB A ROLLCHAN LDA MROLLDM
217 007B 3857 A MUL KR1
218 007C 7486 A RCPY E,T
219 007D 81BB A LDA MROLLM
220 007E 3855 A MUL KR2
221 007F 7C36 A RADD E,T
222 0080 10C0 A RD X'CO' RESET COF
223 0081 8C46 A LDA VRD ROLL ACCEL.
224 0082 7D7B A RADDI *T,A ADD 2TH COMPLEMENT = SUBTRACT
225 0083 E1BB A STA MROLLDD
226
227 ROLL RATE
228
229 MROLLDM = MROLLDM + (KR3*MROLLDD)
230
231 0084 31CE A MUL KR3
232 0085 A862 A ADD MROLLDL L/S PART
233 0086 E861 A STA MROLLDL NEW L/S PART
234 0087 10C0 A RD X'CO' RESET COF
235 0088 81BB A LDA MROLLDM M/S PART
236 0089 7E76 A RADD C E,A
237 008A E1BB A STA MROLLDM NEW M/S PART
238
239 MROLLM = MROLLM + (KR4*MROLLDM)
240
241 008B 31CF A MUL KR4
242 008C A85E A ADD MROLLL L/S PART
243 008D E85D A STA MROLLL NEW L/S PART
244 008E 10C0 A RD X'CO' RESET COF
245 008F 81BB A LDA MROLLM
246 0090 7E76 A RADD C E,A
247 0091 E1BB A STA MROLLM M/S PART

.248	PAGE				
249	*				
250	*	YAW BODY ACCELERATIONS			
251	*				
252	*	TAU	PSI	HI-PASS = 1.5 SEC	
253	*	ZETA	PSI	HI-PASS = .7	
254	*	S	PSI	HP DD = 2 RAD/SEC 2	
255	*	S	PSI	HP D = 1 RAD/SEC	
256	*	S	PSI	HP = 1 RAD	
257	*				
258	*	VHRO		= 2 RAD/SEC 2	
259	*				
260	*	MYAWDD = VHRO - ((KJ1*MYAWDM) + (KJ2*MYAWM))			
261	*				
262	0092	81B9 A	YAWCHAN	LDA MYAWDM	
263	0093	384E A		MUL KJ1	
264	0094	74B6 A		RCPY E,T	
265	0095	81BC A		LDA MYAWM	
266	0096	384C A		MUL KJ2	
267	0097	7C36 A		RADD E,T	
268	0098	10C0 A		RD X'CO'	RESET CDF
269	0099	8C2C A		LDA VHRO	
270	009A	7D7B A		RADDI *T,A	ADD 2TH COMPLEMENT = SUBTRACT
271	009B	E1B6 A		STA MYAWDD	
272	*				
273	*				
274	*				
275	*			MYAWDM = MYAWDM + (KJ3*MYAWDD)	
276	*				
277	009C	31CE A		MUL KJ3	
278	009D	A84B A		ADD MYAWDL	L/S PART
279	009E	E84A A		STA MYAWDL	NEW L/S PART
280	009F	10C0 A		RD X'CO'	RESET CDF
281	00A0	81B9 A		LDA MYAWDM	M/S PART
282	00A1	7E76 A		RADDI E,A	
283	00A2	E1B9 A		STA MYAWDM	NEW M/S PART
284	*				
285	*			MYAWM = MYAWM + (KJ4*MYAWDM)	
286	*				
287	00A3	31CF A		MUL KJ4	
288	00A4	A847 A		ADD MYAWL	L/S PART
289	00A5	E846 A		STA MYAWL	NEW L/S PART
290	00A6	10C0 A		RD X'CO'	RESET CDF
291	00A7	81BC A		LDA MYAWM	
292	00A8	7E76 A		RADDI E,A	
293	00A9	E1BC A		STA MYAWM	NEW M/S PART

294	PAGE	
295		
296	SPECIFIC FORCE ERRORS	
297		
298	$MXDD = KX1 * MPITCHM$	
299		
300 00AA 81BA A	LDA	MPITCHM
301 00AB 3838 A	MUL	KX1
302 00AC 74F6 A	RCPY	E,A
303 00AD E1C1 A	STA	MXDD
304		
305	MYDD = KY1 * MROLLM	
306		
307 00AE 81B8 A	LDA	MROLLM
308 00AF 3835 A	MUL	KY1
309 00B0 74F6 A	RCPY	E,A
310 00B1 E1C2 A	STA	MYDD
311		
312		
313 00B2 484C A	8	G02

PAGE		
314	*	
315	*	
316	*	DATA AND ADRL'S. WHEN SCALED OTHER THAN BO
317	*	THIS IS DONE TO AVOID NECESSARY SHIFTS
318	*	
319	*	WIND TO BODY RESCALING USED WITH SALD 3
320	*	
321	0083 36E0 A KXU1	DEC 428697E-6
322	0084 4E78 A KYV1	DEC 613125E-6
323	0085 2F17 A KZW1	DEC 367875E-6
324	00B6 KSCALE	RES 0
325	*	
326	00B6 6666 A KUBBD	DEC 8E-1
327	00B7 5000 A KVBB	DEC 625E-3
328	00B8 4000 A KWBB01	DEC 25E-2B1
329	00B9 3333 A KWBB02	DEC 2E-1B1
330	*	
331	00BA 0851 A	ADRL VCSAB COSINE ALPHA BODY
332	00BB 0853 A	ADRL VCSB COSINE BETA
333	00BC 0885 A	ADRL VSNB SINE BETA
334	00BD 0883 A	ADRL VSNA8 SINE ALPHA BODY
335	00BE 0888 A	ADRL VSNRB SINE ROLL BODY
336	00BF 0887 A	ADRL VSNPB SINE PITCH BODY
337	00C0 0855 A	ADRL VCSPB COS. PITCH BODY
338	00C1 08E0 A	ADRL VVXPB GROUND SPEED
339	00C2 0801 A	ADRL VPR PITCH RATE
340	00C3 08C5 A	ADRL VHR YAW RATE
341	00C4 0805 A	ADRL VRR ROLL RATE
342	00C5 08C6 A	ADRL VHARD YAW ACCEL. 2B1
343	00C6 0802 A	ADRL VPRD PITCH ACCEL. 2B1
344	00C7 08D6 A	ADRL VRD ROLL ACCEL. 2B2
345	00C8 08B3 A	ADRL VB0G ON/OFF GRD FLAG
346	00C9 OFE0 A	ADRL ACTFL GO4 FOR FREEZE
347	00CA 0880 A BIT4&8	DATA X'0880' FLT & TOTAL FRZE
348	*	
349	00CB 0000 A UB0D	DATA 0 BODY-CENTROID ACCEL. 10M/SEC 2.LONGITUDIN/
350	00CC 0000 A VB0D	DATA 0 8M/SEC 2.LATERAL
351	00CD 0000 A WB0D	DATA 0 40M/SEC 2.VERTICAL
352	*	
353	00CE 52E1 A KUBC	DEC 6475E-4 SALD 3
354	00CF 679A A KVBC	DEC 8094E-4 SALD 4
355	00D0 52E1 A KWBC	DEC 6475E-4 SALD 2

	PAGE	
356		
357	*	
358 0001 4A68 A KX11	DEC	581377E-6
359 0002 1000 A KP1	DEC	11666E-5B1
360 0003 038E A KP2	DEC	01388E-5B1
361 0004 4000 A KP13	DEC	25E-2B1
362 0004 R KP14	EQU	KP13
363 0005 599A A KP15	DEC	7E-1
364 0004 R KP16	EQU	KP13
365 0006 7000 A KY10	DEC	875E-3
366 0007 5829 A KY11	DEC	7122E-4
367 0008 5000 A KR12	DEC	625E-3
368 0009 E000 A KR14	DEC	-125E-3B1
369 000A 599A A KR15	DEC	35E-2B1
370 00DB 2000 A KR16	DEC	125E-3B1
371 00DC 5000 A KR28	DEC	625E-3
372 0000 0000 A TIMER	DATA	0
373 00DE 0000 A LTCOND1	DATA	0
374 00DF FFEC A 20ITERS	DATA	-20
375 00E0 0000 A STOPFLAG	DATA	0
376 *		
377 00E1 7777 A KJ1	DEC	233332E-6B2
378 00E2 38E3 A KJ2	DEC	055552E-6B3
379 *		
380 00E3 E148 A KX1	DEC	-03E-2B3
381 00E4 4CC0 A KY1	DEC	3E-1B1
382 00E5 5165 A KZ2	DEC	635893E-6
		SALD 3

	PAGE	
383	*	
384	*	
385	00E6 0000 A MPITCHDL	DATA 0 PITCH L/S RATE INTEGRATION
386	00E7 0000 A MROLLDL	DATA 0 ROLL
387	00E8 0000 A MYAWDL	DATA 0 YAW
388	*	
389	00E9 0000 A MPITCHL	DATA 0 PITCH
390	00EA 0000 A MROLLL	DATA 0 ROLL
391	00EB 0000 A MYAWL	DATA 0 YAW
392	*	
393	00EC 0000 A BPITCHDL	DATA 0 PITCH BODY DOT L/S INTEGRATION
394	00ED 0000 A BROLLDL	DATA 0
395	*	
396	00EE 0000 A BXM	DATA 0 X BODY MOST INTEGRATION
397	00EF 0000 A BYM	DATA 0 Y
398	00F0 0000 A BZM	DATA 0 Z
399	*	
400	00F1 0000 A BXL	DATA 0 X BODY L/S INTEGRATION
401	00F2 0000 A BYL	DATA 0 Y
402	00F3 0000 A BZL	DATA 0 Z
403	*	
404	00F4 0000 A BXDM	DATA 0 X BODY DOT MOST INTEGRATION
405	00F5 0000 A BYDM	DATA 0 Y
406	00F6 0000 A BZDM	DATA 0 Z
407	*	
408	00F7 0000 A BXDL	DATA 0 X BODY DOT L/S INTEGRATION
409	00F8 0000 A BYDL	DATA 0 Y
410	00F9 0000 A BZDL	DATA 0 Z
411	*	
412	00FA 0000 A BPITCHL	DATA 0 PITCH BODY L/S INTEGRATION
413	00FB 0000 A BROLLL	DATA 0 ROLL
414	*	
415	00FC 0000 A BPITCHM	DATA 0 PITCH BODY MOST INTEGRATION
416	00FD 0000 A BROLLM	DATA 0 ROLL

417	PAGE	
418	*	SPECIFIC FORCES
419	*	
420	*	CENTROID TRANSFORMATION
421	*	
422	*	$UBCD = UBD - (((VPR*VPR)+(VHR*VHR))*KUBC)$
423	*	
424	*	
425 00FE 8DC4 A G02	LDA	VPR
426 00FF 3DC3 A	MUL	VPR
427 0100 20A1 A	SALD	1
428 0101 74B6 A	RCPY	E,T
429 0102 8DC1 A	LDA	VHR
430 0103 3DC0 A	MUL	VHR
431 0104 20A1 A	SALD	1
432 0105 7C36 A	RADD	E,T
433 0106 74F3 A	RCPY	T,A
434 0107 39C7 A	MUL	KUBC
435 0108 20A3 A	SALD	3
436 0109 81AE A	LDA	UBD
437 010A 707E A	RADDI	*E,A
438 010B E9C0 A	STA	UBCD
439	*	SAVE IN E REG.
440	*	MOT.B-AXIS LONGITUDINAL ACC.
441	*	SUBTRACT
		MOT.B-AXIS LONG.ACC.AT CENTROID
442 010C 8DB8 A	LDA	VRR
443 010D 3DB5 A	MUL	VPR
444 010E 20A1 A	SALD	1
445 010F 74F6 A	RCPY	E,A
446 0110 AD85 A	ADD	VHRD
447 0111 39BE A	MUL	KVBC
448 0112 20A4 A	SALD	4
449 0113 74F6 A	RCPY	E,A
450 0114 A1AF A	ADD	VBDM
451 0115 E987 A	STA	WBCD
452	*	MOT.B-AXIS LATERAL ACC.
453	*	MOT.B-AXIS LAT.ACC. AT CENTROID
454	*	
455 0116 8DAE A	LDA	VRR
456 0117 3DAC A	MUL	VHR
457 0118 20A1 A	SALD	1
458 0119 74F6 A	RCPY	E,A
459 011A BDAC A	SUB	VPRD
460 011B 39B5 A	MUL	KWBC
461 011C 20A2 A	SALD	2
462 011D 74F6 A	RCPY	E,A
463 011E A1B0 A	ADD	WBD
464 011F E9AE A	STA	WBCD
		MOT.B-AXIS VERTICAL ACC.
		MOT.B-AXIS VERT.ACC. AT CENTROID

465	PAGE	
466	*	
467	*	LONGITUDINAL SPECIFIC FORCE.
468	*	
469	*	LONGITUDINAL HI-PASS FILTER
470	*	
471	*	TAU X HI-PASS = .7 SEC
472	*	ZETA X HI-PASS = .7
473	*	S X HI DD = 10M/SEC 2
474	*	S X HI D = 10M/SEC
475	*	S X HI = 11.3952 M
476	*	
477	*	BXDD = UBCD - (BPITCHM) - (KX10*BXM) - (KX11*BXM)
478	*	
479	0120 89C0 A	LDA STOPFLAG CALC TO BE STOPPED ?
480	0121 6E3A A	BAN G03 YES
481	0122 89D2 A	LDA BXDM NO
482	0123 7C77 A	RADD A,A FOR KX10 = 2.0
483	0124 A908 A	ADD BPITCHM
484	0125 74B7 A	RCPY A,T SAVE IT
485	0126 89C8 A	LDA BXM
486	0127 39AA A	MUL KX11
487	0128 20A3 A	SALD 3
488	0129 7C36 A	RADD E,T SUM IT
489	012A 89A1 A	LDA UBCD
490	012B 7D7B A	RADDI *T,A SUBTRACT
491	012C E1B1 A	STA BXDD
492	*	
493	*	INTEGRATION
494	*	
495	*	BXM = BXDM + (KX12*BXDD)
496	*	
497	012D 81B1 A	LDA BXDD
498	012E 31CF A	MUL KX12
499	012F A9C8 A	ADD BXDL L/S PART
500	0130 E9C7 A	STA BXDL NEW L/S PART
501	0131 10C0 A	RD X'CO'
502	0132 89C2 A	LDA BXDM M/S PART
503	0133 7E76 A	RADDI E,A
504	0134 E9C0 A	STA BXDM NEW M/S PART
505	*	
506	*	BXM = BXM + (KX13*BXDM)
507	*	
508	0135 31D0 A	MUL KX13
509	0136 A9BB A	ADD BXL L/S PART
510	0137 E9BA A	STA BXL NEW L/S PART
511	0138 10C0 A	RD X'CO'
512	0139 89B5 A	LOA BXM RST CDF
513	013A 7E76 A	RADDI E,A M/S PART
514	013B E9B3 A	STA BXM NEW M/S PART

515 * LONGITUDINAL LOW-PASS FILTER
516 *
517 * TAU THETA LOW-PASS = 2 SEC
518 * ZETA THETA LOW-PASS = .7
519 * S THETA LP DD = 1 RAD/SEC 2
520 * S THETA LP D = 1 RAD/SEC
521 * S THETA LP = 1 RAD
522 *
523 * BPITCHDD = (KP13*UBCD) + (KP14*VSNPB) - (KP16*BPITCHM)
524 * - (KP15*BPITCHDM)
525 *
526 013C 81BF A LDA BPITCHDM
527 013D 3998 A MUL KP15
528 013E 20A1 A SALD 1
529 013F 74B6 A RCPY E,T SAVE
530 0140 8988 A LDA UBCD LONGITUDINAL CENTROID ACCEL.
531 0141 3993 A MUL KP13
532 0142 74A6 A RCPY E,L
533 0143 807C A LDA VSNPB SINE PITCH BODY
534 0144 3990 A MUL KP14
535 0145 7C26 A RADD E,L SUM IN L REG.
536 0146 8986 A LDA BPITCHM
537 0147 398D A MUL KP16
538 0148 702E A RADDI *E,L SUBTRACT IN L REG.
539 0149 74F2 A RCPY L,A
540 014A 7D78 A RADDI *T,A SUBTRACT
541 014B E1BD A STA BPITCHDD
542 *
543 * INTEGRATION
544 *
545 * BPITCHDM = BPITCHDD + (KP17*BPITCHDD)
546 *
547 014C 81BD A LDA BPITCHDD
548 014D 31CF A MUL KP17
549 014E A99E A ADD BPITCHDL L/S PART
550 014F E990 A STA BPITCHDL NEW L/S PART
551 0150 1000 A RD X'CO' RST COF
552 0151 81BF A LDA BPITCHDM M/S PART
553 0152 7E76 A RADD C E,A
554 0153 E1BF A STA BPITCHDM NEW M/S PART
555 *
556 * BPITCHM = BPITCHM + (KP18*BPITCHDM)
557 *
558 0154 31CF A MUL KP18
559 0155 A9A5 A ADD BPITCHL L/S PART
560 0156 E9A4 A STA BPITCHL NEW L/S PART
561 0157 1000 A RD X'CO' RST COF
562 0158 89A4 A LDA BPITCHM M/S PART
563 0159 7E76 A RADD C E,A
564 015A E9A2 A STA BPITCHM NEW M/S PART

565	PAGE
566	*
567	*
568	*
569	*
570	*
571	*
572	*
573	*
574	*
575	*
576	*
577	*
578	*
579	*
580 015B 899A A G03	LDA BYDM
581 015C 397A A	MUL KY10
582 015D 20A2 A	SALD 2
583 015E 74B6 A	RCPY E,T
584 015F 8990 A	LDA BYM
585 0160 3977 A	MUL KY11
586 0161 20A2 A	SALD 2
587 0162 7C36 A	RADD E,T
588 0163 8D5B A	LDA VSNRB
589 0164 3D5C A	MUL VCSPB
590 0165 20A1 A	SALD 1
591 0166 74F6 A	RCPY E,A
592 0167 3975 A	MUL KR28
593 0168 20A2 A	SALD 2
594 0169 7C36 A	RADD E,T
595 016A 8993 A	LDA BROLLM
596 016B 396D A	MUL KR12
597 016C 20A1 A	SALD 1
598 016D 895F A	LDA VBCD
599 016E 7C76 A	RADD E,A
600 016F 7D7B A	RADDI *T,A
601 0170 E1B2 A	STA BYOD

= KY10*2
SAVE
= KY11*2
SAVE SUM
SINE ROLL BODY
COS.PITCH BODY
AND SAVE IN E REG.
SUBTRACT T REG. CONTENTS

602	PAGE		
603	*		
604	*	INTEGRATION	
605	*		
606	*	BYDM = BYDM + (KY12*BYDD)	
607	*		
608	0171 31D4 A	MUL KY12	
609	0172 A986 A	ADD BYDL	L/S PART
610	0173 E985 A	STA BYDL	NEW L/S PART
611	0174 10C0 A	RD X'CO'	RST CDF
612	0175 8980 A	LDA BYDM	M/S PART
613	0176 7E76 A	RADDC E,A	
614	0177 E97E A	STA BYDM	NEW M/S PART
615	*		
616	*	BYM = BYM + (KY13*BYDM)	
617	*		
618	0178 31D0 A	MUL KY13	
619	0179 A979 A	ADD BYL	L/S PART
620	017A E978 A	STA BYL	NEW L/S PART
621	017B 10C0 A	RD X'CO'	RST CDF
622	017C 8973 A	LDA BYM	M/S PART
623	017D 7E76 A	RADDC E,A	
624	017E E971 A	STA BYM	NEW M/S PART

625	PAGE
626	*
627	*
628	*
629	*
630	*
631	*
632	*
633	*
634	*
635	*
636	*
637	*
638 017F 894D A	LDA VBCD
639 0180 31CE A	MUL KR13
640 0181 7486 A	RCPY E,T
641 0182 803C A	LDA VSNRB
642 0183 3956 A	MUL KR14
643 0184 74F6 A	RCPY E,A
644 0185 303B A	MUL VCSPB
645 0186 20A1 A	SALD 1
646 0187 7C36 A	RADD E,T
647 0188 81C0 A	LDA BROLLD0
648 0189 3951 A	MUL KR15
649 018A 7C36 A	RADD E,T
650 018B 8972 A	LDA BROLLM
651 018C 394F A	MUL KR16
652 018D 7C36 A	RADD E,T
653 018E 75FB A	RCPYI *T,A
654 018F E1BE A	STA BROLDD0

LATERAL LOW-PASS FILTER

SAVE
SINE ROLL BODY

SAVE SUM

SAVE SUM

SAVE SUM
FOR - SIGN

		PAGE
655	*	
656	*	INTEGRATION
657	*	
658	*	
659	*	BROLLOM = BROLLOM + (KR17*BROLLOD)
660	*	
661	0190 31CE A	MUL KR17
662	0191 A95C A	ADD BROLLOL
663	0192 E95B A	STA BROLLOL
664	0193 10C0 A	RD X'CO'
665	0194 81C0 A	LDA BROLLOM
666	0195 7E76 A	RADD C
667	0196 E1C0 A	E,A
668	*	STA BROLLOM
669	*	NEW M/S PART
670	*	
671	0197 31CF A	MUL KR18
672	0198 A963 A	ADD BROLLL
673	0199 E962 A	STA BROLLL
674	019A 10C0 A	RD X'CO'
675	019B 8962 A	LDA BROLLM
676	019C 7E76 A	RADD C
677	019D E960 A	E,A
		STA BROLLM
		NEW M/S PART

PAGE		
678	*	
679	*	
680	*	VERTICAL HI-PASS FILTER
681	*	
682	*	TAU Z HI-PASS = .7 SEC
683	*	ZETA Z HI-PASS = .7
684	*	S Z HP DD = 40 M/SEC 2
685	*	S Z HP D = 10 M/SEC
686	*	S Z HP = 49.854 M
687	*	BZDD = WBCD - (.5*BZDM) - (KZ2*BZM)
688	*	
689	019E 8952 A	LDA BZM
690	019F 3946 A	MUL KZ2
691	01A0 20A3 A	SALD 3
692	01A1 74B6 A	RCPY E,T SAVE
693	01A2 8954 A	LDA BZDM
694	01A3 2001 A	SARS 1 * .5
695	01A4 7C37 A	RADD A,T SAVE SUM
696	01A5 8928 A	LDA WBCD
697	01A6 7D78 A	RADDI *T,A SUBTRACT
698	01A7 E1B3 A	STA BZDD
699	*	
700	*	INTEGRATION
701	*	
702	*	BZDM = BZDM + (KZ3*BZDD)
703	*	
704	01AB 3105 A	MUL KZ3
705	01A9 A950 A	ADD BZDL L/S PART
706	01AA E94F A	STA BZDL NEW L/S PART
707	01AB 10C0 A	RD X'CO' RST CDF
708	01AC 894A A	LDA BZDM M/S PART
709	01AD 7E76 A	RADDI E,A
710	01AE E948 A	STA BZDM NEW M/S PART
711	*	
712	*	BZM = BZM + (KZ4*BZDM)
713	*	
714	01AF 3106 A	MUL KZ4
715	01B0 A943 A	ADD BZL L/S PART
716	01B1 E942 A	STA BZL NEW L/S PART
717	01B2 10C0 A	RD X'CO' RST CDF
718	01B3 8930 A	LDA BZM M/S PART
719	01B4 7E76 A	RADDI E,A
720	01B5 E93B A	STA BZM
721	01B6 44FD A	B *PROGRETN NEW M/S PART

		PAGE	
722	*		
723	*		
724	*	EQUALS	TABLE AT END OF PROGRAM
725	*		
726	10CE A KP3	EQU	KPRJ3
727	10CE A KR3	EQU	KPRJ3
728	10CE A KJ3	EQU	KPRJ3
729	*		
730	10CE A KR17	EQU	KPRJ3
731	10CE A KR13	EQU	KPRJ3
732	*		
733	10CF A KP4	EQU	KPRJ4
734	10CF A KR4	EQU	KPRJ4
735	10CF A KJ4	EQU	KPRJ4
736	*		
737	10CF A KJ11	EQU	KPRJ4
738	10CF A KX12	EQU	KPRJ4
739	*		
740	10CF A KR18	EQU	KPRJ4
741	10CF A KP17	EQU	KPRJ4
742	10CF A KP18	EQU	KPRJ4
743	*		
744	*		
745	10D0 A KX13	EQU	KXY13
746	10D0 A KY13	EQU	KXY13
747	*		
748	*		
749	10D1 A KP19	EQU	KR19
750	10D1 A KJ5	EQU	KR19
751	*		
752	*		
753	10D3 A KP24	EQU	KPR2423
754	10D3 A KR23	EQU	KPR2423
755	*		
756	*		
757	10D2 A KR20	EQU	KPRJ206
758	10D2 A KJ6	EQU	KPRJ206
759	*		
760	00D2 R KR1	EQU	KP1
761	00D3 R KR2	EQU	KP2
762	*		
763	*		
764	0000 A	END	

0 ERRORS
EQUALS ERROR MAINMN1

A	0007 X	ACTFLG04	0FE0 X	B	0005 X	BASE10	008D X
BIT&8	00CA R	BPITCHDD	10BD X	BPITCHDL	00EC R	BPITCHDM	10BF X
BPITCHL	00FA R	BPITCHM	00FC R	BROLLD	10BE X	BR0LLDL	00ED R
BROLLM	10C0 X	BROLLL	00FB R	BROLLM	00FD R	BX0D	10B1 X
BXDL	00F7 R	BXDM	00F4 R	BXL	00F1 R	BXM	00EE R
BYDD	10B2 X	BYDL	00F8 R	BYDM	00F5 R	BYL	00F2 R
BYM	00EF R	BZ0D	10B3 X	BZDL	00F9 R	BZDM	00F6 R
BZL	00F3 R	BZM	00F0 R	E	0006 X	G01	0062 R
G02	00FE R	G03	0158 R	KJ1	00E1 R	KJ11	10CF A
KJ2	00E2 R	KJ3	10CE A	KJ4	10CF A	KJ5	1001 A
KJ6	10D2 A	KPRJ206	10D2 X	KPRJ3	10CE X	KPRJ4	10CF X
KPR2423	10D3 X	KP1	00D2 R	KP13	00D4 R	KP14	00D4 R
KP15	00D5 R	KP16	00D4 R	KP17	10CF A	KP18	10CF A
KP19	10D1 A	KP2	00D3 R	KP24	10D3 A	KP3	10CE A
KP4	10CF A	KR1	00D2 R	KR12	00D8 R	KR13	10CE A
KR14	00D9 R	KR15	00DA R	KR16	00D8 R	KR17	10CE A
KR18	10CF A	KR19	10D1 X	KR2	00D3 R	KR20	10D2 A
KR23	10D3 A	KR28	00DC R	KR3	10CE A	KR4	10CF A
KSCALE	00B6 R	KUBBD	00B6 R	KUBC	00CE R	KVBB0	00B7 R
KVBC	00CF R	KWBBD1	00B8 R	KWBBD2	00B9 R	KWBC	00D0 R
KXU1	00B3 R	KXY13	10D0 X	KX1	00E3 R	KX11	00D1 R
KX12	10CF A	KX13	10D0 A	KYV1	00B4 R	KY1	00E4 R
KY10	00D6 R	KY11	00D7 R	KY12	10D4 X	KY13	10D0 A
KZW1	00B5 R	KZ2	00E5 R	KZ3	10D5 X	KZ4	10D6 X
L	0002 X	L00P1	0007 R	L00P2	0011 R	LTCOND	00DE R
MAINMN1	0000 R	MFZWB	10AA X	MPITCHDD	10B4 X	MPITCHDL	00E6 R
MPITCHDM	10B7 X	MPITCHL	00E9 R	MPITCHM	10BA X	MROLLDL	10B5 X
MROLLDL	00E7 R	MROLLM	10B8 X	MROLLL	00EA R	MROLLM	10B8 X
MXDD	10C1 X	MYAWDD	10B6 X	MYAWDL	00E8 R	MYAWDM	10B9 X
MYAWL	00EB R	MYAWM	10BC X	MYOD	10C2 X	M3	00D8 X
NOFRZE	0004 R	ONGROUND	0010 R	PROGRETN	00FD X	ROLLCHAN	007A R
STOPFLAG	00E0 R	T	0003 X	TIMER	00D0 R	TIMEUP	0057 R
TIMEX	0053 R	TRANSFOR	0017 R	UBCD	00CB R	UBD	10AE X
UWD	10AB X	VBCD	00CC R	VBDM	10AF X	VB0G	0B8J X
VCSAB	0851 X	VCSB	0853 X	VCSPB	0855 X	VHR	08C5 X
VHRD	08C6 X	VPR	08D1 X	VPRD	08D2 X	VRR	08D5 X
VRD	08D6 X	VSNAB	08B3 X	VSNB	08B5 X	VSNPB	0887 X
VSNRB	0888 X	VVXBP	08E0 X	VWD	10AC X	WBCD	00CD R
WBD	10B0 X	WWD	10AD X	YAWCHAN	0092 R	Z	0000 X
ZERO	0014 R	Z0ITERS	00DF R				

APPENDIX B, PART 2

1 * KSS B-747 MAIN MOTION SIMULATION. PART 2.
2 *
3 * TEST PILOT : CAPTAIN J.L. VELDHUYZEN VAN ZANTEN
4 *
5 * DESIGN : IR. M. BAARSPUL
6 *
7 * SOFTWARE : B.BAARSCHERS
8 *
9 * ASSEMBLE THIS PROGRAM WITH :
10 * EXT. X-REF
11 * SLV SP
12 * MOTION X-REF
13 * FLIGHT INT. X-REF
14 *
15 * ISSUE 3
16 * AUG. 1975
17 *
18 * DEF MAINMN2
19 *
20 * SREF MOTION,MZ
21 *
22 * CSECT
23 * ORG X'0000'
24 *
25 0000 8C61 A MAINMN2 LDA ACTFLG04 FLIGHT OR TOTAL FREEZE ?
26 0001 9861 A AND BIT4&8
27 0002 6404 A BAZ NDFREEZE
28 0003 808E A LDA BASE8
29 0004 74D7 A RCPY A,B RESTORE BASE REG.
30 0005 44FD A B *PROGRETN EXIT
31 *
32 * BASE X'1000'
33 *

34	PAGE
35	*
36	* SUM OF BODY ROTATIONAL ACCELERATIONS
37	*
38	* SPITCHDD = BPITCHDD + (2.0 * MPITCHDD)
39	*
40 0006 81B4 A NOFREEZE	LDA MPITCHDD
41 0007 2021 A	SALS 1 2.0 *
42 0008 A1BD A	ADD BPITCHDD
43 0009 E86C A	STA SPITCHDD
44	*
45	* SROLLD = BROLLDD + MROLLD
46	*
47 000A 81B5 A	LDA MROLLD
48 000B A1BE A	ADD BROLLD
49 000C E86A A	STA SROLLD
50	*
51	* SUM OF BODY ROTATIONAL RATES
52	*
53	* SPITCHDM = BPITCHDM + MPITCHDM
54	*
55 000D 81B7 A	LDA MPITCHDM
56 000E A1BF A	ADD BPITCHDM
57 000F E868 A	STA SPITCHDM
58	*
59	* SROLLDM = BROLLDM + MROLLDM
60	*
61 0010 81B8 A	LDA MROLLDM
62 0011 A1C0 A	ADD BROLLDM
63 0012 E866 A	STA SROLLDM

64 PAGE
65 *
66 * EULER RATE : PITCH
67 *
68 * MPITCHSD = (SPITCHDM*COS(MROLLSM))-(MYAWDM*SIN(MROLLSM))
69 *
70 0013 8857 A LDA MROLLSM
71 0014 3848 A MUL KR24 SCALING FOR SINE/COS
72 0015 74F6 A RCPY E,A
73 0016 75A1 A RCPYI P,L
74 0017 44E9 A B *LOOKYCOS
75 0018 E858 A STA CMROLLSM COSINE ROLLSM
76 0019 385E A MUL SPITCHDM
77 001A 20A1 A SALD 1
78 001B 74B6 A RCPY E,T SAVE
79 001C 884E A LDA MROLLSM
80 001D 383F A MUL KR24 SCALING FOR SINE/COS
81 001E 74F6 A RCPY E,A
82 001F 75A1 A RCPYI P,L
83 0020 44E8 A B *LOOKYSIN
84 0021 E84F A STA SMROLLSM SINE ROLLSM
85 0022 31B9 A MUL MYAWDM
86 0023 20A1 A SALD 1
87 0024 7D3E A RADDI *E,T ADD 2TH COMPL TO T REG. = SUB.
88 0025 74F3 A RCPY T,A
89 0026 E840 A STA MPITCHSD

90		PAGE
91	*	EULER RATE : ROLL
92	*	
93	*	MROLLSD = SROLLDL +(SPITCHDM*SIN(MROLLSM)*SIN(MPITCHSM) / COS(MPITCHSM) +(MYAWDM*COS(MROLLSM)*SIN(MPITCHSM) / COS(MPITCHSM))
94	*	
95	*	LDA MPITCHSM MUL KP25 SCALE FOR SINE/COS RCPY E,A
96	0027 8842 A	RCPYI P,L
97	0028 3834 A	B *LOOKYSIN
98	0029 74F6 A	STA SPITCHSM SINE MPITCHSM = SIN SIM.CAB.P1
99	002A 75A1 A	LDA MPITCHSM
100	002B 44E8 A	MUL KP25 SCALE FOR SINE/COS
101	002C E843 A	RCPY E,A
102	002D 883C A	RCPYI P,L
103	002E 382E A	B *LOOKYCS
104	002F 74F6 A	STA CPITCHSM COS.MPITCHSM = COS.SIM.CAB.PIT
105	0030 75A1 A	LDA SPITCHDM SUM OF PITCH ROT.RATES
106	0031 44E9 A	MUL SMROLLSM SINE MROLLSM
107	0032 E840 A	SALD 1
108	0033 8844 A	RCPY E,A SINE MPITCHSM
109	0034 383C A	MUL SPITCHSM COS.MPITCHSM
110	0035 20A1 A	DIV CPITCHSM SAVE
111	0036 74F6 A	RCPY A,T
112	0037 3838 A	MUL LOA MYAWDM
113	0038 583A A	MUL CMROLLSM COSINE MROLLSM
114	0039 74B7 A	DIV SALD 1
115	003A 81B9 A	RCPY E,A SINE OF MPITCHSM
116	003B 3838 A	MUL SPITCHSM COS MPITCHSM
117	003C 20A1 A	DIV CPITCHSM
118	003D 74F6 A	RADD T,A SUM OF ROLL ROT.RATES
119	003E 3831 A	ADD SROLLDL
120	003F 5833 A	STA MROLLSD
121	0040 7C73 A	
122	0041 A837 A	
123	0042 E825 A	
124	*	
125	*	
126	*	EULER RATE : YAW
127	*	
128	*	MYAWSO = (SPITCHDM*SIN(MROLLSM) / COS(MPITCHSM) +(MYAWDM*COS(MROLLSM) / COS(MPITCHSM))
129	*	
130	*	
131	0043 8834 A	LDA SPITCHDM
132	0044 382C A	MUL SMROLLSM SINE MROLLSM
133	0045 582D A	DIV CPITCHSM
134	0046 74B7 A	RCPY A,T SAVE
135	0047 81B9 A	LDA MYAWDM
136	0048 382B A	MUL CMROLLSM COSINE MROLLSM
137	0049 5829 A	DIV CPITCHSM COSINE MPITCHSM
138	004A 7C73 A	RADD T,A
139	004B E810 A	STA MYAWSO

PAGE			
140	*		
141	*		
142	*	RETURN TO GROUND CHECK	
143	*		
144	004C 8C13 A	LDA DISOP075	RETURN TO GRD ?
145	004D 90C6 A	AND BIT12	
146	004E 6402 A	BAZ RETNGRD	YES
147	004F 482A A	B G05	NO
148	0050 C0D8 A RETNGRD	LDX M3	
149	0051 74F0 A	RCPY Z,A	CLEAR
150	0052 EA14 A	STA MPITCHMD+3,1	CLEAR EULER RATE WASHOUT
151	0053 EA16 A	STA MPITCHSD+3,1	CLEAR EULER RATE
152	0054 EA18 A	STA MPITCHSM+3,1	CLEAR EULER ANGLE MOST
153	0055 EA1A A	STA MPITCHSL+3,1	CLEAR EULER ANGLE LEAST
154	0056 67FB A	BIX RETNGRD+1	LOOP
155	0057 EC09 A	STA VVXB	TO ZERO THE GROUND SPEED
156	0058 4821 A	B G05	
157	*		

158 PAGE
159 * ALL CONSTANTS SCALED OTHER THAN BO , THIS SCALING
160 * IS TO AVOID SHIFTING AFTER A MULTIPLY
161 *
162 0059 5000 A KX16 DEC 625E-3 SALD 2
163 005A C000 A KX17 DEC -25E-281
164 005B 0B44 A KP20 DEC 044E-3B1
165 005C 517D A KP25 DEC 31831E-5B1 SCALE FOR SINE/COSINE
166 *
167 005D 6666 A KY16 DEC 8E-1
168 10D5 A KY17 EQU KZ3 IN BASE
169 *
170 005C R KR24 EQU KP25 SCALE FOR SINE/COS
171 *
172 005E 0888 A ADRL VSNRB SINE ROLL BODY AT 2B0
173 005F 01B9 A ADRL DISOP075
174 0060 08E0 A ADRL VVXPB
175 0061 0FE0 A ADRL ACTFLG04
176 *
177 0062 0880 A BIT4&8 DATA X'0880' FOR FLIGHT & TOTAL FREEZE
178 *
179 005C R KJ9 EQU KP25 SCALE FOR SINE / COS
180 *
181 0063 0000 A MPITCHMD DATA 0 EULER RATE WASHOUT
182 0064 0000 A MROLLMD DATA 0
183 0065 0000 A MYAWMD DATA 0
184 *
185 0066 0000 A MPITCHSD DATA 0 EULER RATE
186 0067 0000 A MROLLSD DATA 0
187 0068 0000 A MYAWSO DATA 0
188 *
189 0069 0000 A MPITCHSM DATA 0 EULER ANGLE M/S PART
190 006A 0000 A MROLLSM DATA 0
191 006B 0000 A MYAWSM DATA 0
192 *
193 006C 0000 A MPITCHSL DATA 0 EULER ANGLE L/S PART
194 006D 0000 A MROLLSL DATA 0
195 006E 0000 A MYAWSL DATA 0
196 *
197 006F 0000 A SPITCHSM DATA 0 SINE MPITCHSM (EULER ANGLE M/S
198 0070 0000 A SMROLLSM DATA 0 MROLLSM
199 0071 0000 A SMYAWSM DATA 0 MYAWSM
200 *
201 0072 7FFF A CPITCHSM DATA X'7FFF' COSINE MPITCHSM (EULER ANGLE M
202 0073 7FFF A CMROLLSM DATA X'7FFF' MROLLSM
203 0074 7FFF A CMYAWSM DATA X'7FFF' MYAWSM

204 PAGE
205 *
206 * SUM OF ROTATIONAL ACCEL' & RATES
207 *
208 0075 0000 A SPITCHDD DATA 0 PITCH ACC. SUM
209 0076 0000 A SROLLDD DATA 0 ROLL ACC. SUM
210 0077 0000 A SPITCHDM DATA 0 PITCH RATE SUM
211 0078 0000 A SROLLDM DATA 0 ROLL RATE SUM
212 *

213	PAGE
214	*
215	*
216	*
217	*
218	*
219	*
220	*
221	*
222 0079 89F0 A G05	TAU THETA ROTATIONAL = 200 SEC
223 007A 31D3 A	S THETA (MOTION) = 1 RAD
224 007B 89EB A	MPITCHMD = MPITCHSD - (KP24*MPITCHSM)
225 007C 7D7E A	LDA MPITCHSM
226 007D E9E6 A	MUL KP24
227	LDA MPITCHSD
228	RADDI *E,A ADD 2TH COMPLEMENT
229	STA MPITCHMD
230	*
231	*
232 007E 31CF A	INTEGRATION
233 007F A9ED A	MUL KP18
234 0080 E9EC A	ADD MPITCHSL L/S PART
235 0081 10C0 A	STA MPITCHSL NEW L/S PART
236 0082 89E7 A	RD X'CO'
237 0083 7E76 A	LOA MPITCHSM RESET OVERFLOW
238 0084 E9E5 A	RADDI E,A M/S PART
239	STA MPITCHSM NEW M/S PART
240	*
241	*
242	COMPENSATION
243	*
244 0085 89DE A	MPITCHC = MPITCHSM + (KP19*MPITCHMD) + (KP20*SPITCHDD)
245 0086 31D1 A	LDA MPITCHMD
246 0087 74B6 A	MUL KP19
247 0088 89ED A	RCPY E,T
248 0089 39D2 A	LDA SPITCHDD SUM OF PITCH ACCELERATIONS
249 008A 7C36 A	MUL KP20
250 008B 89DE A	RADD E,T
251 008C 7C73 A	LDA MPITCHSM
252 008D E1C7 A	RADD T,A
	STA MPITCHC

253 PAGE
254 *
255 * ROTATIONAL WASHOUT.
256 *
257 * TAU, PHI ROTATIONAL = 200 SEC
258 * S PHI (MOTION) = 1 RAD
259 *
260 * MROLLMD = MROLLSM - (KR23*MROLLSM)
261 *
262 008E 89DC A LDA MROLLSM
263 008F 31D3 A MUL KR23
264 0090 89D7 A LDA MROLLSD
265 0091 7D7E A RADDI *E,A ADD 2TH COMPLEMENT
266 0092 E9D2 A STA MROLLMD
267 *
268 * INTEGRATION
269 *
270 * MROLLSM = MROLLSM + (KR18*MROLLMD)
271 *
272 0093 31CF A MUL KR18
273 0094 A9D9 A ADD MROLLSL L/S PART
274 0095 E9D8 A STA MROLLSL NW L/S PART
275 0096 10C0 A RD X'CO' RESET CDF
276 0097 89D3 A LDA MROLLSM M/S PART
277 0098 7E76 A RADDI E,A
278 0099 E9D1 A STA MROLLSM NEW M/S PART
279 *
280 * COMPENSATION
281 *
282 * MROLLC = MROLLSM + (KR19*MROLLMD) + (KR20*SROLLDD)
283 *
284 009A 89CA A LDA MROLLMD
285 009B 31D1 A MUL KR19
286 009C 74B6 A RCPY E,T
287 009D 89D9 A LDA SROLLDO SUM OF ROLL ACCELERATIONS
288 009E 31D2 A MUL KR20
289 009F 7C36 A RADDI E,T
290 00A0 89CA A LDA MROLLSM
291 00A1 7C73 A RADDI T,A
292 00A2 E1C8 A STA MROLLC

293	PAGE
294	*
295	*
296	*
297	*
298	*
299	*
300	*
301	*
302 00A3 89C8 A	LDA MYAWSM
303 00A4 31CF A	MUL KJ11
304 00A5 89C3 A	LDA MYAWSD
305 00A6 7D7E A	RADDI *E,A ADD 2TH COMPLEMENT
306 00A7 E9BE A	STA MYAWMD
307	*
308	*
309	*
310 00A8 31CF A	MUL KJ4
311 00A9 A9C5 A	ADD MYAWSL L/S PART
312 00AA E9C4 A	STA MYAWSL NEW L/S PART
313 00AB 10C0 A	RD X'CO' RESET COF
314 00AC 898F A	LDA MYAWSM M/S PART
315 00AD 7E76 A	RADD C E,A
316 00AE E9BD A	STA MYAWSD NEW M/S PART
317	*
318	*
319	*
320 00AF 89B6 A	MYAWC = MYAWSM + (KJ5*MYAWMD) + (KJ6*MYAWDD)
321 00B0 31D1 A	LDA MYAWMD
322 00B1 74B6 A	MUL KJ5
323 00B2 81B6 A	RCPY E,T SAVE
324 00B3 31D2 A	LDA MYAWDD
325 00B4 7C36 A	MUL KJ6
326 00B5 89B6 A	RADD E,T
327 00B6 7C73 A	LDA MYAWSM
328 00B7 E1C6 A	RADD T,A
	STA MYAWC

329	PAGE	
330		
331		GENERATE SINE AND COSINE OF MYAWSM
332		FOR BODY TO INERTIAL TRANSFORMATION.
333		
334		
335 00B8 89B3 A	LDA	MYAWSM
336 00B9 39A3 A	MUL	KJ9
337 00BA 74F6 A	RCPY	E,A
338 00BB 75A1 A	RCPYI	P,L
339 00BC 44E8 A	B	*LOOKYSIN
340 00BD E9B4 A	STA	SMYAWSM
341		SINE OF MYAWSM
342 00BE 89AD A	LDA	MYAWSM
343 00BF 399D A	MUL	KJ9
344 00C0 74F6 A	RCPY	E,A
345 00C1 75A1 A	RCPYI	P,L
346 00C2 44E9 A	B	*LOOKYCOS
347 00C3 E9B1 A	STA	CMYAWSM
348		COSINE OF MYAWSM
349		SUMMATION OF TRANSLATIONAL ACCELERATIONS
350		
351 00C4 81B1 A	LDA	BXDD
352 00C5 A1C1 A	ADD	MXDD
353 00C6 E1CC A	STA	SXDD
354		
355 00C7 81B2 A	LDA	BYDD
356 00C8 A1C2 A	ADD	MYDD
357 00C9 E1CD A	STA	SYDD
358		

359	PAGE
360	*
361	*
362	*
363	*
364	*
365	*
366	*
367 00CA 89AA A	LDA CMYAWSM COS.MYAWSM
368 00CB 39A4 A	MUL SPITCHSM
369 00CC 20A1 A	SALD 1
370 00CD 74F6 A	RCPY E,A
371 00CE 39A2 A	MUL SMROLLSM
372 00CF 20A1 A	SALD 1
373 00D0 74B6 A	RCPY E,T SAVE
374 00D1 89A2 A	LDA CMROLLSM
375 00D2 399F A	MUL SMYAWSM SINE OF MYAWSM
376 00D3 20A1 A	SALD 1
377 00D4 74F3 A	RCPY T,A
378 00D5 707E A	RADDI *E,A
379 00D6 31CD A	MUL SYDD
380 00D7 20A1 A	SALD 1
381 00D8 74F6 A	RCPY E,A
382 00D9 3984 A	MUL KY16
383 00DA 20A1 A	SALD 1
384 00DB 74B6 A	RCPY E,T SAVE
385 00DC 8998 A	LDA CMYAWSM
386 00DD 3995 A	MUL CPITCHSM
387 00DE 20A1 A	SALD 1
388 00DF 74F6 A	RCPY E,A
389 00EO 31CC A	MUL SXDD
390 00E1 20A1 A	SALD 1
391 00E2 7C36 A	RADD E,T SUM IT
392 00E3 74F3 A	RCPY T,A
393 00E4 E1C9 A	STA MXSDD

394 PAGE
395 * BODY TO INERTIAL TRANSFORMATION FOR : Y
396 *
397 * MYSDD = (KX16*SXDD*COS(MPITCHSM)*SIN(MYAWSM))
398 * + (SYDD*SIN(MROLLSM)*SIN(MPITCHSM)*SIN(MYAWSM))
399 * + (COS(MROLLSM)*COS(MYAWSM)))
400 *
401 00E5 898E A LDA CMROLLSM
402 00E6 398E A MUL CMYAWSM
403 00E7 20A1 A SALD 1
404 00E8 7486 A RCPY E,T SAVE
405 00E9 8987 A LDA SMROLLSM
406 00EA 3985 A MUL SPITCHSM
407 00EB 20A1 A SALD 1
408 00EC 74F6 A RCPY E,A
409 00ED 3984 A MUL SMYAWSM
410 00EE 20A1 A SALD 1
411 00EF 7C36 A RADD E,T
412 00F0 74F3 A RCPY T,A
413 00F1 31CD A MUL SYDD
414 00F2 20A1 A SALD 1
415 00F3 74B6 A RCPY E,T SAVE
416 00F4 81CC A LDA SXDD
417 00F5 3964 A MUL KX16
418 00F6 20A2 A SALD 2 = KX16*2
419 00F7 74F6 A RCPY E,A
420 00F8 397A A MUL CPITCHSM
421 00F9 20A1 A SALD 1
422 00FA 74F6 A RCPY E,A
423 00FB 3976 A MUL SMYAWSM
424 00FC 20A1 A SALD 1
425 00FD 7C36 A RADD E,T SUM IT
426 00FE 74F3 A RCPY T,A
427 00FF E1CA A STA MYSDD

428	PAGE
429	*
430	*
431	*
432	*
433	*
434	*
435	*
436 0100 896F A	LDA SPITCHSM SINE MPITCHSM
437 0101 31CC A	MUL SXDD
438 0102 20A1 A	SALD 1
439 0103 74F6 A	RCPY E,A
440 0104 3956 A	MUL KY17
441 0105 74B6 A	RCPY E,T SAVE IT
442 0106 896C A	LDA CPITCHSM COSINE MPITCHSM
443 0107 3969 A	MUL SMROLLSM
444 0108 20A1 A	SALD 1
445 0109 74F6 A	RCPY E,A
446 010A 31CD A	MUL SYDD
447 010B 20A1 A	SALD 1
448 010C 74F6 A	RCPY E,A
449 010D 3105 A	MUL KY17
450 010E 7C36 A	RADD E,T SUM IT IN T REG
451 010F 8963 A	LDA CPITCHSM
452 0110 3963 A	MUL CMROLLSM
453 0111 20A1 A	SALD 1
454 0112 74F6 A	RCPY E,A
455 0113 31B3 A	MUL BZDD
456 0114 20A1 A	SALD 1
457 0115 7C36 A	RADD E,T SUM IT IN T REG
458 0116 74F3 A	RCPY T,A
459 0117 E1CB A	STA MZDD

460 PAGE
461 *
462 * TRANSLATIONAL WASHOUT FOR : X
463 *
464 * TAU X TRANSLATIONAL = 2 SEC
465 * ZETA X TRANSLATIONAL = .7
466 *
467 * MXMDD = MXSDD - (KX18*MXD) - (KX19*MXM)
468 *
469 0118 886F A LDA MXDM
470 0119 3874 A MUL KX18
471 011A 20A1 A SALD 1
472 011B 74B6 A RCPY E,T
473 011C 886D A LOA MXM
474 011D 3871 A MUL KX19
475 011E 7C36 A RAOD E,T
476 011F 81C9 A LDA MXSDD
477 0120 707B A RADDI *T,A ADD 2TH COMPLEMENT OF SUM
478 0121 E869 A STA MXMDD
479 *
480 * INTEGRATION
481 *
482 * MXDM = MXDM + (KX12*MXD)
483 *
484 0122 31CF A MUL KX12
485 0123 A863 A ADD MXDL L/S PART
486 0124 E862 A STA MXDL NEW L/S PART
487 0125 10CO A RD X'CO' RESET CDF
488 0126 8861 A LOA MXDM
489 0127 7E76 A RADDC E,A
490 0128 E85F A STA MXDM M/S PART
491 *
492 * MXM = MXM + (KX13*MXD)
493 *
494 0129 31D0 A MUL KX13
495 012A A85E A ADD MXL L/S PART
496 012B E85D A STA MXL NEW L/S PART
497 012C 10CO A RD X'CO' RESET CUF
498 012D 885C A LOA MXM
499 012E 7E76 A RADDC E,A
500 012F E85A A STA MXM NEW M/S PART

	PAGE
501	*
502	*
503	*
504	*
505	*
506	*
507	*
508 0130 8857 A	LOA MXDM
509 0131 385A A	MUL KX14
510 0132 7486 A	RCPY E,T
511 0133 8857 A	LDA MXMDD
512 0134 3858 A	MUL KX15
513 0135 7C36 A	RADD E,T
514 0136 8853 A	LDA MXM
515 0137 7C73 A	RADD T,A
516 0138 E1C3 A	STA MXC

PAGE	
517	
518	*
519	*
520	*
521	*
522	*
523	*
524	*
525	*
526 0139 8857 A	LDA MYDM
527 013A 385B A	MUL KY18
528 013B 20A1 A	SALD 1
529 013C 74B6 A	RCPY E,T
530 013D 8855 A	LDA MYM
531 013E 3858 A	MUL KY19
532 013F 7C36 A	RADD E,T
533 0140 81CA A	LDA MYSDD
534 0141 7D7B A	RADDI *T,A
535 0142 E851 A	STA MYMDD
536	*
537	*
538	*
539	*
540	*
541 0143 31D4 A	MUL KY12
542 0144 A84B A	ADD MYDL
543 0145 E84A A	STA MYDL
544 0146 10C0 A	RD X'CO'
545 0147 8849 A	LDA MYDM
546 0148 7E76 A	RADDC E,A
547 0149 E847 A	STA MYDM
548	*
549	*
550	*
551 014A 31D0 A	MUL KY13
552 014B A846 A	ADD MYL
553 014C E845 A	STA MYL
554 014D 10C0 A	RD X'CO'
555 014E 8844 A	LDA MYM
556 014F 7E76 A	RADDC E,A
557 0150 E842 A	STA MYM

TRANSLATIONAL WASHOUT FOR : Y

TAU Y TRANSLATIONAL = 2 SEC

ZETA Y TRANSLATIONAL = .7

MYMDD = MYSDD - (KY18*MYDM) - (KY19*MYM)

ADD 2TH COMPLEMENT OF SUM

INTEGRATION

MYDM = MYDM + (KY12*MYMDD)

L/S
NEW L/S PART
RESET COF

M/S PART

MYM = MYM + (KY13*MYDM)

L/S PART
NEW L/S PART
RESET COF

M/S PART

	PAGE
558	*
559	*
560	*
561	*
562	*
563	*
564 0151 883F A	LDA MYDM
565 0152 3839 A	MUL KY14
566 0153 7486 A	RCPY E,T
567 0154 883F A	LDA MYMDD
568 0155 383F A	MUL KY15
569 0156 7C36 A	RAOO E,T
570 0157 883B A	LDA MYM
571 0158 7C73 A	RAOO T,A
572 0159 E1C4 A	STA MYC

573 PAGE
574 *
575 * TRANSLATIONAL WASHOUT FOR : Z
576 *
577 * TAU Z TRANSLATIONAL = 2 SEC
578 * ZETA Z TRANSLATIONAL = .7
579 *
580 * MZMDD = MZSDD - (KZ8*MZDM) - (KZ9*MZM)
581 *
582 015A 883E A LDA MZM
583 015B 384J A MUL KZ8
584 015C 74B6 A RCPY E,T SAVE IT
585 015D 883D A LDA MZM
586 015E 3841 A MUL KZ9
587 015F 7C36 A RADD E,T SUM IT IN T REG
588 0160 81CB A LDA MZSDD
589 0161 7D78 A RADDI *T,A SUBTRACT T IN A REG
590 0162 E839 A STA MZMDD
591 *
592 * INTEGRATION
593 *
594 * MZDM = MZDM + (KZ3*MZMDD)
595 *
596 0163 31D5 A MUL KZ3
597 0164 A833 A ADD MZDL L/S PART
598 0165 E832 A STA MZDL NEW L/S PART
599 0166 10C0 A RD X'CO' RESET COF
600 0167 8831 A LDA MZM M/S PART
601 0168 7E76 A RADD C E,A
602 0169 E82F A STA MZM NEW M/S PART
603 *
604 * MZM = MZM + (KZ4*MZDM)
605 *
606 016A 31D6 A MUL KZ4
607 016B A82E A ADD MZL L/S PART
608 016C E82D A STA MZL NEW L/S PART
609 016D 10C0 A RD X'CO' RESET
610 016E 882C A LDA MZM M/S PART
611 016F 7E76 A RADD C E,A
612 0170 E82A A STA MZM NEW M/S PART

	PAGE
613	
614	*
615	*
616	*
617	*
618 0171 8827 A	LDA MZDM
619 0172 382A A	MUL KZ5
620 0173 74B6 A	RCPY E,T
621 0174 8827 A	LDA MZMDD
622 0175 3828 A	MUL KZ6
623 0176 7C36 A	RADD E,T
624 0177 8823 A	LDA MZM
625 0178 7C73 A	RADD T,A
626 0179 E1C5 A	STA MZC
	SAVE IT
	SUM IT IN T REG

627	PAGE	
628		
629	SUMMATION OF OUTPUTS TO MOTION OUTPUT PROGRAM.	
630		
631 017A COEO A	LDX M6	
632 017B 83C9 A	LDA MXC+6,1	COMPENSATED SIGNALS
633 017C EE08 A	STA MOTION,1	INTO OUTPUT PROGRAM
634 017D 67FE A	BIX \$-2	LOOP
635		
636	RESTORE BASE FOR OUTPUT PROGRAM	
637		
638 017E 80BE A	LDA BASE8	
639 017F 74D7 A	RCPY A,B	RESTORE BASE REG.
640		
641	BASE \$BASE8	
642		
643	RUNWAY BUMPS	
644		
645 0180 8C05 A	LDA MZ	
646 0181 A120 A	ADD BUMPS	COMPUTED BUMPS FROM RNWYBMPs
647 0182 EC03 A	STA MZ	HEAVE MOTION
648		
649		
650		
651 0183 44FD A	8 *PROGRETN	EXIT

PAGE			
652	*	ALL CONSTANTS SCALED OTHER THAN BO THIS SCALING	
653	*	IS TO AVOID SHIFTING AFTER A MULTIPLY	
654	*		
655	*		
656	0184 0000 E	ADRL	MOTION
657	0185 0000 E	ADRL	MZ
658	*		FOR OUTPUT PROGRAM
659	0186 0000 A MXDL	DATA	HEAVE MOTION
660	0187 0000 A MXDM	DATA	
661	0188 0000 A MXL	DATA	
662	0189 0000 A MXM	DATA	
663	018A 0000 A MXMDD	DATA	
664	018B 3EE8 A KX14	DEC	24572E-5B1
665	018C 09E3 A KX15	DEC	038613E-6B1
666	018D 599A A KX18	DEC	7E-1
667	018E 48EE A KX19	DEC	28488E-5B1
668	*		
669	018F 0000 A MYDL	DATA	0
670	0190 0000 A MYDM	DATA	0
671	0191 0000 A MYL	DATA	0
672	0192 0000 A MYM	DATA	0
673	0193 0000 A MYMDD	DATA	0
674	0188 R KY14	EQU	KX14
675	0194 07E8 A KY15	DEC	03089E-5B1
676	0195 7000 A KY18	DEC	875E-3
677	0196 5B29 A KY19	DEC	3561E-4B1
678	*		
679	0197 0000 A MZDL	DATA	0
680	0198 0000 A MZDM	DATA	0
681	0199 0000 A MZL	DATA	0
682	019A 0000 A MZM	DATA	0
683	019B 0000 A MZMDD	DATA	0
684	019C 0E61 A KZ5	DEC	056164E-6B1
685	019D 090A A KZ6	DEC	035302E-6B1
686	019E 2CCD A KZ8	DEC	175E-3B1
687	019F 4FC4 A KZ9	DEC	311587E-6B1

688	PAGE		
689	*		
690	*		
691	*		
692	10CE A KP3	EQU	KPRJ3
693	10CE A KR3	EQU	KPRJ3
694	10CE A KJ3	EQU	KPRJ3
695	*		
696	10CE A KR17	EQU	KPRJ3
697	10CE A KR13	EQU	KPRJ3
698	*		
699	10CF A KP4	EQU	KPRJ4
700	10CF A KR4	EQU	KPRJ4
701	10CF A KJ4	EQU	KPRJ4
702	*		
703	10CF A KJ11	EQU	KPRJ4
704	10CF A KX12	EQU	KPRJ4
705	*		
706	10CF A KR18	EQU	KPRJ4
707	10CF A KP17	EQU	KPRJ4
708	10CF A KP18	EQU	KPRJ4
709	*		
710	*		
711	1000 A KX13	EQU	KXY13
712	1000 A KY13	EQU	KXY13
713	*		
714	*		
715	1001 A KP19	EQU	KR19
716	10D1 A KJ5	EQU	KR19
717	*		
718	*		
719	1003 A KP24	EQU	KPR2423
720	1003 A KR23	EQU	KPR2423
721	*		
722	*		
723	1002 A KR20	EQU	KPRJ206
724	1002 A KJ6	EQU	KPRJ206
725	*		
726	*		
727	*		
728	0000 A	END	

0 ERRORS
EQUALS ERROR MAINMN2

\$BASE8	0800 X	A	0007 X	ACTFLG04	0FEO X	B	0005 X
BASE8	008E X	BIT12	00C6 X	BIT4&8	0062 R	BPITCHDD	108D X
BPITCHDM	108F X	BR0LLDD	108E X	BR0LLDM	10C0 X	BUMPS	0820 X
BXDD	1081 X	BYDD	10B2 X	BZDD	10B3 X	CWROLLSM	0073 R
CWYAWSM	0074 R	CPITCHSM	0072 R	DISOP075	01B9 X	E	0006 X
G05	0079 R	KJ11	10CF A	KJ3	10CE A	KJ4	10CF A
KJ5	10D1 A	KJ6	10D2 A	KJ9	005C R	KPRJ206	10D2 X
KPRJ3	10CE X	KPRJ4	10CF X	KPR2423	10D3 X	KP17	10CF A
KP18	10CF A	KP19	10D1 A	KP20	005B R	KP24	10D3 A
KP25	005C R	KP3	10CE A	KP4	10CF A	KR13	10CE A
KR17	10CE A	KR18	10CF A	KR19	10D1 X	KR20	10D2 A
KR23	10D3 A	KR24	005C R	KR3	10CE A	KR4	10CF A
KXY13	1000 X	KX12	10CF A	KX13	10D0 A	KX14	018B R
KX15	018C R	KX16	0059 R	KX17	005A R	KX18	018D R
KX19	018E R	KY12	10D4 X	KY13	10D0 A	KY14	018B R
KY15	0194 R	KY16	005D R	KY17	10D5 A	KY18	0195 R
KY19	0196 R	KZ3	10D5 X	KZ4	10D6 X	KZ5	019C R
KZ6	019D R	KZ8	019E R	KZ9	019F R	L	0002 X
L00KYC0S	00E9 X	L00KYSIN	00E8 X	MAINMN2	0000 R	MOTION	0184 E
MPITCHC	10C7 X	MPITCHDD	1084 X	MPITCHDM	10B7 X	MPITCHMD	0063 R
MPITCHSD	0066 R	MPITCHSL	006C R	MPITCHSM	0069 R	MROLLC	10C8 X
MR0LLDD	10B5 X	MR0LLDM	10B8 X	MR0LLMD	0064 R	MR0LLSD	0067 R
MR0LLSL	006D R	MR0LLSM	006A R	MXC	10C3 X	MXDD	10C1 X
MXDL	0186 R	MXDM	0187 R	MXL	0188 R	MXM	0189 R
MXMDD	018A R	MXSDD	10C9 X	MYAWC	10C6 X	MYAWDD	10B6 X
MYAWDM	10B9 X	MYAWMD	0065 R	MYAWSO	0068 R	MYAWSL	006E R
MYAWSM	0068 R	MYC	10C4 X	MYDD	10C2 X	MYDL	018F R
MYDM	0190 R	MYL	0191 R	MYM	0192 R	MYMDD	0193 R
MYSD0	10CA X	MZ	0185 E	MZC	10C5 X	MZDL	0197 R
MZDM	0198 R	MZL	0199 R	MZM	019A R	MZMDD	019B R
MZSDD	10C8 X	M3	0008 X	M6	00E0 X	NOFREEZE	0006 R
P	0001 X	PROGRETN	00FD X	RETNGRD	0050 R	SMROLLSM	0070 R
SMYAWSM	0071 R	SPITCHDD	0075 R	SPITCHDM	0077 R	SPITCHSM	006F R
SR0LLDD	0076 R	SR0LLDM	0078 R	SXDD	10CC X	SYDD	10CD X
T	0003 X	VSNRB	0888 X	VVXBPP	08E0 X	Z	0000 X

APPENDIX B, PART 3

1 * X-REF PART FOR MOTION SYSTEM.
2 *
3 * B-747 FILE NO: K 820
4 * JULY 1975
5 * B. BAARSCHERS.
6 * ISSUE 1
7 *
8 ASELECT
9 ORG X'10A8'
10 *
11 *
12 10AB 0000 A MFXWB DATA 0 WIND/BODY AXIS LONG.FORCE/GW
13 10A9 0000 A MFYWB DATA 0 WIND/BODY-AXIS LAT. FORCE/GW
14 10AA 0000 A MFZWB DATA 0 WIND/BODY-AXIS VERT.FORCE/GW
15 *
16 * ON/OFF GROUND FUNCTIONS AFTER RESCALING.
17 *
18 10AB 0000 A UWD DATA 0 W/B-AXIS LONGITUDINAL ACCEL.
19 10AC 0000 A VWD DATA 0 W/B-AXIS LATERAL ACCEL.
20 10AD 0000 A WWD DATA 0 W/B-AXIS VERTICAL ACCEL
21 *
22 * ON/OFF GROUND FUNCTIONS.
23 *
24 10AE 0000 A UBD DATA 0 MOTION BODY-AXIS LONGITUD.ACCEL
25 10AF 0000 A VBDM DATA 0 MOTION BODY AXIS LATERAL ACCEL
26 10B0 0000 A WBD DATA 0 MOTION BODY-AXIS VERTICAL ACCEL
27 *
28 * BODY - AXIS FUNCTIONS
29 *
30 10B1 0000 A BXDD DATA 0 X BODY DOUBLE DOT
31 10B2 0000 A BYDD DATA 0 Y BODY DOUBLE DOT
32 10B3 0000 A BZDD DATA 0 Z BODY DOUBLE DOT
33 *
34 10B4 0000 A MPITCHDD DATA 0 PITCH ACCEL
35 10B5 0000 A MROLLDD DATA 0 ROLL
36 10B6 0000 A MYAWDD DATA 0 YAW
37 *
38 10B7 0000 A MPITCHDM DATA 0 PITCH RATE
39 10B8 0000 A MROLLDM DATA 0 ROLL
40 10B9 0000 A MYAWDM DATA 0 YAW
41 *
42 10BA 0000 A MPITCHM DATA 0
43 10BB 0000 A MROLLM DATA 0
44 10BC 0000 A MYAWM DATA 0
45 *
46 10BD 0000 A BPITCHDD DATA 0 PITCH ACCEL BODY
47 10BE 0000 A BR0LLDD DATA 0 ROLL

48	PAGE		
49 10BF 0000 A BPITCHOM	DATA	0	PITCH RATE BODY
50 10CO 0000 A BROLLM	DATA	0	ROLL
51 *			
52 10C1 0000 A MXDD	DATA	0	X SPEC. FORCE ERROR
53 10C2 0000 A MYDD	DATA	0	Y
54 *			
55 *	COMPENSATED SIGNALS TO MOTION OUTPUT		
56 *			
57 *			
58 10C3 0000 A MXC	DATA	0	X-AXIS
59 10C4 0000 A MYC	DATA	0	Y-AXIS
60 10C5 0000 A MZC	DATA	0	Z-AXIS
61 *			
62 10C6 0000 A MYAWC	DATA	0	YAW
63 10C7 0000 A MPITCHC	DATA	0	PITCH
64 10C8 0000 A MROLLC	DATA	0	ROLL
65 *			
66 *			
67 *			
68 10C9 0000 A MXSDD	DATA	0	X INERTIAL ACCEL
69 10CA 0000 A MYSDD	DATA	0	Y
70 10CB 0000 A MZSDD	DATA	0	Z
71 *			
72 *	SUM OF TRANSLATIONAL ACCEL'S		
73 *			
74 10CC 0000 A SXDD	DATA	0	
75 10CD 0000 A SYDD	DATA	0	
76 *			
77 *	THIS DATA IS SCALED AT B1 TO AVOID ALL THE SALD 1 INSTR'		
78 *			
79 10CE 199A A KPRJ3	DEC	1E-1B1	
80 10CF OCCO A KPRJ4	DEC	05E-2B1	
81 10D0 08JC A KXY13	DEC	043878E-6B1	
82 10D1 47AE A KR19	DEC	28E-2B1	
83 10D2 1687 A KPRJ206	DEC	088E-3B1	
84 10D3 0148 A KPR2423	DEC	005E-3B1	
85 10D4 0A3D A KY12	DEC	04E-2B1	
86 10D5 3333 A KZ3	DEC	2E-1B1	
87 10D6 0291 A KZ4	DEC	010029E-6B1	
88 *			
89 TAPE			
TAPE			
!KEY-IN			
!GO			
1 *			
2 0000 A	END		

771308